Geol. Bull. Univ. Peshawar, 1983, Vol. 16, pp. 105–184

METAMORPHIC EVOLUTION OF AN OBDUCTED ISLAND ARC : EXAMPLE OF THE KOHISTAN SEQUENCE (PAKISTAN) IN THE HIMALAYAN COLLIDED RANGE

JEAN–PIERRE BARD

Lab. Petrologie des Zones Profondes, 34060, Montpellier-Cedex, France

ABSTRACT

In the northern Pakistan, the extraordinary 40km thick Kohistan sequence of mafic, ultramafic and calc-alkaline layered plutonic and volcanic (mainly andesitic to rhyodacitic) rocks has been interpreted as the only complete vertical section of an intraoceanic island arc presently exposed anywhere in the world. Plate-scale models have been suggested to explain the origin and the tectonic evolution of this arc in the Himalayan collided range. Despite some noticeable differences in the models, there is a general agreement that the Kohistan sequence represents the crust of an arc obducted onto the Indian plate before the Oligocene collision of India against Asia.

The purpose of the present paper is to give new data on the tectono-metamorphic evolution of the Kohistan sequence and to try to estimate its changing metamorphic conditions on petrological, mineralogical and crystal chemistry grounds. The structural, textural and mineralogical data suggest two main tectono-metamorphic events that have affected the Kohistan arc before late lower grade overprints. From various geothermometry estimates as well as from field zonations, it is concluded that the major (D_1) phase developed with a thermal structure strongly controlled by thermal anomalies in the metamorphic pile. These anomalies seem centered around isolated bodies of two-pyroxenes and cpx-garnet granulites. Because the petrographical evidences indicate the latter are derived from large pre-tectonic layered calc-alkaline intrusion(s), the former anomalies are interpreted as remnant magmatic heat source(s) within the arc. This interpretation fits nicely with theoretical thermal models. Assuming D_1 is contemporaneous with obduction of the arc and together with the geochronological data, it is suggested that the tectonic

emplacement of the Kohistan arc was 20±5 m.y. after the intrusion of enormous calc-alkaline pluton(s) within the arc crust. Such a relatively short elapsed time between a strong magmatic activity and a tectono-metamorphic event may explain why the T–P paths during D_1 produced sinuous geotherms in the petrogenetic grid, i.e. the dT/dP are varying from 35°C ± 5°C/km upto 100°C/km in the 40km thick pile.

The second (D_2) phase is contemporaneous with synkinematic low- to mid-grade retrogressions upto the epidote-amphibolite facies conditions. The T–P curve during this phase is a classical one and the D_2-geotherm approached 25°C ± 5°C/km within a re-equilibriated thermal structure. Scarce geochronological data suggest that D_2 was contemporaneous with the Oligocene collision of India against Asia and possibly synchronous with the Oligocene Barrovian metamorphism which has affected the Indian plate south of Kohistan. The origin of the rocks of the Kohistan granulites as well as the significance of a blueschist belt under the Kohistan metamorphic pile are briefly discussed.

INTRODUCTION

In the northern Pakistan (Fig. 1) amphibolite to granulite facies mafic and ultramafic rocks have been interpreted by Jan (1977) as possible relicts of Archean and Tethyan crust and/or crystalline mushes of alpine-type ultramafites emplaced in the latter crust during the Himalayan collision (but see also, Jan, 1980). Recently, Tahirkheli *et al.* (1979) and Bard *et al.* (1980) claimed that the metamorphites and associated calcalkaline plutonic and volcanic rock make up a 40km thick sequence, representative of intraoceanic arc crust (the so-called "Kohistan arc sequence"). Tahirkheli *et al.* (opt. cit.) suggested that the Kohistan sequence is possibly the only cross-section of such a crust presently exposed in the world. They proposed that a Cretaceous oceanic island arc, formed in response to a Cretaceous northwards subduction in the paleo-Tethys, was obducted onto the Indian plate in Lower Eocene (i.e. before the Oligocene collision of India against Asia).

Fig. 1. Geological sketch map of northern Pakistan and Kashmir with special reference to Kohistan area (slightly modified after Bard *et al.*, 1980). 1 : fossils (Mid-Cretaceous to Lower Eocene); 2 : serpentines and allochthonous ultrabasics; 3 : Blueschist belt and associated "tectonic melange" under the Main Mantle Thrust (M.M.T.) paleosuture; 4 : Jijal-Patan mafic-ultramafic complex and western equivalents near Mingora (Swat Valley); 5 : Southern amphibolitic series; 6 : Kohistan "granulitic belt" (metamorphic calc-alkaline layered lopolith); 7 : Northern amphibolitic series; 8 : Kalam metasedimentary and volcanosedimentary series; 9 : Utror volcanics (mainly andesitic to dacitic lavas and tuffs); 9 : late dioritic granitic intrusives; 10 : Yasin-group (Mid-Cretaceous); 11 : Indian plate (I.P.) orthogneissic rocks; 12 : late kinematic I-P granitoids; 13 : (I.P.) metasediments (Upper Precambrian to Paleozoic); 14 : Upper Paleozoic to Triassic Series of Srinagar and Panjal Traps; 15 : Foreland Cenozoic deposits (Murree formation, etc. ....). AB : Abbottabad; AS : Astor; AT : Attock; BAB : Babusar Pass; BUZ : Burzil Pass; CH : Chilas; DRO : Drosh; DS : Dras; GI : Gilgit; ISL : Islamabad; J : Jallalabad; K : Kalam; M : Mingora; NP : Nanga Parbat; P : Peshawar; R : Rakaposhi Mountain; SH : Srinagar; SK : Skardu; Y : Yasin.

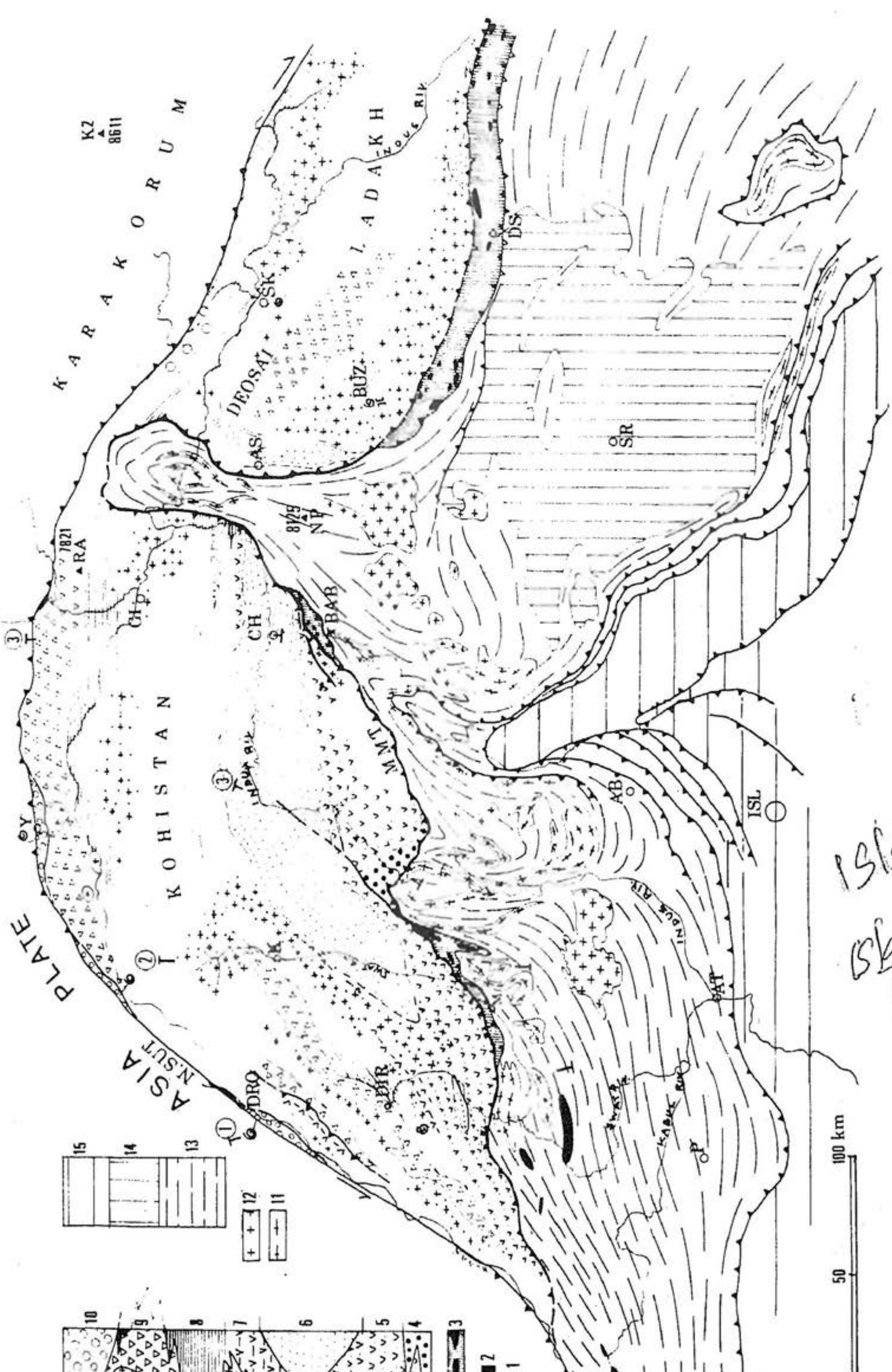

Island

Island Arc

The purpose of this paper is to describe the petrological and mineralogical features related to the metamorphic evolution of the Kohistan sequence. This data is used to determine the history of the rocks with respect to T and P during the tectono-metamorphic stages and to compare possible dynamo-thermal structures with the plate-scale models which have been proposed for this area by Tahirkheli *et al.* (opt. cit.) and, more recently, by Brookfield and Reynolds (1981).

THE KOHISTAN SEQUENCE

The 60–70° northward dipping rocks in Kohistan (Fig. 1, 6) comprise of a lithological complex disrupted near Dir and Kalam by a northward dipping cataclastic fault. There is a late open synform and antiform in the northern part of the area but evidence for older isoclinal recumbent folds and nappes is not obvious (see further discussion). The sequence in the southern and central part of Kohistan is assumed not to have major significant tectonic repetitions in a grossly northwards dipping foliation monocline. In the absence of exhaustive structural studies that might change estimates of the thickness and the relative age of the major lithological units, the Kohistan sequence has been subdivided into six series (Bard *et al.*, 1980); the lowermosts are the oldest and grossly the most highly metamorphosed. As shown by the Fig. 1, the lower part of the sequence is cut by a steep northward plunging megashear zone, the so-called MMT (Tahirkheli *et al.*'s (1979) Main Mantle Thrust) which has been interpreted as a major paleosuture in the western Himalayan collided range. The rocks under the overthrust sequence are a complex of slices of metaharzburgites + serpentinites + various ultramafic rocks, high–P (with blueschist facies minerals) metamorphic "tectonic melanges" or Precambrian to Lower Paleozoic metamorphic rocks and orthogneisses which belong to the Indian plate. The northern contact of the Kohistan sequence against the Hindu Kush-Karakorum series is also a major tectonic zone called (Tahirkheli *et al.*, opt. cit. ; Gansser, 1980) the Northern Megashear Zone or the Main Karakorum Thrust (MKT). The Kohistan sequence itself is made up of six major units with an estimated total thickness of approximately 40km. These are, from the apparent base upward (Fig. 5):

1. *The Southern Amphibolite unit.* This includes 6–8km folded and refolded fine- to coarse-grained striped or homogeneous amphibolites, Flaser-gabbros and blastomylonitic amphibolites. The striped-amphibolites are sometimes migmatitic in aspect with *lit par lit* quartzo-feldspathic injections. They are cut off by various folded and/or sheared leucocratic rocks that form a swarm of dioritic-trondhjemitic veins and dykes. Apparently the lower part of the unit encloses two large "patches" of mafic-ultramafic rock (mainly harzburgites, dunites, diopsidites and garnet-spinel diopsidites) surrounded by more or less amphibolitized and/or garnetified metanoritic gneisses (two-pyroxene retrogranulites). These are (Fig. 1) the North Mingora (Bar Bandai) complex in Swat Valley and, over all, the Jijal-Patan complex (Jan, 1977; Jan and Howie, 1981) in Indus Valley.

2. *The Metanoritic (granulitic) unit.* This is a 1–12km thick "belt" mainly composed of pyriclasites which is interpreted to be a grossly homogeneous

stratiform calc-alkaline lopolith now transformed into granulites. The main rock types are mesocratic two-pyroxene ± hornblende granulites cut by coarse-grained poorly deformed (schistosed) hornblende-plagioclase pegmatites. The southern parts of the granulites show intensely developed foliation with isoclinal folding affecting a primary layering (S_o). Sharp contacts between the granulites and lenses of websteritic rocks suggest that the parental intrusives (leucogabbros and/or leuconorites) were injected locally by ultramafic dykes prior to deformation, folding and boudinage. Intensity of deformation seems to decrease northwards (?) and around Chilas (Fig. 1) S_o appears clearly as a prekinematic surface which separates mainly metric to hectometric long pyroxene-rich/plagioclase-rich cumulative layers (Fig. 3). At some localities, the layering is well-developed with sedimentary-like magmatic structures and intramagmatic laminations. Some melanocratic beds are metric thick metadunites and metawebsterites with local extrusive structures throughout neighbouring metatroctolitic, noritic and anorthositic layered rocks. Despite strong annealing, inherited cumulative-like textures are still recognizable (Fig. 3) in the latter rocks when S_o is well exposed.

3. *The Northern Amphibolitic unit* "overlies" the metanoritic unit. The rocks are also heterogeneous striped-amphibolites, probably mainly from basaltic tuffaceous origin, locally interlayered with silico-aluminous, siliceous, calcareous and epidotic lenses. Southeast of Timurgara (Fig. 1), this amphibolite unit grades into the southern amphibolite belt. In this area the granulites seem to pinch out, a feature which may be related to the geometry of their parental rocks (i.e. a wide stratiform noritic intrusive). One of the more striking characteristics of the northern and southern amphibolites is their strongly migmatic aspect adjacent to the granulitic unit. At both the localities, they are coarse-grained amphibolites (from "retrogranulites") or striped heterogeneous amphibolites injected by veinlets of dioritic-leucodioritic leucosomes which may concentrate into weakly-folded and foliated quartz-dioritic bodies.

4. *The Volcano-Sedimentary unit* (Kalam series) overlies conformably or with tectonic contact the northern amphibolite unit. It contains meso- to epimetamorphic metagreywackes, chlorite-schists and phyllites with thick zones of fine-layered metacherts enclosing bands and lenses of calcareous metasediments. Some basic metatuffites and low-grade epidote-amphibolites occur locally together with pillowed metabasalts. In Gilgit district (Fig. 1) this unit is very thick (at least 8–10km) and much more greywacke-rich (with flyschoid patterns). The cherts are not massive but outcrop as centimetric black-grey levels within greywackes containing some marbles. Mesometamorphic conditions transform these rocks into "quartzites", micaschists with or without andalusite and garnet, and calc-silicate gneisses and skarns.

5. *The Calc-alkaline Volcanic unit* (Utror volcanics) occurs above the Kalam sequence, either with intraformational conglomerates, volcanic (andesitic) agglomerates or with andesitic flows. Near Utror village (Fig. 1), the volcanic unit is 5–8km thick and grossly composed of more or less schistose meta-andesitic agglomerates or lavas, metadacites and, towards the top, by rhyodacites with ignim-

britic structures. Syn- to post-kinematic tonalitic, granodioritic and dioritic plutons intrude the volcanics (Majid and Paracha, 1980).

6. *The Upper Detritic sequence* (Yasin group) contains shales, wackes, calcareous beds and some volcanics. It lies unconformably upon the Utror unit and begins with a polygenic conglomerate containing pebbles of Utror volcanics and some dioritic to granophyric rocks. Cretaceous (Aptian) fossils have been found (Rossi-Ronchetti, 1965) near Gilgit within the calcareous lenses of the Yasin group; this proves that the former calc-alkaline volcanics (Utror) and underlying metasediments and some amphibolites are at least Lower Cretaceous.

Another striking feature of the Kohistan is the scarcity of sialic rocks (aside some scarce post-kinematic granitic s. l. intrusions) within 40km thick pile where mafic, ultramafic and calc-alkaline plutonic to volcanic rocks are dominant. As this feature is not normal for cross-section of continental crust or ophiolites, Tahirkheli *et al.* (1979) have suggested that the Kohistan sequence represents the crust of a volcanic island arc showing its 40km deep root as well as its subaerial top. The amphibolitic series would represent the oceanic crust "basement" of this arc (Tahirkheli *et al.*, opt. cit.), but in our opinion this is not obvious and we regard at least parts of these rocks as basaltic lavas and tuffs emplaced in the earlier arc building stages. Evidence for this suggestion is present in Dir and Gilgit districts where thick flyschoid sequences of cherts, phyllites and metagreywackes contain basaltic metatuffs, lavas and pillowed flows. Rather than assuming that the previously described cherts are part of the classical *Fersmann trilogie* of ophiolitic models, they are thought to represent siliceous deposits in a confined basin environment (Steinberg *et al.*, 1977) i.e. in arc basin. The large stratiform and layered metanoritic (granulitic) rocks are interpreted as the deepest levels of the volcanic arc. If this interpretation is correct, the Kohistan sequence indicates that the roots of oceanic island arcs are made up of enormous lopolithic intrusions of layered and differenciated calc-alkaline rocks (e.g. Arculus and Will, 1980) from which andesites, dacites and possibly rhyodacites may have (?) escaped. As suggested by Tahirkheli *et al.* (opt. cit.), the North Mingora, and, in particular, the thick Jijal-Patan complex of harzburgitic rocks, dunites, websterites, diopsidites, pyrigarnites (i.e. garnet-diopsidites), garnetites, hornblendites and plagio-pyrigarnites may not be remnants of the "petrological" upper-mantle and oceanic crust underlying the arc. The field relations as well as the textural and mineralogical evidence presented are better understood when these rocks are considered to be part of metamorphic cumulative rocks which represent either the top of an ascending mantle diapir emplaced during arc formation or the lower (N) part of the noritic pluton the granulitic belt comes from (Fig. 5). This problem will be discussed further.

METAMORPHIC EVOLUTION OF THE KOHISTAN SEQUENCE

Prograde polyphase metamorphism affects the Kohistan sequence. This paper concentrates on the medium and high grade metamorphic rocks which are mainly mafites and ultramafites overlain by siliceous and (rarely) calcareous metasediments and metagreywackes.

Structural and Metamorphic Aspects of the Amphibolite Units.

Striped-amphibolites are the dominant rock-type of the southern and northern amphibolite units but field data indicates that the banding of these rocks has four main origins :

i) it may be an original layering formed during deposition of basaltic-pyroclastics, so that the main components quartz + plagioclase + hornblende ± garnet ± epidote built centimetric upto decimetric layers with various modal compositions.

ii) the layering may have formed by synkinematic metamorphic processes that produced centimetric sharp modal and/or sharp grain-size variations. At some places this may represent either tectonic dismembering of volcano-sedimentary layers or inherited textural patterns in the form of (deformed) basic dykes and/or sills. As shown by Fig. 2, intense shearing along ductile shear zones may also progressively transform, with strong strain gradients, some Flaser-gabbros and/or coarse-grained massive amphibolites (some of them being retrogranulites) into fine-grained striped-blastomylonites containing centimetric rounded plagioclase, garnet and hornblende porphyroclasts. The latter are moulded by the shear zone foliation.

iii) the layering may be related to a metamorphic differentiation process along the foliation planes and to the segregation of mafic/felsic components in centimetric thick layers.

iv) the fourth origin is that the layering may correspond to the emplacement of centimetric/metric thick injections of leucocratic material; in this case the "layers" are fine- to coarse-grained felsic veins and veinlets which cut across, with low angle, the S_1 schistosity exposed by the neighbouring rocks. These veins are currently folded, boudinaged, and tectonically dispersed during a transposing folding phase (Fig. 2).

From these structural patterns and because of the occurrence of numerous "cold" more or less reworked shearing planes and joints, one may infer three main tectonic events to have deformed the Kohistan amphibolites (Fig. 3). The first major tectonic phase (D_1) corresponds to the development of an S_1 regional foliation synchronous with centimetric to decimetric isoclinal folding (vergence perhaps to the south). This phase is contemporaneous with a low to high grade metamorphic regime and the partial melting of the amphibolite units indicating that the temperature reached ≃ 750–850°C. It is noteworthy that no large kilometric scale structures such as large recumbent folds were observed that can be attributed to D_1. In the Indus Valley around Jalkot as well as near Timurgara in Dir district, numerous shear zones developed late in the D_1 phase. These shear zones are marked by strongly foliated blastomylonites. The geometrical relationships between the foliation of the blastomylonites and S_1 in the neighbouring coarse-grained amphibolites, as well as some rotational features exposed by the porpyroclasts (Fig. 2) strongly suggest that at least some of these shear zones have worked with northwards movements during the late D_1 phase or (?) during D_2. After and/or during the emplacement of various leucocratic (sometimes pegmatitic) injections, D_1 structures have been affected by a second event that produced centi-

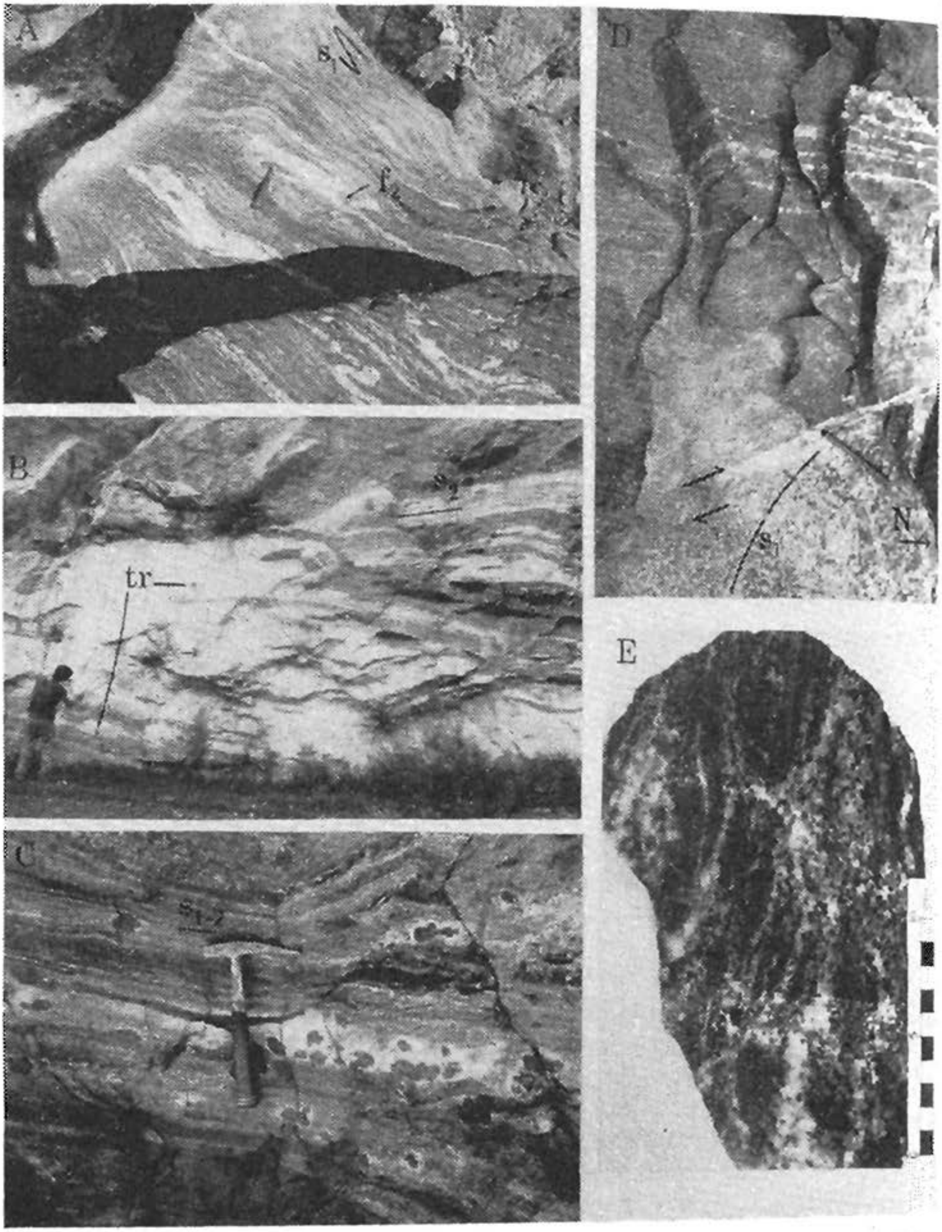

Fig. 2. Field aspects of Kohistan amphibolitic series; A : D_2 isoclinaly folded (f_2) leucocratic injections in epidote amphibolites near Tal, Swat (refolded and transposed surface is S_1); B : pinched and swelled trondhjemitic injections (tr) within striped-amphibolites (felsitic fine bands are precoceous pre-D_2 (S_2) veins) (3km south of Jalkot in Indus Valley); C : striped-amphibilites near Pirkala village (Swat Valley) showing late-S_1 / pre-S_2 garnet megablasts at the expense of amphiboles in coarse grained bands; D : blastomylonitic ductile shear zone, with apparent northwards movements, affecting a coarse-grained amphibolite (Flaser-gabbro) 8km north of Patan (Indus Valley); E : Migmatitic amphibolite "overlying" the granulitic belt north of Chilas (Indus Valley) (leucocratic metatects contain garnets).

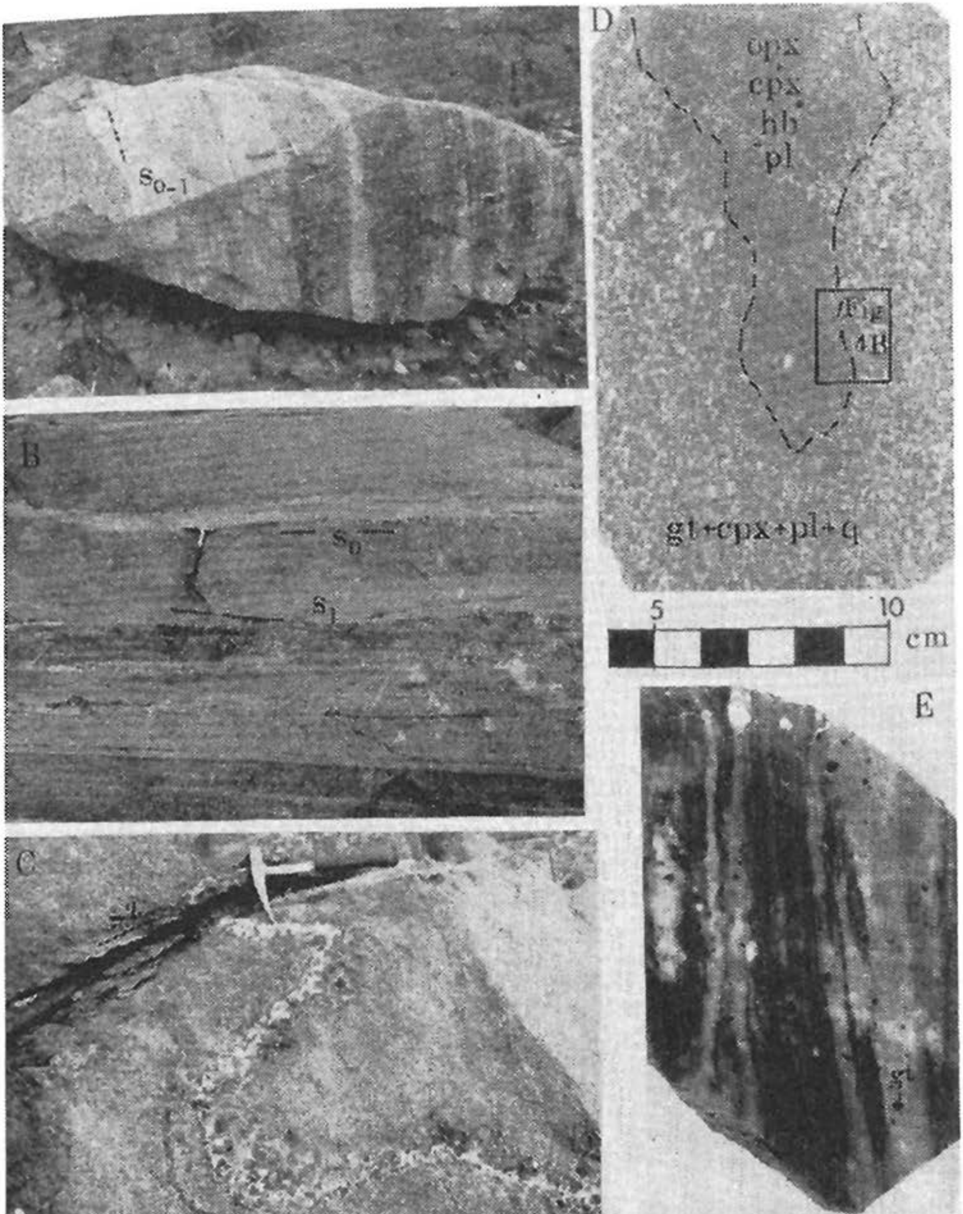

Fig. 3. Field aspects of some granulitic rocks in Kohistan; A : inherited cumulative layering with various inherited relationships between troctolitic, noritic and leuconoritic layers (regional foliation = subparallel S_0 and S_1) (8km east of Chilas in Indus Valley); B : Some outcrops with S_1 slightly oblique to layering (S_0); C : D_2 - fold affecting pegmatoid garnet and garnet-plagioclase veins crosscutting poorly foliated plagiopyrigarnites (SZ : late D_1 pre-D_2 shear zone) (Patan village, Indus Valley); D : patch of inherited hornblende pyriclasite invaded by garnet- blasts giving rise to the overall mass of the Jijal-Patan complex plagiopyrigarnites (500m north of Patan); E): strongly blastomylonitic amphibolites with rounded plagioclase and garnet porphyroclasts (10km north of Patan as well as in Jijal, Indus Valley).

metric to hectometric, more or less open to sub-isoclinal/isolinal folds. A second schistosity (S_2) is closely associated with D_2 (Fig. 2). Flattening, rotation and truncation of syn- to late D_1 porphyroblasts can be seen to be clearly related to D_2 at some localities. Around Timurgara, Tal, Fathehpur, Jalkot and Patan, numerous D_2 folds show apparent northwards vergence with "Z" aspects. D_2 would be contemporaneous with the first collisional stages affecting the northern Pakistan Himalayas according to Tahirkheli *et al.*'s (1979) model. The northward vergence poses the same problems as does the evidence for northwards movements along the late D_1 ductile shear zones. The very late structures (D_3) in the amphibolite units and neighbouring rocks are mainly sets of conjugate joints and microstrike-slip faults. Inverse faults north of Dir and NE–SW (wrench ?) fault near Alpurai-Jalkot may be syn-D_3. Epidote-amphibolite to greenschist facies retrogressions occur at the expense of the amphibolite and granulite units along and nearby these fractures.

Regarding the metamorphic patterns of the amphibolite units, no very spectacular changes occur within the ± 15km thick sequences during D_1 (and D_2). The less metamorphosed rocks show transitional greenschist to epidote-amphibolite facies and sub-facies associations. The latter develop within the A*h* zone of Fig. 5, with the quartz bearing assemblages :

(1a) Plagioclase An5–15 + chlorite + actinolite or blue-green Ca-amphibole + clinozoisite/pistacite + sphene + ilmenite/sulfides.

(1b) Plagioclase An5–15 + chlorite + biotite + white mica + blue-green Ca-amphibole + clinozoisite/pistacite + sphene + ilmenite/sufides.

The first prograde syn-D_1 steps are the appearance of garnet together with greenish hornblende + clinozoisite + andesitic plagioclase ± quartz. This would correspond to the garnet-amphibolite facies "in" conditions (Winkler, 1967) and the amphibolites show the association of the B*h* zone, i.e. :

(2a) Quartz + plagioclase An25–35 + green hornblende + clinozoisite + garnet + sphene and/or rutile + ilmenite + sulfides.

(2b) Quartz + plagioclase An25–35 + green hornblende + clinozoisite/pistacite + sphene and/or rutile + ilmenite + sulfides.

(2c) Quartz + plagioclase An25–35 + greenish hornblende + biotite + clinozoisite/pictacite + sphene/rutile ± white mica + ores.

Assuming that the colour changes of the Ca-amphiboles from mafic rocks are related to prograde processes (Miyashiro, 1972), it is suggested that the brownish/greenish-brown tint of the hornblende from some amphibolite presenting sometimes partial melting patterns, would allow to draw a high grade C*h* zone in the Kohistan pile. Although the accurate boundaries of this zone are not well established because either greenish or brownish-green hornblendes may occur in alternating beds in the studied rock, it is apparent from exposures that the C*h* zone develops (Fig. 5) towards the lowermost part of the Kohistan sequence and also towards the granulitic belt and the north Mingora/Jijal-Patan ultramafic complexes.

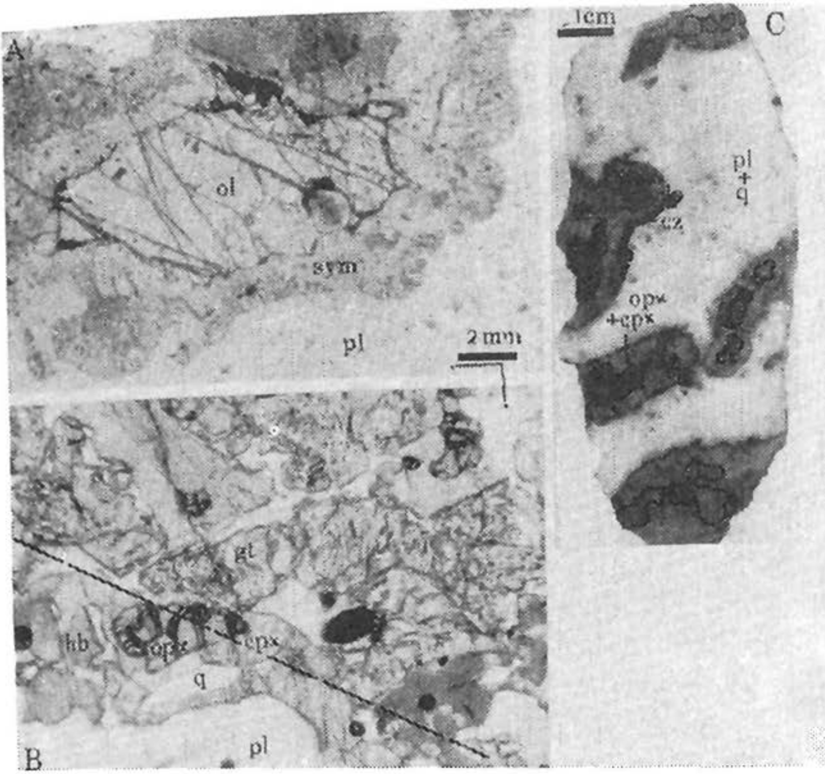

Fig. 4. Some reactional textures in the granulitic rocks; A : coronitic rims of opx + (cpx + spinel) vermicular symplectite + (Mg-pargasitic hb + spinel vermicular symplectite around relictual olivine Fo_{80}) in a metatroctolitic layer 8km west of Chilas (Indus Valley); B : microscopic relationships between hb-opx-cpx pyriclasites and garnet cpx plagiopyrigarnite in the sample from Fig. 3D; C : Coarse-grained plagiopyrigarnite with coronitic rims of gt + sp ± clinozoisite around relictual opx + cpx (and ? olivine) (Duber Stream, Indus Valley; Jan's collection with courtesy).

The mineralogical associations are similar to the B*h* zone except within some coarse-grained more or less strongly foliated and sheared amphibolites from altered pyriclasites; in these rocks relict opx and cpx are rimmed by zoned greenish-brown hornblende (frequently cloudy in aspects) and/or anthophyllite. Within all these rocks, the relations between crystallization and deformation sometimes allow to discriminate the D_1 and D_2 mineralogical assemblages (see Table 8). This is not always the situation and if such features like the late growth of some pistacite or zoisite, chlorite, clear albite rims around plagioclase, sphene (armouring rutile), blue-green fringes around greenish/greenish-brown hornblende, etc., have been related to late D_2, it is not certain that this is the correct relative age. Epidotes related to the late D_1 metamorphic stage are clear more or less zoned blasts frequently exposed as quartz-clinozoisite symplectites with cauliflower aspects. Garnet phenoblasts with diameters sometimes upto 10cm develop preferentially within hornblende-poor/plagioclase-rich layers or veinlets. This is not a rule and mafic

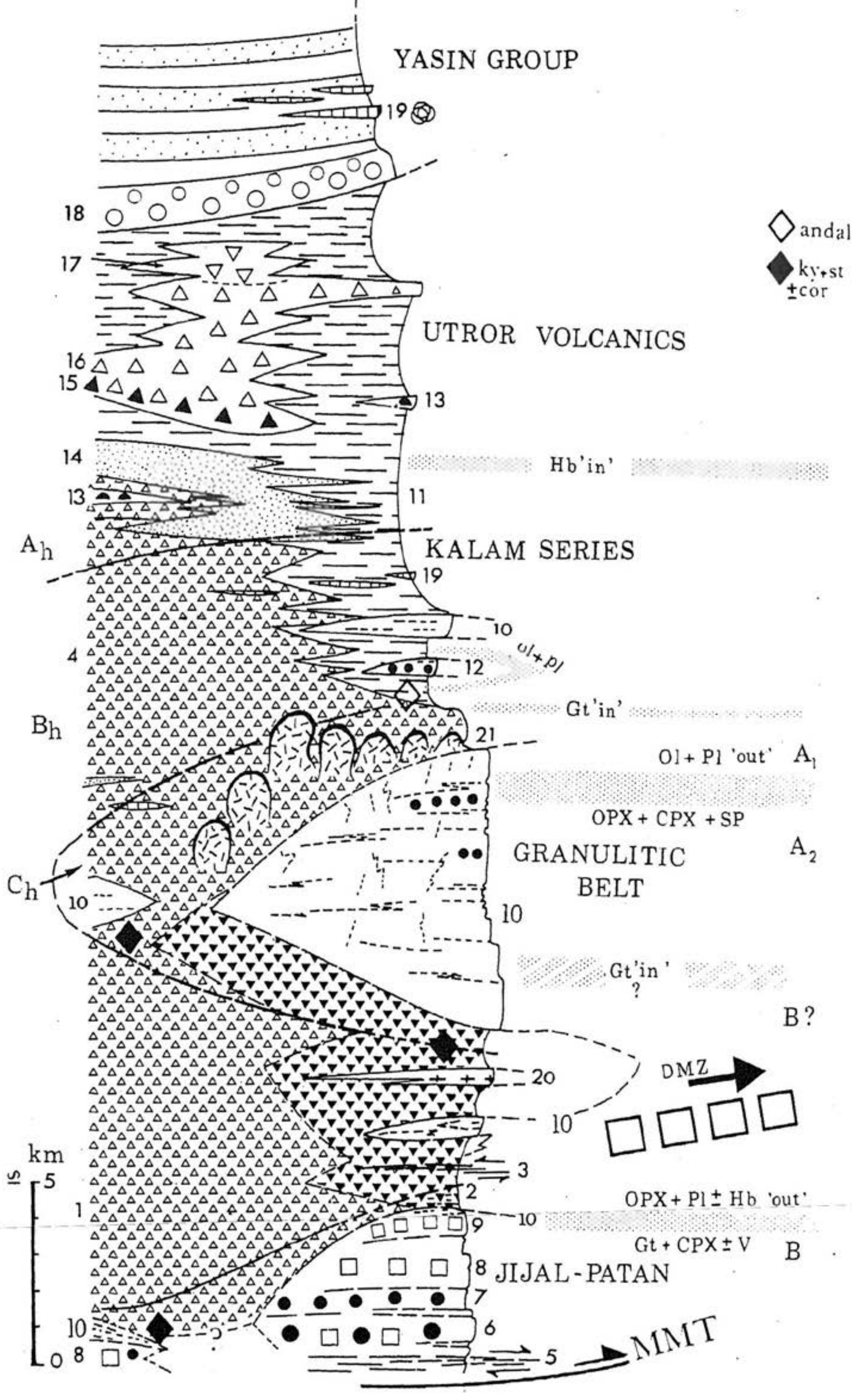
YASIN GROUP
19
18
17
andal
ky+st
±cor
UTROR VOLCANICS
16
15
13
14
Hb'in'
13
11
A_h
KALAM SERIES
19
10
4
ol+pl
12
Gt'in'
B_h
21
Ol + Pl 'out'
A_1
OPX + CPX + SP
GRANULITIC
BELT
A_2
C_h
10
10
Gt'in'
?
B?
20
DMZ
10
km
5
3
2
OPX + Pl ± Hb 'out'
1
10
9
Gt + CPX ± V
B
8
JIJAL-PATAN
7
10
6
0
8
5
MMT

hornblende-rich levels also contain automorphic garnets embaying helicitic inclusions of quartz ± clinozoisite ± hornblende ± sphene ± rutile. Flattening of the matrix around rotating garnets is related to D_2; in this case the garnets are corroded and rimmed by a polycrystalline corona of quartz + plagioclase ± green hornblende ± clinozoisite suggesting reactional processes such as the retrogression of eclogites (Vogel, 1967; Engels, 1972; Lasnier, 1977). Leucocratic halos around some garnets in leucosome metatects from zone *Ch* suggest that the blastesis of the garnets was associated with Fe-Mg mass transfers towards the garnets nuclei (Fig. 2C). Rutile seems to become more abundant in the zone *Ch* and *Bh*. It is either alone, rimming ilmenite grains, or associated with sphene and/or mantling the latter.

The previously described folded and foliated (D_2) leucocratic dykes and sills which intrude the striped and massive amphibolites are leucodioritic-leucotrondhjemitic aplites, pegmatites and coarse-grained quartz-diorites. These are older in emplacement than late D_2 heterogeneous late-kinematic dioritic-tonalitic melts, possibly related to the partial anatexis of the amphibolite units. The former leucocratic injections are quartz-plagioclase (An_{20}-An_{40})-rich rocks with more or less subordinate pale-green/green hornblende ± biotite ± garnet ± clinozoisite ± white mica ± sphene ± rutile + apatite + sulfides. A critical paragenesis sometimes develops in the pegmatitic injections ; it is :

(3) Quartz + plagioclase An30–35 + clinozoisite + kyanite + staurolite + paragonite + rutile + chlorite + green hornblende + apatite.

In these pegmatitic veins, the clinozoisite forms large euhedral crystals enclosing kyanite (mainly towards its borders), paragonite (Table 6), chlorite and cloudy plagioclase. The quartz-plagioclase annealed matrix contains scarce staurolite poikiloblasts, white mica, fine tabular kyanite (or sillimanite ?) and hornblende grains; the latter amphibole is optically similar to the amphibole of the clinozoisite-hornblende ± garnet bearing neighbouring amphibolites. This significant

---

Fig. 5. The Kohistan sequence; 1 : southern striped amphibolites; 2 : coarse-grained metagabbros and amphibolites with blastomylonites in ductile (northwards) shear zones (3); 4 : northern striped amphibolites and amphibolitic schists; 5 : blastomylonites near the MMT paleosuture; 6 : ultramafics (metaharzburgites, websterites, dunites, pyroxenites); 7 : dunites and diopsidites; 8 : pyrigarnites (garnet-diopsidites and garnetites); 9 : plagiopyrigarnites; 10 : pyriclasites + amphiclasites + metatroctolites and meta, dunites from the layered calc-alkaline lopolith; 11 : shales and metagreywackes; 12 : coarse grained metagabbros and associated layered dunites and pyroxenites; 13 : pillowed metabasalts; 14 : metacherts with alternating wackes and shales; 15 : andesitic agglomerates with granophyric pebbles; 16 : andesites; 17 : dacites with local ignimbritic aspects; 18 : unconformable massive heterogeneous conglomerates and breccias (mainly volcanics and dioritic blocks and pebbles); 19 : marbles calc-silicate bearing gneisses and skarns; 20 : dioritic-trondhjemitic deformed injections (Jalkot type); 21 : foliated heterogeneous late-anatectic diorites (late-to post-kinematic intrusives are not shown); DMZ : ductile megashear zone; Ah : "chlorite + epidote" zone; Bh : "blue-green Ca-amphibole + epidote" zone; Ch : "garnet + green/greenish brown hornblende ± clinozoisite" zone (including incipient anatexis of "wet" mafic rocks); A_1 : low grade olivine + plagioclase bearing granulites; A_2 : two-pyroxene granulites; **B** : garnet - cpx (granulites note the two "garnet-in isograds" i.e. within the amphibolitic rocks and within the granulites).

assemblage will be discussed further together with staurolite ± kyanite ± corundum ± garnet ± clinozoisite associations from late-D_1 veinlets and patches which develop in coarse-grained amphibolitized gabbroic rocks near Timurgara (Jan and Kempe, 1973) and Bar Bandai (north Mingora ultramafic-granulitic complex).

Structural and Metamorphic Aspects of the Metanoritic (Granulite) Unit.

The granulitic rocks of Kohistan are either massive and homogeneous rocks or strongly foliated and layered gneisses separated from the amphibolites by a transitional zone of either retrogranulites or some discontinuous inclusions of partially "degranulitized" rocks enclosed within coarse-grained amphibolites (Jan, 1982). The layering (S_0) when compositional, appears clearly to be an inherited feature from a magmatic cumulative process. Good examples are exposed around Chilas and along the Indus river (Fig. 4). Centimetric up to plurimetric layers of leuconoritic, noritic, troctolitic, (scarce) websteritic and dunitic rocks may alternate either with gradational (graded-bedding like) or sharp contacts. In this second situation, the structural relationships between the layers may reflect dynamic features during the magmatic "deposition" of the layers. The foliation (S_1) of the granulitic rocks is broadly sub-parallel to the S_0 layering and has the same attitude as the regional foliation of the neighbouring amphibolite units. In the homogeneous granulites further evidence of magmatic origin is given by dispersed enclaves of mafic-ultramafic rocks. In some cases it is possible that some "inclusions" may represent dismembered layers or dykes along S_1. As shown by Fig. 4, syn-S_1 folding and boudinage are obvious. Textural evidence suggests that except for some relict olivine in reaction coronas from metatroctolites, primary (magmatic) minerals have completely disappeared.

All the granulites have suffered a strong annealing before or during the emplacement of coarse-grained hornblende-plagioclase pegmatites and before their static or dynamic alteration under the amphibolite to the greenschist facies conditions. The D_2 deformation is not evident except near the borders of the noritic unit where an S_2 schistosity sometimes cut S_1/S_0. D_2 is mainly associated with the "degranulitization" (strong amphibolitization) but this process probably continues further during the formation of sets of conjugate shearing planes linked to North-South compressive constraints. With grade increasing toward the base of the Kohistan sequence, syn-D_1 metamorphism in the granulites is marked by the incipient blastesis of late-D_1 to post-D_1 garnet in leucocratic, sometimes pegmatitic, veinlets. South of the main metanorite unit (Fig. 1 and 5) some lenses and bands of garnet-pyriclasites/amphiclasites which outcrop above the Jijal-Patan complex, show relict opx ± cpx ± greenish-brown hornblende and local reemplacement of these phases by coronas of garnet ± clinozoisite + green spinel or by garnet ± cpx ± zoisite ± clinozoisite ± rutile. These features suggest (Jan, 1977) that a garnet "in" – opx "out" zone may cut across the granulites towards the lowermost part of the Kohistan sequence and may separate two main metamorphic zones A and B within the granulitic rocks, i.e. (Fig. 5) :

a) an *Upper Zone* "A" where the most common rocks are pyriclasites with the association :

(4a) Plagioclase An40–55 + opx + pale-green or brownish-green hornblende± quartz + biotite + ore + apatite ± K-fel.

Around Chilas the well exposed stratiform metadunitic, websteritic, troctolitic, cumulates respectively show :

(4b) Olivine Fo_{80} + opx ± pale-brown/pale-green hornblende ± ores.

(4c) Cpx + opx ± pale-brown/greenish-brown hornblende ± ores.

(4d) Plagioclase An40–60 + cpx + opx + relict olivine (Fo_{80}) + pale-green hornblende ± green spinel + apatite + ores ± biotite + quartz.

In the case of association (4c) the textural evidences obviously suggest that the olivine is a relict phase of magmatic origin rimmed by the coronitic assemblages cpx + opx + spinel and amphibole + spinel. In agreement with the crystal chemistry affinities of the opx + cpx pairs (Jan and Howie, 1980; the present data next pages), this places the reactional destruction of the plagioclase-olivine-bearing metatroctolites as a metamorphic process of the kind (Fig. 6) :

Olivine + anorthite + H_2O ⇄ opx + cpx ± Mg-pargasite
+ vermicular symplectitic green spinel.

This reaction is critical and may separate (Fig. 5) the zone A granulites into an upper sub-zone A_1 where olivine + plagioclase would be stable and a lower (more) metamorphic sub-zone A_2 where these phases are unstable in rocks with similar bulk-chemistry.

b) a *Lower Zone* "B" with garnet-bearing pyriclasites and amphiclasites and the common assemblages :

(5a) Quartz + plagioclase An40–50 + cpx + opx ± brownish-green/pale/green hornblende ± biotite + ores.

(5b) Quartz + plagioclase An40–50 + cpx + opx ± brownish-green hornblende + clinozoisite + zoisite + K-fel ± scapolite.

(5c) Quartz + plagioclase An35–45 + garnet + cpx + greenish-brown/green hornblende (+ relict opx) + clinozoisite + rutile + ores.

The association (5c) suggests the appearance of garnet + quartz at the expense of earlier opx ± hornblende. This association is sporadic within the uppermost part of the zone B and the garnet growth is not clearly related to a sharp garnet "in" isograd in the granulite unit. The abundance of garnet seems to increase rapidly towards the lowermost part of the Kohistan pile when entering the Jijal-Patan complex. This is marked by the development of a network of fracture-like (jointing) planes along which numerous pinkish garnet grows and invades (Fig. 6) the surrounding pyriclasites/amphiclasites. These features are quite similar to those described by Blattner (1976) in New Zealand granulites. As in this area, some leucocratic and pegmatitic veins and veinlets containing garnet megablasts (Fig. 4) as well as some garnet-rich enfilled cracks and fractures are associated with the latter network. These veins are late-D_1 : they cut across the "garnetified"

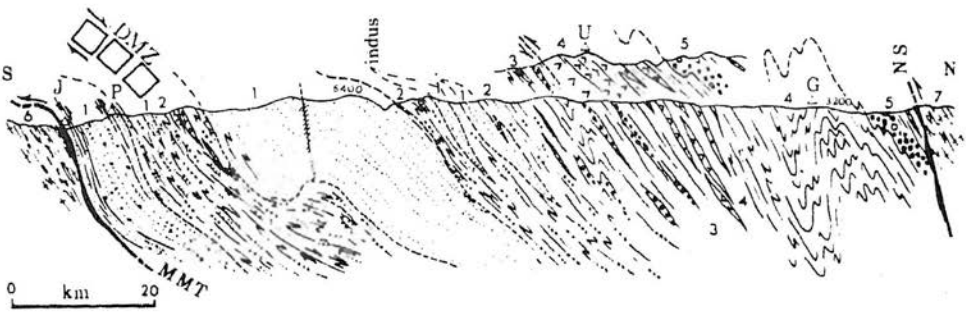

Fig. 6. Simplified cross-section of the Kohistan from Jijal (J) to Gilgit (G). 1 : layered metaplutonic rocks i.e. the Jijal-Patan (P) complex, the main granulitic belt and some associated small lopoliths; 2 : undifferenciated amphibolitic series; 2 : Kalam metasediments (greywackes, shales, cherts and marbles) with pillowed metabasalts; 4 : Utror (U) calc-alkaline volcanics (mainly andesites) and associated metasediments (greywackes and shales); 5 : Yasin sedimentary group (Mid-Cretaceous) with basal conglomerates; 6 : Indian plate metamorphics; 7 : Asia metamorphics; MMT : Main Mantle Thrust; NS : Northern Suture (for simplicity, the numerous syn- to late D_2 dioritic intrusives (see map, Fig. 1) have not been drawn); DMZ : possible ductile late D_1 megashear zone.

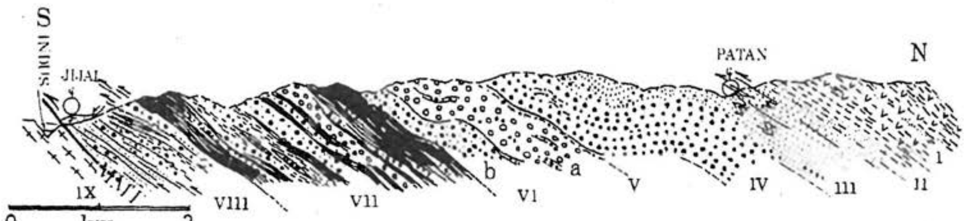

Fig. 7. The Jijal-Patan cross-section (explanation in the text) along the Karakorum Highway (DMZ : possible ductile late D_1 megashear zone).

pyriclasites/amphiclasites of the uppermost Jijal-Patan rocks and similar veinlets are found in the lowermost parts of the granulitic belt (Fig. 5). K-feldspar in zone B pyriclasites is scarce and develops lately as myrmekitic intergrowths at quartz-(antiperthitic) plagioclase contacts. Some scapolite with optical properties of mizzonitic wernerites are present in some samples; these scapolites are anhedral annealed phases in apparent textural equilibrium with the surrounding minerals.

The Ultramafic-Mafic Complexes of Jijal-Patan and North Mingora (Bar Bandai).

South of Patan and north of Mingora (Fig. 1, 5), the deepest parts of the southern amphibolite unit are separated from the MMT paleosuture by mafic-ultramafic rocks which comprise the Jijal-Patan complex in the Indus Valley and some outcrops north of Mingora (Bar Bandai) in the Swat Valley. The Jijal-Patan complex is an extraordinary formation of garnet-granulites and ultramafites (Jan and Howie, 1981). A detailed cross-section (Fig. 7) along the Karakorum Highway shows that this complex is made up of the following main levels, from the top to the apparent base :

i) coarse-grained amphibolites, retropyriclasites, basic blastomylonites and retrogranulites;

ii) more or less "garnetified" pyriclasites and amphiclasites;

iii) sheared garnet-bearing hornblendites and more commonly 0.5 to 1km thick homogenous or striped and sheared plagiopyrigarnites (plagioclase + garnet + pyroxenes bearing granulites) with flat late-D_1 and/or syn-D_2 blastomylonitic to cataclastic shear zones. These are cut across by a late to post-D_1 swarm of folded (D_2) decimetric/metric thick garnet-bearing leucocratic sometimes pegmatitic dykes and/or coarse-grained garnet-rich veinlets and cracks. The latter locally contain garnet megablasts rimmed by quartz + plagioclase ± clinozoisite corona;

iv) massive bands of pyrigarnites (≃ 1.5km thick) grading upwards to the former plagiopyrigarnites either with progressive contacts or as metric-hectometric enclave-like inclusions within the plagiopyrigarnites. These inclusions seem tectonically dispersed layers of homogeneous plagioclase-free pyrigarnites. Downwards the latter enclose some decametric levels of plagiopyrigarnites and grade to grossly layered massive garnetites, diopsidites and, mainly, coarse-grained pyrigarnites (garnet-diopsidites);

v) foliated hornblendites and garnet-bearing hornblendites (≃ 200m);

vi) thick series (≃ 3km) of a grossly layered dunites and (b) garnet-free clinopyroxenites (diopsidites); in the dunites a primary foliation marked by chromite layers and elongated cpx patches is cut across by disrupted sub-parallel centimetric thick vermicules and layers of coarse-grained Cr-Cpx. Chromite bands and cpx patches are sometimes affected by centimetric to metric isoclinal intrafoliation (D_1) microfolds (Fig. 6). The diopsidites also show a layering drawn by grain size variations and thin chromite-rich bands. Deformed, squeezed dykes of plagioclase + hornblende + clinozoisite ± garnet pegmatoids as well as a system of sub-parallel Cr-Cpx enfilled fractures cut across the clinopyroxenite foliation;

vii) thick layered alternating series (≃ 2-3km) of foliated chromiferous harzburgitic rocks, dunites and clinopyroxenites cut by Cr-diopside pyroxenites bands and websteritic dykes. Some blastomylonitic flat shear zones similar to those described within the amphibolite units (but with southwards displacements) occur within the clinopyroxenites. This late to syn-(?)D_2 feature increases towards the apparent bottom of the series i.e. towards the MMT suture zone;

viii) layered foliated pyroxenites, pyrigarnites and websterites (≃ 1000m) with numerous "levels" of mafic blastomylonites containing porpyroclasts of garnet, hornblende, opx, cpx and some plagioclase; these rocks are strongly sheared garnet-amphibolites, pyrigarnites and plagiopyrigarnites;

ix) MMT suture at Jijal village and Indian sialic metamorphites (mainly gneissic and granitic rocks).

Petrographical characters of these various units may be summarized as follow :

Level ii) are retrogressive pyriclasites with relictual cpx and opx embayed within green zoned hornblende or colorless to pale-green actinolitic amphibole. The common associations are :

(6a) Quartz + plagioclase An45−55 + opx + brownish-green (pargasitic) hornblende ± greenish hornblende ± actinolite ± biotite + ores + apatite + rutile or sphene + paragonitic mica + clinozoisite (+late chlorite + calcite).

The felsic garnet-bearing patches and veinlets which occur at place within these retropyriclasites show the assemblage :

(6b) Quartz + plagioclase An30−40 + garnet + clinozoisite + rutile or sphene ± white mica ± biotite (+ sec. chlorite).

As previously said, these retropyriclasites are crosscut by a network of joints "enfilled" by garnet, diopsidic cpx and late greenish blue hornblende + clinozoisite (in symplectitic cauliflower intergrowths with vermicular quartz) and rutile. The development of these minerals is related to an overprinting metamorphic stage and as will be discussed below, the crystallization of garnet ± clinozoisite ± quartz ± hornblende 2 during this second, at least late–D_1 event, is mainly at the expense of the association opx + hornblende ± (?) cpx 1 + An-member of the plagioclase from the pyriclasites/amphiclasites formed during earlier high-pressure reactions. This is supported by the growth of polycrystalline garnet ± cpx ± rutile aggregates mimetic after opx ± hornblende aggregates and by the late intergrowths of quartz + hornblende ± clinozoisite and cpx + clinozoisite symplectites.

The level iii) are striped massive or foliated plagiopyrigarnites in alternating, sometimes strongly sheared, coarse to fine-grained "layers". Field aspects of these plagiopyrigarnites are similar to the two-pyroxenes pyriclasites and despite different metamorphic grade, it is suggested that both rock-types may have the same parental (dioritic/noritic) magmatic origin. The common mineralogical association is :

(6c) Quartz + plagioclase An45−55 + garnet + cpx ± clinozoisite ± greenish-brown/green hornblende + rutile and/or sphene ± ores + apatite.

The plagioclase is always quite cloudy and pseudomorphosed by zoisite/clinozoisite ± sericite ± calcite. The diopsidic cpx forms oblong, locally granulated, aggregates or monoblasts grossly oriented within the mesoscopic foliation. As the other components, plagioclase has recrystallized during a strong annealing process and formed symplectitic tabular exsolution-like intergrowths with clinozoisite. The garnets are either enclosed as little sub-automorphic grains within the cpx or as aggregates or chains of euhedral/sub-euhedral grains which contain rutile, quartz, hornblende and clinozoisite. They are sometimes broken and show rims, cracks and fractures enfilled by late clinozoisite ± quartz ± chlorite. Clinozoisite forms either cauliflower-like symplectites with quartz vermicules of large poikiloblasts enclosing plagioclase, garnet and cpx. Hornblende is often poorly zoned with pale-brownish-green to greenish-blue tints. Rutile is found as coarse grains or needles; it occurs within the garnet and cpx porphyroblasts or within the quartz—plagioclase—clinozoisite matrix. This mineral is sometimes rimmed by sphene and, as this latter, it may armour ilmenite grains. Paragonitic white mica forms patches together with chlorite ± clinozoisite/pistacite. Some flat centimetric to metric thick, blastomylonitic shear zones containing relict cpx and/or garnet porphyroclasts cut through, with low angles, the plagiopyrigarnites and show southwards displacements. These blastomylonites are post D_1 and anterior to the emplacement of plagioclase-garnet bearing veins which have been in turn folded by D_2 (fig. 3).

The levels iv) and v) are mainly plagioclase-free pyrigarnites with a few garnet-hornblendites, plagioamphigarnites and garnet-hornblende pegmatites. The main rock-types are coarse-grained garnet-diopsidites grading either to garnetites or to diopsidite bands. Textures of these pyrigarnites are heterogranular interlobated with frequent triple junctions. Some of these rocks are porphyroclastic with mortar-like aspects. Garnets sometimes grow at triple "points" and tend to form mono- to polycrystalline aggregates with chains hobits; they are locally fractured and the cracks contain clinozoisite ± chlorite ± rutile ± quartz. Diopsidic cpx with Schiller's inclusions are anhedral and locally rimmed by a thin corona of white mica and/or blue-green Ca-amphibole needles. They are currently megaclasts welded by polygonized anhedral annealed cpx microblasts. Some lithofacies contain a pale brown to green hornblende; this phase is interstitial but in apparent textural equilibrium with the cpx and the garnet. Common assemblages are :

(7) Diopside ± pale brown or green hornblende + ores (± chlorite ±pistacite). ± pistacite).

(7′) Diopside ± garnet ± pale brown/green hornblende+rutile+ores.

(7″) Garnet ± pale brown-green hornblende + ores ± rutile (+ actinolite ± epidote ± quartz).

Level vi) rocks are grossly layered medium to coarse-grained ultramafites ranging from serpentinized chromite-bearing harzburgites to dunites and diopsidites with some hornblende-diopsidites and ± green spinel ± hornblende pyroxenites and websterites. Inherited textures of the harzburgitic rocks are mainly interlobated to porphyroclastic. The dunites and diopsidites show similar patterns; olivine or diopside grains have currently smooth curved boundaries except when noticeable tectonic overprints have produced mortar-like textures followed by partial annealing. Chromite within all these rocks is interstitial or it forms thin "beds". The websteritic rocks are generally porphyroclastic with abraded and/or kinked pyroxenes surrounded by fine polygonal grains of annealed pyroxenes. Green spinel and ores are interstitial or apparently enclosed as vermicules within the diopsidic pyroxenes. Scarce pale-brown to pale-green hornblende is not obviously late and seems in textural equilibrium with the pyroxene and/or the olivine. Blastomylonitic shear zones cut across with low angle the regional foliation of these ultramafites; this led to the development of various heterogranular granoblastic eyed textures with relict clasts of pyroxene pinched by a fine-grained foliated matrix of pyroxene. The main mineralogical associations in the ultramafites are :

(8) (Olivine Fo_{92-89}) ± (opx) ± cpx ± pale-brown hornblende ± serpentine ± chlorite ± tremolite ± ores (chromite + magnetite).

(8′) (Olivine Fo_{90-92}) + pale-brown hornblende± chromite + (serpentine ± chlorite).

(8″) Diopside ± pale-brown hornblende ± chromite ± (chlorite ± calcite ± clinozoisite ± quartz).

(8‴) Diopside + opx ± green spinel ± pale-brown/green hornblende ± ores ± apatite.

North Mingora (Bar Bandai) ultramafites. In Swat Valley, north of Mingora town and near Bar Bandai a 2km thick heterogeneous complex of mafic-ultramafic rocks outcrops "under" rocks of the southern amphibolite unit. Because of discontinuities in the exposure and strong post D_1-retrogression, the cross-section of this complex does not have the quality of the Jijal-Patan outcrops; one may observe however the following rocks, from apparent top to base :

i) striped garnet-amphibolites with numerous garnet-bearing felsitic injections and garnet enfilled cracks.

ii) coarse to fine-grained "retropyriclasites" (≃ 1.5km).

iii) various ± garnet ± zoisite ± spinel ± hornblende clinopyroxenites enclosing lenses of serpentinites and intruded by pegmatoid hornblendites and some plagioclase-rich veins (200m); numerous shear zones affect the latter rocks transforming them into blastomylonitic gneisses.

The retropyriclasites of level ii) are similar to those which outcrop towards the top of the Jijal-Patan complex. The retrogression of the pyriclasites into fine-grained foliated amphibolites is quite complete and relict opx and cpx occur as corroded inclusions within patches of blue-green cloudy and spongy hornblende porphyroblasts or within late polycrystalline aggregates of chlorite + actinolite. Some brownish hornblende relicts suggest the parental pyriclasites also cotained high-grade Ca-amphiboles. The blastesis of the greenish amphibole is contemporaneous with clinozoisite and both minerals show symplectitic intergrowths with quartz. The plagioclases are cloudy and altered into patches of white mica ± calcite ± zoisite ± clinozoisite. Rutile is scarce but sphene is common, sometimes armouring ilmenite and/or rutile grains.

The level iii) corresponds to a perhaps crudely layered (?) ultramafic complex of possible cumulative origin. The plagioclase-free parental rocks are meta-websterites with mainly pale hornblende + green-dark cloudy spinel + clinozoisite + chlorite + actinolite + white mica + rutile/sphene. Some chlorite + paragonite + clinozoisite pods contain polycrystalline poikiloblasts of garnet or kyanite ±

staurolite and staurolite ± corundum; they occur in places in coarse-grained amphibolitized clinozoisite-metaclinopyroxenites. The garnets enclose grains of rutile + quartz + bluish-green hornblende. Green aluminous spinels develop in some metapyroxenites as early (relict) minerals with two textural aspects. These are either intercumulus-like grains which are rimmed by a corona of quartz + clinozoisite surrounded by chlorite, or vermicular (symplectitic) intergrowths within cpx ± a pale-green hornblende. The latter habit is similar to the aspect of spinel in the coronas which armour relictual olivine in the Indus Valley layered (cumulative) troctolites. Olivine-bearing ultramafites have been described (Jan and Kempe, 1973) in Bar Bandai area but apart from some serpentinite lenses (metadunitic) enclosed within spinel-metaclinopyroxenites, no fresh olivine-bearing rocks have been found in this outcrop (see also Ahmed, 1977).

MINERALOGY

As a basis for an attempt to determine the P, T history of the obducted Kohistan island arc, mineralogical data that complements those published by Jan (1977) and Jan and Howie (1980, 1981, 1982) are presented here.

Pyroxenes

Twenty-three Ca-rich and thirty Ca-poor pyroxenes from different rocks have been analysed (Tab. 1 & 2) in the Jijal-Patan complex (websterites, diopsidites, pyrigarnites, plagiopyrigarnites), the granulite unit (pyriclasites, dunites and troctolites), one retrogranulite and one opx-garnet gneiss bordering the top of the granulitic belt. This, with Jan and Howie's (opt. cit.) data, covers most rock-types from the lowermost to the middle part of the Kohistan sequence.

Clinopyroxenes

Several comments can be made about the Ca-Fe^T-Mg ratios of the analyzed cpx (Fig. 8) :

i) In agreement with Jan and Howie the pyrigarnites and the plagiopyrigarnites cpx are mainly diopsidic to salitic, whereas those from the garnet-free Jijal-Patan websterites and clinopyroxenites are Mg-rich diopsides locally Cr-bearing.

ii) The cpx from the layered (metanoritic) granulitic belt are salites or sub-augites in two pyroxene pyriclasites and troctolites but diopsides in webste-ritic metacumulates. In the plagioclase-bearing rocks the plagiopyrigarnites-cpx are richer in Mg than the pyriclasites-cpx; they differ from the latter by their relatively higher Ca contents. On the other hand, the Na contents of the analyzed cpx are lower than those of eclogitic clinopyroxenes and rather similar to the granulitic cpx. From Fig. 9 it seems the bulk compositions broadly control the Al_2O_3 and Na_2O contents of the cpx with the following patterns :

a) The cpx from the plagiopyrigarnites (together with some data from Jan

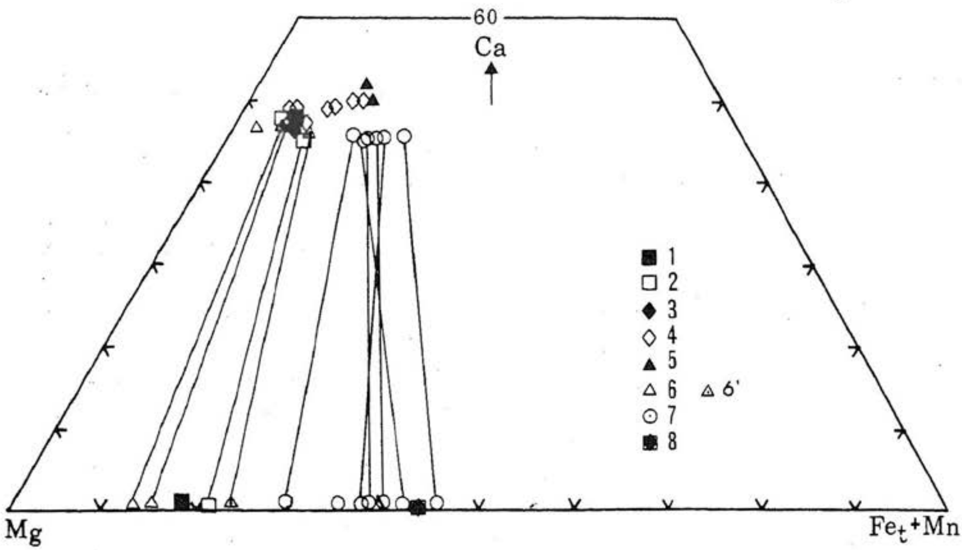

Fig. 8. Plots of the Kohistan cpx and opx (granulitic belt and Jijal-Patan complex) on the Ca-Mg-Fe^T triangle (mol. prop.); 1 : dunitic metacumulates; 2 : metatroctolites; 3 : metaclinopyroxenites; 4 : pyrigarnites; 5 : plagiopyrigarnites; 6 : metawebsterites; 6′ : two-pyroxene spinel pyroxenite; 7 : pyriclasites; 8 : garnet opx-biotite gneiss (tie-lines for coexisting pyroxenes).

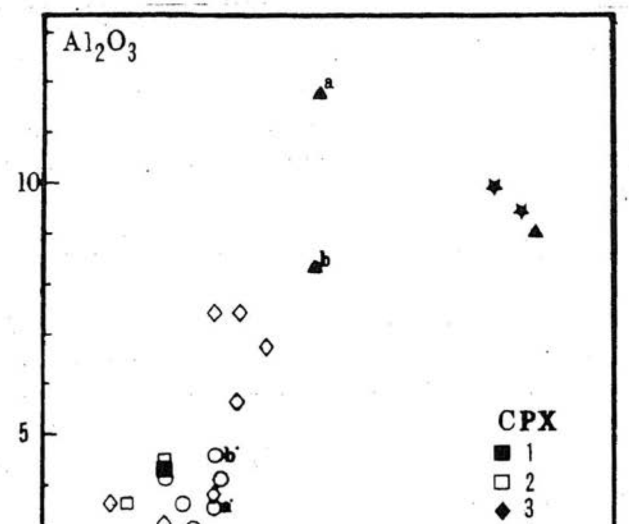

Fig. 9. Al_2O_3 versus Na_2O (weight %) in the Kohistan cpx from the granulitic belt and the Jijal-Patan complex. 1 : metadunites; 2 : metatroctolites; 3 : metaclinopyroxenites; 4 : pyrigarnites; 5 : plagiopyrigarnites; 6 : metawebsterites; 7 : pyriclasites; 9 : plagiopyrigarnites (SI 290 and SI 238 from Jan and Howie, 1981).

(1977)) plot within Al_2O_3 /Na_2O-rich field with $8.5 < Al_2O_3 < 12.0$ and $1.0 < Na_2O < 2.0$.

b) The cpx from the websterites and clinopyroxenites are the poorest in Al_2O_3 and Na_2O with $0.9 < Al_2O_3 < 1.5$ and $0.05 < Na_2O < 0.2$.

c) The cpx in the dunites, troctolites, pyriclasites, and pyrigarnites form an intermediate group with positively correlated Na_2O and Al_2O_3 contents.

The fact that Na_2O and Al_2O_3 contents of the cpx in the granulite unit in plagioclase-bearing pyriclasites are lower than in the deeper plagioclase-free pyrigarnites suggests that the relatively high Na and Al-contents of the latter would reflect higher P,T metamorphic conditions. A similar conclusion may be drawn when comparing the Na and Al contents of the deep seated plagiopyrigarnites-cpx and the apparent lower grade pyriclasites-cpx, i.e. the Na and Al-contents of the cpx from two andesine-bearing rocks. As shown by the Fig. 10 and 11 the positive correlations between Na, Al [iv] and Al [vi] reflect both host rock dependence and higher P, T conditions for the Jijal-Patan rocks as compared to the granulitic belt pyriclasites. A slight negative correlation (Fig. 11) between Ca and Al [vi] indicates a progressive (but clearly not grade-dependent) substitution of the Ca-Tschermak's molecule by the jadeite ("first") end-member. Scattered Na *vs.* Fe_T'' correlation (Fig. 10) grossly indicates Mg $\rightleftharpoons$ Fe″ and possibly 2Ca $\rightleftharpoons$ NaAl (jadeite) and/or 2Ca $\rightleftharpoons$ NaFe″ (acmite) substitutions. Papike *et al.*'s (1974) recalculation method of the possible Fe‴ contents suggest together with Jan and Howie's (1981) conclusions that most cpx would have Fe‴ in sufficient amount to consume Na in forming acmite "first" preferentially over jadeite. Both methods (Edgar *et al.*, 1969) suggest that the Kohistan clinopyroxenes are more similar to the intermediate-P granulite facies cpx than to the eclogitic (omphacitic) cpx. This is in agreement with the Al [vi]/Al [iv] ratios which are 5 in the websteritic and pyrigarnitic-cpx and 1.0 ± 0.2 in the cpx from the plagioclase-bearing pyriclasites and plagiopyrigarnites; following White (1964), both ratios are from intermediate pressure ($\simeq 13 \pm 2$Kb) granulitic facies-mafic rocks.

Orthopyroxenes

The Ca–Fe_T'' (+Mn)–Mg ratios of Kohistan opx (mainly from websterites, dunites, troctolites, pyriclasites, one opx-spinel diopsidite and one garnet-opx gneiss) show (Fig. 8) that they are bronzites in the Mg-rich rocks and hypersthenes (En50 to En65) in the pyriclasites. Enstatite components (Table 2) seem mainly host-rock controlled. On a small scale, there is no clear relation between Al_2O_3 ($0.0 < Al_2O_3 < 5.4$), the positions of the rocks in the metamorphic pile and the mineral assemblages. The Ca versus Al contents (Fig. 12) suggest a negative correlation similar to that of cpx with a scattered distribution of the pyriclasites and associated rocks. The tendency for some Ca-poor opx to show high Al contents ($\simeq 0.20$) reflects high Al [iv] compositions rather than Al [vi] contents in M_1. This would indicate high Al content of the whole-rock (case of the opx-garnet (para) gneiss) and/or higher Al solubility in some opx in response to MgSi $\rightleftharpoons$ AlAl

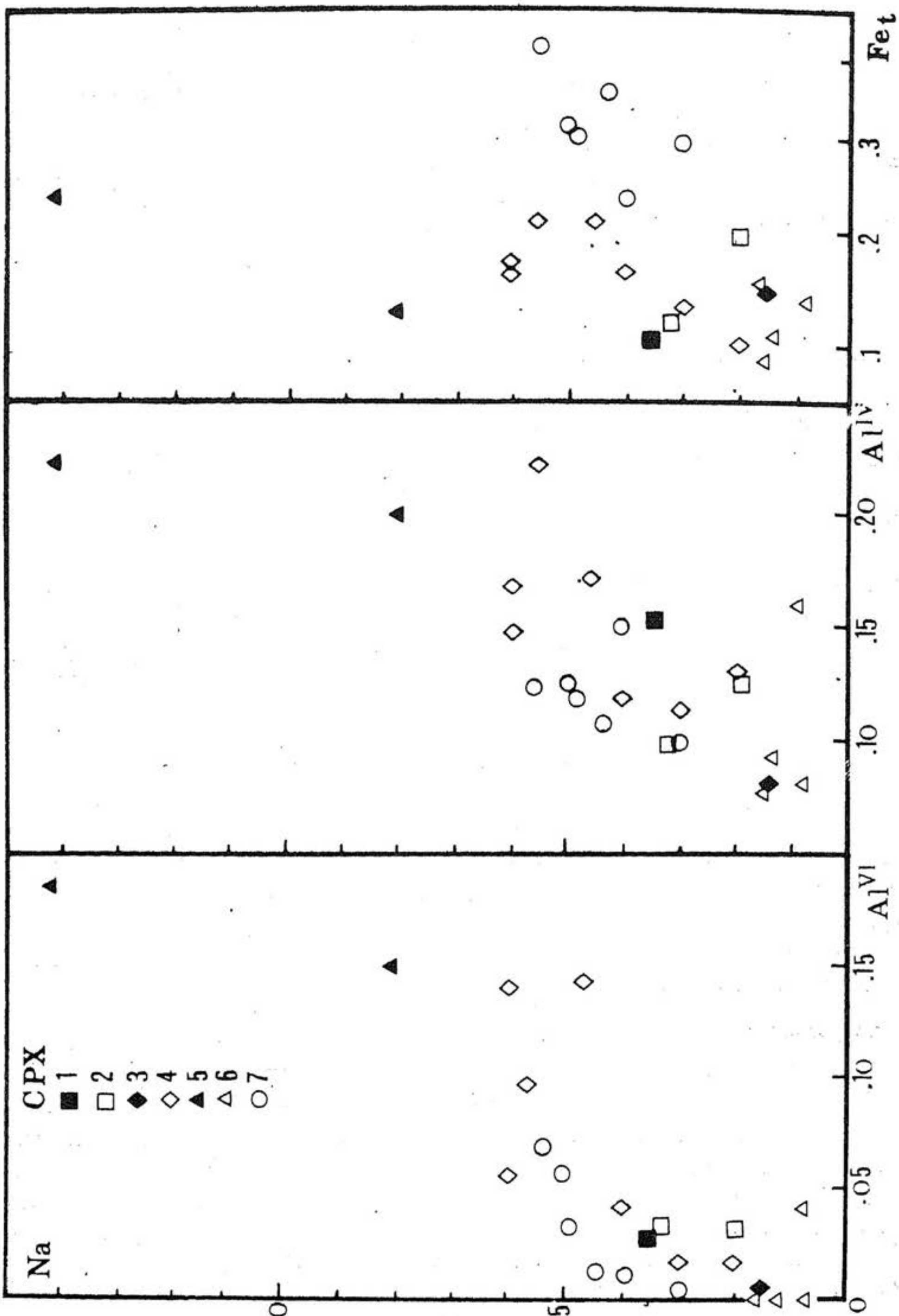

Fig. 10. Na versus Al [vi], Al [iv] and Fe^T (total iron as Fe″; cation numbers from structural formula) for the Jijal-Patan and the granulitic belt cpx (same symbols as for Fig. 9).

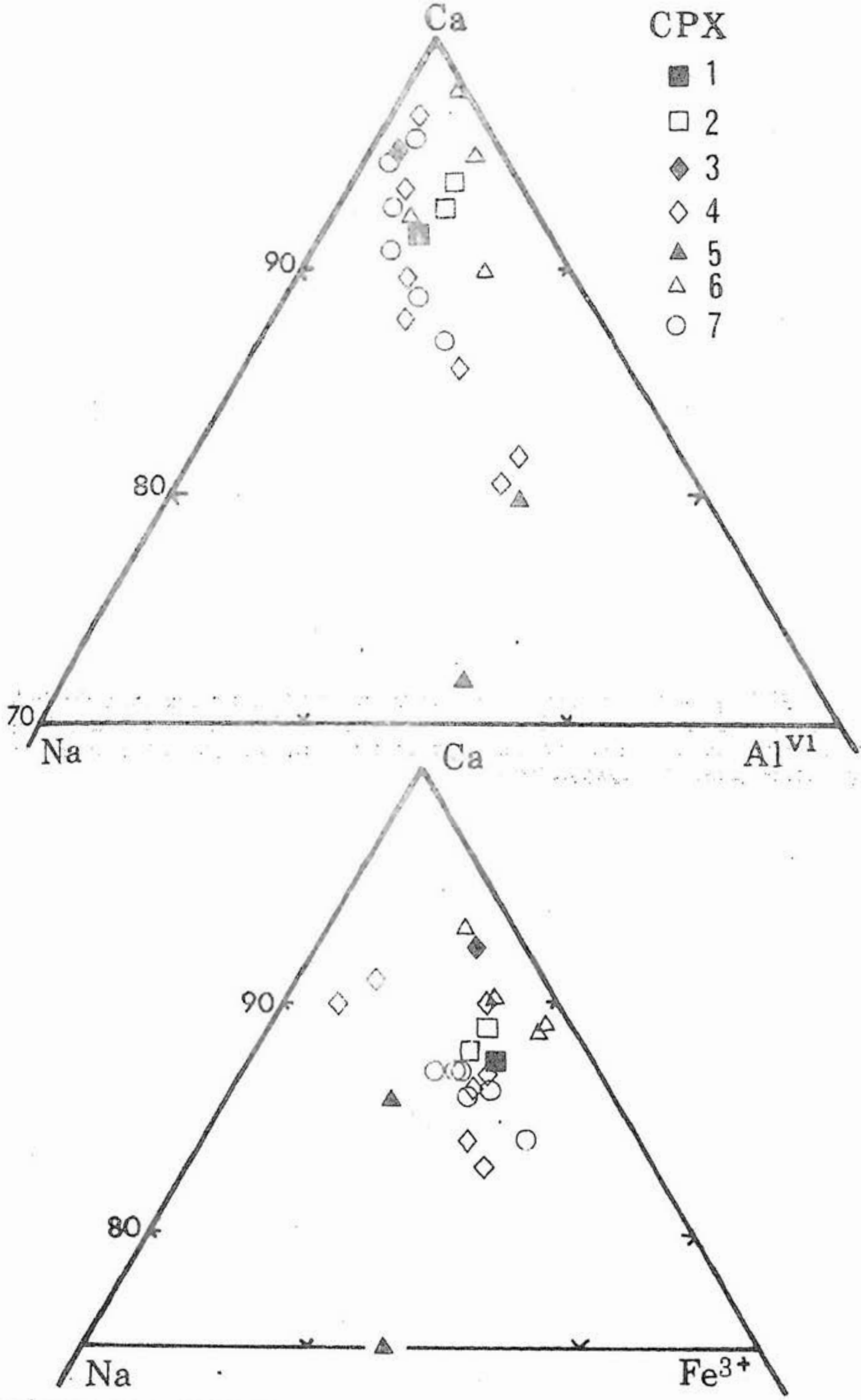

Fig. 11. Plots of the Kohistan cpx in the Ca-Na-Al [vi] (the "jadeitic" trends) and Ca-Na-Fe‴ (the "acmite" trends) triangles (Fe‴ estimates from Papike *et al.*'s (1974) method). 1 : metadunites; 2 : metatroctolites; 3 : metaclinopyroxenites; 4 : pyrigarnites; 5 : plagiopyrigarnites; 6 : metawebsterites; 7 : pyriclasites.

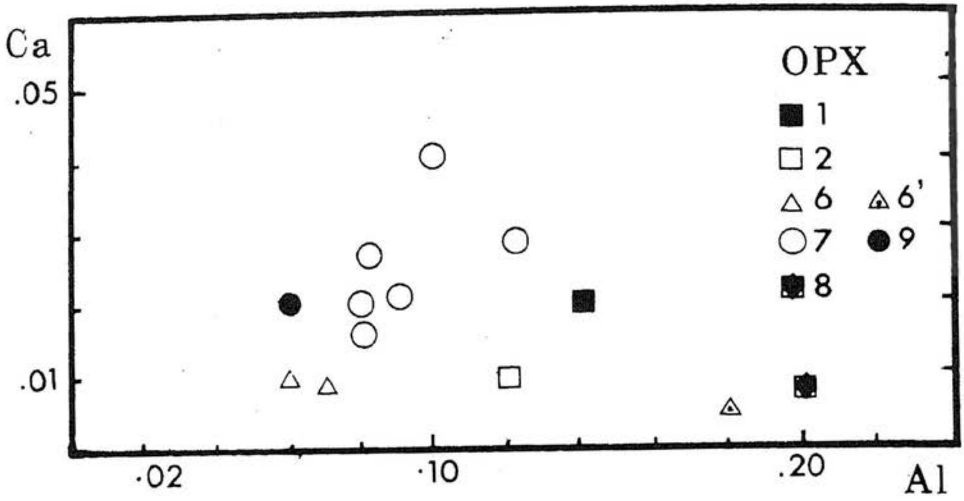

Fig. 12. Ca *vs.* Al [iv] + [vi] (cation numbers from str. form) in the opx from the Jijal-Patan complex and the granulitic belt rocks. 1 : metadunites; 2 : metatroctolites; 6 : metawebsterites; 6′ : two pyroxene spinel-pyroxenites; 7 : pyriclasites; 8 : garnet-opx-biotite gneiss; 9 : opx-pyriclasite.

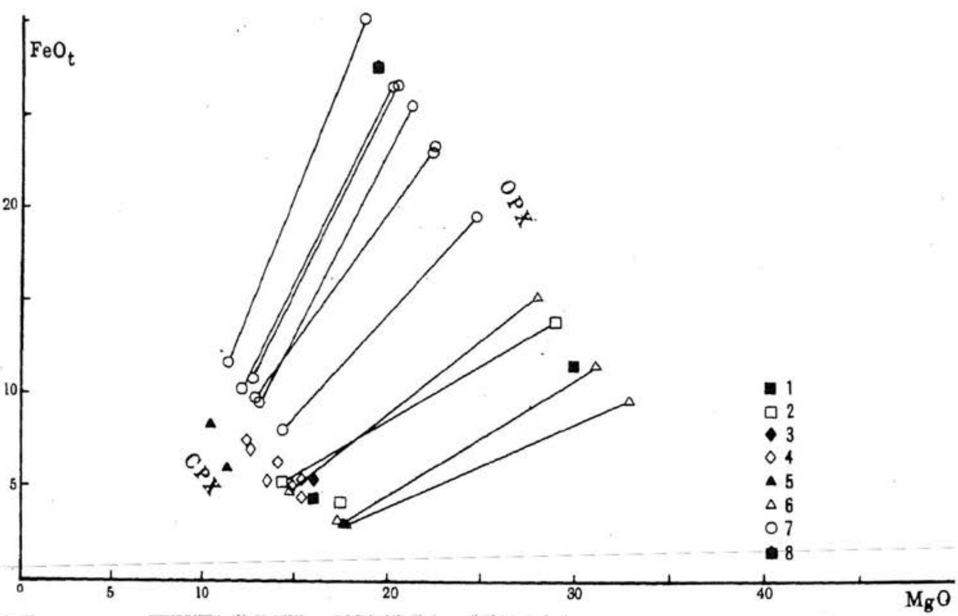

Fig. 13. FeO^T *vs.* MgO (weight %) in two or one pyroxene granulite rocks in Kohistan. 1 : metadunites; 2 : metatroctolites; 3 : clinopyroxenites; 4 : pyrigarnites; 5 : plagio-pyrigarnites; 6 : metawebsterites; 7 : pyriclasites; 8 : garnet-opx-biotite gneiss.

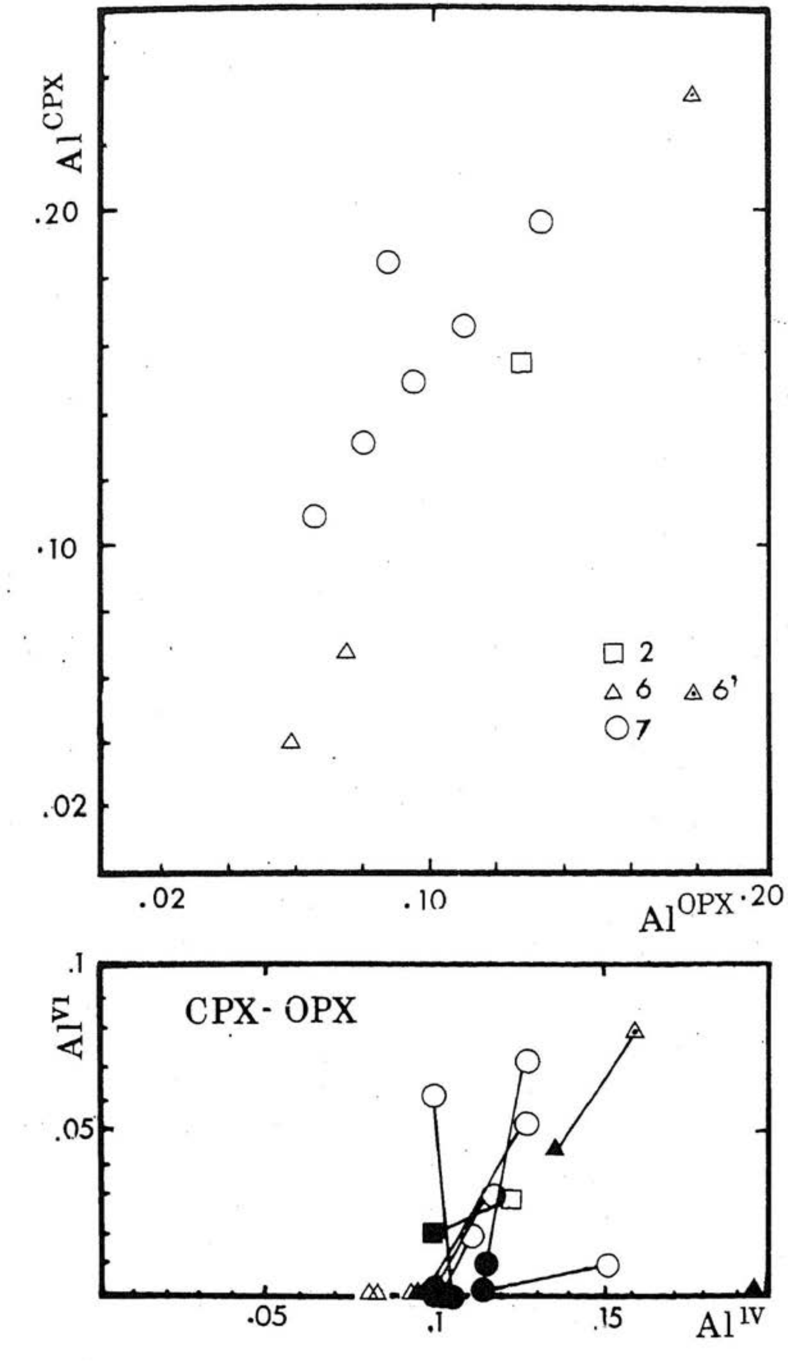

Fig. 14. Upper : Total Al (Al [iv] + [vi]) in cpx *vs.* total Al in coexisting opx; 2 : metatroctolites; 6 : metawebsterites; 6′ : two pyroxene spinel-pyroxenites; 7 : pyriclasites. Lower : Al [vi] *vs.* Al [iv] in coexisting two-pyroxenes pairs (black symbols : opx; white symbols : cpx; same symbols as Fig. 13).

substitution. In agreement with Jan and Howie (1981), the Ca and Al absolute values of Kohistan granulitic opx are not clearly related to prograde T and P changes (Kuno, 1968; Hess, 1960; Perkins and Newton, 1980; Mercier, 1980) during syn- to late D_1 equilibration process; as pointed out by various authors (Howie, 1965; Green, 1964; Medaris, 1972) accurate whole-rock data are necessary to discuss this dependence.

Two pyroxene associations in websterites, troctolites and pyriclasites show clearly that the Mg and Fe+Mn contents of both phases are mostly related to host-rock composition (Fig. 8 and 13) with fan-like aspects of the opx-cpx tie-lines suggesting near-equilibrium distrbiution of these elements at least during the late-D_1 annealing stage. The Al-distribution between coexisting apparently stable cpx and opx (Fig. 14) is grossly positively correlated with host-rock so the Al-poorest pairs are from the websteritic rocks (together with harzburgites; Jan and Howie, 1981) and the Al-richest from the plagioclase-bearing rocks (pyriclasites) plus some scarce opx-bearing plagiopyrigarnites and a plagioclase-free opx + Al-spinel diopsidite. The latter shows pyroxenes which have the highest Al-contents in the studied pairs and it is suggested that parts of the Al-contents in both phases may also correspond to higher P,T conditions (Atkins, 1969; Fleet, 1974) in those Jijal-Patan ultramafic rocks which may have (?) contained some plagioclase before an opx 1 + plagioclase reaction during D_1 high-grade metamorphic stage. This is in accord with the higher jadeitic content of some Jijal-Patan cpx and possibly, to the fact that the solubility of Al more or less increases (Boyd and England, 1964; Boyd, 1970; Anastasiou and Seifert 1972; Green and Ringwood, 1970; Wood and Banno, 1973; Wood, 1974; Mysen and Boettcher, 1976; Mercier, 1980) in opx-cpx and/or in opx ± cpx garnet associations in response to increasing T,P. In the Al-poor cpx-opx pairs (Fig. 14), if we accept that SiO_2 has been estimated with the same accuracy in all samples (see Powel, 1978 and Rollinson, 1981 for discussion), it seems obvious that all Al is expressed as quite equal Al [iv] contents between the opx and the cpx. For the pyriclasites, Al [iv] is slightly higher in the opx and the coexisting cpx than the latter group and Al [vi] tends to be higher in the cpx. Al [vi] is very low in the pyriclasitic-opx; when present it is related to some low Ca-Tschermak's molecule contents i.e. also to some low Ca content which has not been expelled (?) as late-D_1 diopsidic demixing blades in the opx. As previously discussed, calculated Fe''' and calculation methods do not allow clear estimates of the Al [vi] in the analysed cpx. This is unfortunate since the P,T dependent Al [vi] Al [iv] $\rightleftharpoons$ Mg Si (Boyd and England, 1964; Boyd, 1970; Anastasiou and Seifert, 1972) cannot be correctly advocated to demonstrate the Na and the Al [vi] richness of the cpx from the Jijal-Patan opx + Al-spinel diopsidites which are related to higher T,P conditions than those applied on the granulites of the central granulitic belt.

The partitioning of Ca, Mg and Fe_T between coexisting cpx and garnets (gt) in Jijal-Patan pyrigarnites (Fig. 15) strongly suggests (Jan and Howie, 1981) that these phases have crystallized and/or re-equilibrated under broadly the same T,P conditions. Sub-parallel tie-lines indicate possible cpx-gt near-equilibrium for slight'y different host-rocks. This possibility is not confirmed by the chemical data from

TABLE 1. MICROPROBE ANALYSES OF CLINOPYROXENES

Analysis	1	2	3	4	5	6	7	8	9	10°	11°	12	13
Sample	P21	PK22	PK23A	PK23B	PK23C	PK23E	GI5A	P23C	P23D	P24	P24	P24′	GI9A
SiO_2	47.28	52.51	50.21	47.17	49.82	50.96	52.11	51.37	51.22	48.45	46.16	50.91	49.23
Al_2O_3	7.33	1.14	7.32	9.37	5.29	3.04	2.00	3.71	6.86	8.17	11.67	3.46	5.37
FeO^T	7.40	3.19	7.11	8.32	6.44	4.84	5.09	5.27	5.35	5.12	5.89	4.05	5.65
MgO	12.52	17.47	11.94	10.64	13.85	15.39	16.30	15.50	13.45	12.63	11.40	15.87	15.54
MnO	.00	.20	.00	.04	.13	.02	.23	.27	.00	.01	.05	.03	.10
CaO	23.17	24.44	22.99	20.92	23.29	24.20	23.29	22.95	22.82	22.55	22.02	24.89	21.86
Na_2O	.78	.23	.67	1.96	.86	.49	.23	.66	.89	1.13	1.08	.26	.22
K_2O	.00	.00	.00	.00	.03	.02	.03	.00	.01	.00	.02	.00	.00
TiO_2	.69	.07	.74	.68	.56	.15	.14	.34	.71	.76	1.05	.40	.48
Cr_2O_3	.00	.46	.05	.05	.07	.00	.20	.00	.21	.00	1.06	.00	.78
ZnO	.00	.00	.00	.00	.00	.19	.00	.11	.00	.37	.00	.00	.00
TOTAL	99.19	99.71	100.85	99.16	100.33	99.30	99.62	100.20	101.52	99.22	100.38	99.85	99.24
FeO*	2.42	.00	5.92	3.32	2.14	.96	2.75	1.73	4.55	2.01	3.15	.52	3.81
Fe_2O_3*	4.53	3.22	1.08	4.54	3.91	3.53	2.13	3.22	.73	2.83	2.49	3.21	1.60

Table 1 continued (Microprobe analyses of clinopyroxenes).

Analysis	14	15	16	17	18	19	20	21°	22°	23
Sample	GI9B	GI25B	GI7	GI41	GI53	GI58	P130	GI42	GI42	GI45
SiO_2	51.97	52.20	51.64	49.72	49.59	51.03	49.57	50.59	49.60	50.08
Al_2O_3	.91	3.12	1.20	3.71	2.41	3.61	4.13	3.39	4.45	3.06
FeO^T	4.28	4.27	3.65	8.29	10.49	6.93	10.15	9.44	11.63	10.21
MgO	17.70	16.57	17.60	13.99	14.56	15.60	12.69	13.29	11.35	12.29
MnO	.17	.08	.14	.31	.36	.17	.21	.38	.35	.31
CaO	24.66	23.25	24.75	22.38	21.68	22.63	21.46	21.86	21.19	21.83
Na_2O	.13	.47	.19	.56	.46	.27	.69	.67	.73	.59
K_2O	.00	.00	.00	.04	.00	.16	.00	.00	.00	.03
TiO_2	.06	.00	.04	.42	.18	.00	.36	.48	.34	.19
Cr_2O_3	.00	.01	.42	.11	.00	.09	.01	.43	.05	.00
ZnO	.01	.22	.03	.97	.00	.00	.05	.00	.16	.00
TOTAL	99.88	100.18	99.64	100.49	99.73	100.49	99.31	100.52	99.86	100.65
FeO*	.10	1.11	.63	3.27	6.10	3.40	6.72	6.34	8.96	6.59
Fe_2O_3*	3.90	2.87	3.89	4.56	3.65	3.21	3.12	2.82	2.43	3.37

* Recalculated iron after Papike *et al.* (1974).
°° Two cpx rocks.

TABLE 2. MICROPROBE ANALYSES OF ORTHOPYROXENES

Analysis	1	2	3	4	5	6	7	8	9	10	11°	12°	13
Sample	GI9A	GI9B	GI7	P135	GI41	GI53	GI56	GI58	P130	P155	GI42a	GI42b	GI45
SiO_2	52.30	54.05	54.19	51.00	51.47	50.31	53.73	53.28	50.61	48.99	50.93	49.67	50.25
Al_2O_3	4.27	1.45	1.82	1.95	2.41	1.33	3.51	3.00	1.91	4.68	2.13	2.98	1.81
FeO^T	15.30	11.11	9.66	23.17	19.80	25.13	11.57	14.17	24.95	26.84	23.84	27.74	26.46
MgO	27.95	31.69	32.99	23.00	24.82	21.69	30.12	28.92	21.70	18.84	22.31	18.05	20.37
MnO	.35	.28	.27	.55	.48	.84	.24	.33	.69	.28	.24	.03	.69
CaO	.17	.38	.29	.50	1.03	.60	.60	.30	.42	.24	.59	.68	.68
Na_2O	.07	.02	.00	.01	.05	.01	.00	.01	.03	.00	.00	.00	.00
K_2O	.02	.00	.00	.01	.00	.00	.00	.00	.00	.04	.00	.08	.00
TiO_2	.11	.06	.01	.04	.06	.11	.01	.03	.08	.13	.10	.03	.16
Cr_2O_3	.00	.11	.45	.04	.00	.08	.00	.00	.00	.08	.00	.08	.12
ZnO	.00	.00	.03	.00	.00	.00	.09	.00	.00	.00	.00	.00	.00
TOTAL	100.54	99.13	99.70	100.27	100.11	100.25	99.87	100.03	100.38	100.14	100.16	100.01	100.54
FeO*	12.47	7.86	5.96	19.30	15.88	20.55	9.52	11.74	21.11	23.97	20.76	24.90	23.03
Fe_2O_3*	2.57	2.95	3.36	3.52	3.56	4.16	1.86	2.21	3.39	2.69	2.80	2.56	3.12

* Recalculated iron after Papike *et al.* (1974).

° ° Two opx rocks.

one cpx-gt pair which shows a cross-cutting tie-line, possibly related to a significant unknown physio-chemical process. Assuming that experimental data from Raheim and Green (1974) are relevant for the present discussion, the pair with cross-cutting tie-lines would more likely correspond to a lower (late-D_1) temperature readjustment causing an anticlockwise shifting of the cpx and gt plots (cpx richer in Mg and Ca; gt poorer in Mg and Ca) rather than higher acting (late-D_1)

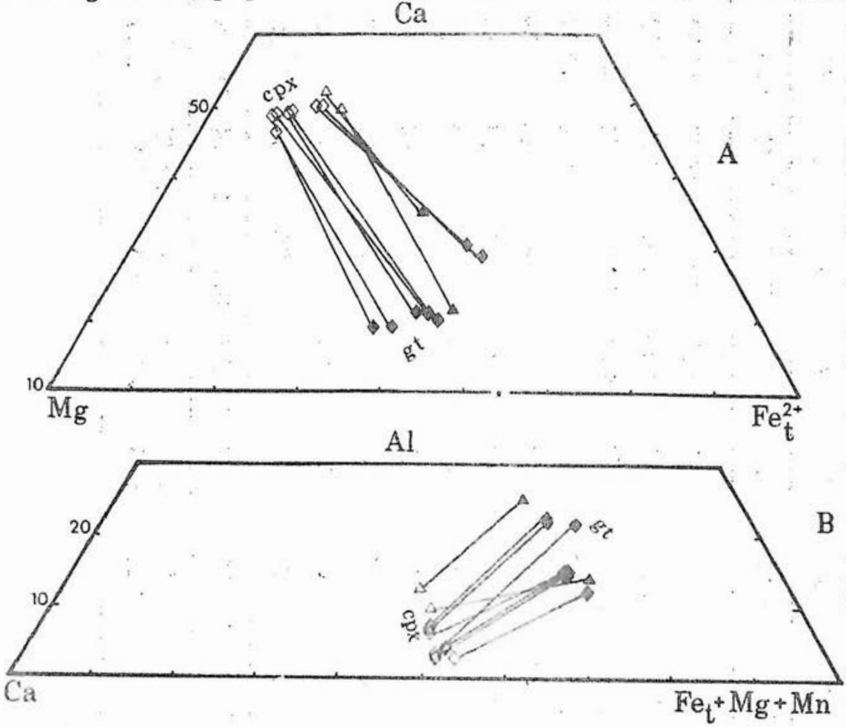

Fig. 15. Plots of coexisting clinopyroxenes (white) and garnets (black) in the Ca-Mg-Fe″ and Al^T-Ca-(Fe″+Mg+Mn) triangles (mol. %); (losangic symb.: pyrigarnites; triangles: plagiopyrigarnites).

P_1 (with quite identical topological effects) for sub-isochemical bulk compositions [X_{MG} = 100Mg/(Mg + Fe″) (mol. prop.) ≃ 70±5; Jan and Howie, 1981]. The plagiopyrigarnites' cpx-gt are from much more heterogeneous plagioclase bearing rocks with bulk compositions ranging from $55 < X_{MG} < 65$. The tie-lines (Fig. 15A) for their coexisting cpx-gt pairs may be cross-cutting either together or with the cpx-gt tie-lines from plagioclase-free pyrigarnites whose X_{MG} are probably around 55. Field aspect and textural evidences for a strongly cross-cutting cpx-gt plagiopyrigarnite pair show this sample is a coarse-grained foliated quartz-clinozoisite plagio-pyrigarnitic gneiss whose feldspars are strongly cloudy and whose garnets are strongly cataclastic with fractures enfilled by late epidote + greenish blue hornblende. It is suggested that both cpx and gt have suffered diffusive transfers during an overprinting shearing phase and possibly have attempted to re-equilibriate at lower P during the D_2 tectonometamorphic stage. This would be in agreement with Raheim and Green (1974) data i.e. a major decrease in P favours clockwise rotation of the cpx-gt tie-lines in the Ca-Mg-Fe_T'' triangle. Similar conclusions may be obtained when considering Al versus Ca and Mg+Fe_T''+Mn (Fig. 15B).

Equilibrium has probably been approached and maintained for the cpx-gt pairs under similar high-grade T,P conditions except in the plagiogarnetite sample which shows a cross-cutting tie-line. Decreasing Ca-Tschermak's molecule from the plagiopyrigarnites-cpx upto the pyrigarnites-cpx as well as decreasing Al-contents in the coexisting garnets are more likely host-rock dependent than related to opposite P and/or T variationships. Cpx-trends are accordingly not turned towards significant Mg-enrichments or decreases respectively in response to increasing P and T. In the same way the garnet-trends are not significantly turned toward grossular enrichment or diminution in response to increasing P or decreasing T except (?) for one pyrigarnite. The latter cross-cutting tie-line is linked to a grossular-poor garnet suggesting the sample comes from an area which has maintained (or reached) higher T (?) during D_1 metamorphism. The possible retrogression of the cpx-garnet (+plagioclase) from a sheared plagiopyrigarnite is again apparent with the garnet plot shifted towards the Fe_T+Mg+Mn corner (Fig. 15B) mainly as the result of a post-D_1 (almandinous) Fe-enrichment. More data are necessary to be sure this interpretation is the good one to explain the chemical patterns of this particular cpx-gt pair and moreover the coexisting garnet chemistry. At this respect one must remember the garnet blastesis in some plagiopyrigarnites is sometimes an overprinting late-D_1 feature along a network of joints affecting amphibolitized two-pyroxenes pyriclasites. As previously described (see also Fig. 4) the latter garnet growth is related to a petrological process of a "garnetization" at the expense of hb+opx which brings together a newly formed garnet with an inherited cpx not chemically reequilibriated with the garnet(?). As will be discussed, this alternative (together with the possible selective retrogression of some plagiopyrigarnites garnets) may be an explanation for the apparent temperature discrepancies which occur when applying the cpx-gt geothermometric methods to the uppermost cpx-gt bearing plagiopyrigarnites in the Jijal-Patan complex.

Amphiboles

Thirty six amphiboles (with one member showing significant compositional zoning) from one or two-amphibole rocks (three samples) have been analysed in mid to high-grade mafic to ultramafic rocks. Structural formulae (Table 3) calculated on the anhydrous basis of 23 oxygens with total iron as FeO show the following main characteristics :

a) greenish brown, brownish green, green, pale brown amphiboles from the high-grade C*b* zone striped-amphibolites as well as those from the garnet-bearing or garnet-free pyriclasites, metatroctolites, metadunites and metawebsterite are pargasite-rich hornblendes in Leake's (1978) classification, i.e. they show : $1.6 < Al[iv] < 2.2$, $0.6 < (Na+K)^A < 0.95$ and almost all Na in the "vacant space A" (Fig. 16).

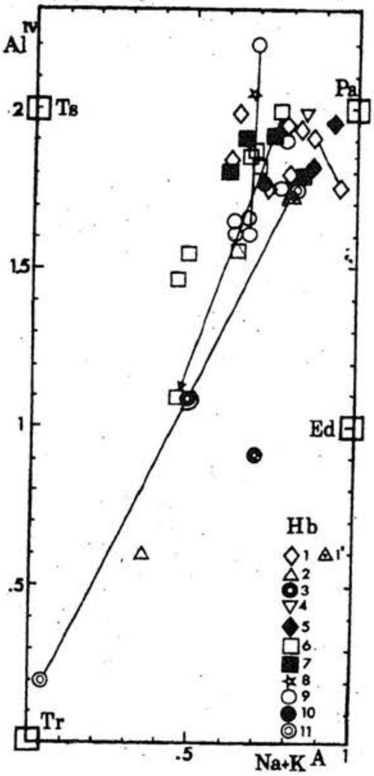

Fig. 16. Al [iv] *vs.* $(Na+K)^A$ contents of the Kohistan amphiboles. 1 : pyrigarnites; 1′ : garnetites; 2 : plagiopyrigarnites; 3 : metawebsterites; 4 : plagioamphigarnites; 5 : metadunites; 6 : garnet-free amphibolites; 7 : garnet amphibolites; 8 : ky-st-clinozoisite rock near Jalkot (Indus Valley); 9 : pyriclasites; 10 : metatroctolites; 11 : retropyriclasites. (Arrows for zoned amphiboles; tie-lines for two amphibole rocks).

b) Blue-green outer rim of a C*b* zoned hornblende from a coarse-grained amphibolite (Flaser-gabbro) as well as two pale-green hornblendes from metawebsteritic rocks fall within the "common hornblendes" field suggesting these minerals are late (perhaps syn-D_2 amphiboles). Al-poor amphiboles (tremolite-actinolite) also develop in some plagiopyrigarnites from Jijal-Patan complex and within strongly altered retropyriclasites. In the latter case, the amphibole is clearly late at the expense of relict cpx and/or pargasitic hornblende.

Because it is now well established that pargasitic amphiboles from metamorphic mafic-ultramafic rocks are stable under the granulite temperatures (i.e. 700–850°C) one may infer that the syn- to late D_1 metamorphic stage was at least under these T conditions throughout the lowermost part of the Kohistan amphibolites and near the granulitic (metanoritic) belt. With respect to Al [iv] and $(Na + K)^A$ and despite the fact that they are almost green to greenish blue, zone B*b* hornblendes do not seem clearly different (Fig. 16) from zone C*b* hornblendes. The apparent lower grade character of one B*b* hornblende appears more obvious when considering the P-dependent parameter Al [vi] (Kostyuk and Sobolev, 1969; Bard, 1970).

TABLE 3. MICROPROBE ANALYSES OF AMPHIBOLES

Analysis	1	2	3	4	5	6	7	8	9°	10°	11	12	13
Sample	P21	PK23A	PK22″	PK23B	PK23C	PK23E	P23C	P23D	P24′	P24′	GI9A	GI12A	GI25
SiO_2	42.29	41.82	42.72	49.91	42.51	41.30	43.27	41.73	42.12	42.17	42.01	41.86	41.96
Al_2O_3	15.03	15.62	16.78	5.23	14.96	14.66	13.65	15.11	14.96	13.44	16.07	17.27	14.96
FeO^T	9.84	10.76	14.15	10.18	9.96	8.86	7.96	9.70	7.81	15.09	8.61	9.11	6.45
MgO	14.13	13.67	9.94	16.31	14.85	15.20	16.81	15.09	16.15	11.85	15.03	13.78	16.71
MnO	.00	.00	.28	.11	.00	1.17	.08	.07	.06	.19	.07	.24	.11
CaO	12.05	11.86	8.87	11.85	12.07	11.86	11.98	12.19	12.45	12.16	11.76	11.35	11.89
Na_2O	2.29	2.28	3.87	1.17	2.85	2.78	2.64	2.91	3.01	2.88	2.36	3.15	3.15
K_2O	.02	.02	.64	.08	1.13	.09	.02	.13	.24	.74	.22	.34	.33
TiO_2	.89	.90	.69	.22	1.13	1.17	.87	1.01	.83	.27	.96	1.32	1.51
Cr_2O_3	.08	.06	.00	.00	.00	.02	.03	.03	.05	.12	.16	.00	.14
ZnO	.00	.00	.00	.04	.00	.00	.07	.00	.00	.00	.03	.00	.00
TOTAL	96.63	96.79	97.95	95.11	98.37	97.12	97.39	97.98	97.69	98.91	97.28	98.42	97.21
FeO^*	8.06	8.58	14.15	10.18	9.96	8.86	8.86	9.70	7.81	13.53	6.61	9.11	5.65
$Fe_2O_3^*$	1.62	1.98	.01	.01	.01	.01	.01	.01	.01	1.42	1.82	0.01	.73

Table 3 continued (microprobe analyses of amphiboles).

Analysis	14	15	16	17	18	19	20	21	22	23	24	25	26°
Sample	GI20A	GI21A	GI16	GI19	GI7	GI18	P135	GI41	GI53	GI56	GI57	P130	GI42
SiO_2	40.47	43.65	41.38	43.51	48.58	40.71	40.24	42.16	41.37	42.6	42.01	41.60	43.22
Al_2O_3	15.12	12.94	14.56	12.33	7.76	17.06	13.04	10.87	11.30	16.09	16.31	12.78	11.90
FeO^T	15.55	11.76	16.37	15.81	4.69	18.60	15.12	12.56	14.78	5.90	8.48	14.88	13.95
MgO	10.19	13.32	10.06	11.57	20.40	7.97	11.34	13.54	12.56	16.31	14.84	11.63	12.38
MnO	.47	.21	.33	.40	.12	.01	.58	.18	.22	.07	.07	.11	.10
CaO	11.16	11.80	11.17	11.03	12.67	10.85	11.48	11.95	11.51	11.47	12.09	11.15	11.48
Na_2O	1.80	1.46	1.99	2.20	1.79	2.17	1.18	1.02	1.40	3.00	2.43	1.62	1.23
K_2O	.86	.40	.20	.06	.00	.19	2.34	1.73	1.13	.13	.22	1.65	1.67
TiO_2	.82	.61	1.06	1.12	.29	.57	2.16	2.14	1.38	.00	.12	2.02	2.07
Cr_2O_3	.00	.13	.30	.07	.69	.00	.05	.00	.00	.00	.00	.00	.05
ZnO	.00	.00	.13	.00	.00	.00	.00	.00	.00	.00	.00	.00	.00
TOTAL	96.44	96.28	97.55	98.10	96.99	98.13	97.53	96.15	95.65	95.57	96.57	97.44	98 05
FeO*	14.02	9.70	14.54	14.93	.92	18.31	13.20	10.16	11.18	5.80	6.39	14.59	13.75
Fe_2O_3*	1.39	1.87	1.67	.80	3.43	.26	1.74	2.18	3.27	0.09	1.50	0.26	.18

Table 3 continued (microprobe analyses of amphiboles).

Analysis	27†	28	29	30	31	32	33	34°	35°	36†	37°
Sample	GI.42	P.136	P.140	P.142	P.127	P.291	P.292	P.293	P.293	P.297	P.297
SiO_2	37.58	40.20	41.40	40.90	44.88	39.94	40.39	41.09	53.71	47.20	39.30
Al_2O_3	21.07	14.34	12.91	17.55	13.22	13.87	13.92	11.96	.78	9.73	17.64
FeO^T	21.08	15.32	18.05	13.63	13.09	19.88	18.33	15.66	10.81	12.81	15.66
MgO	3.90	10.22	9.20	10.62	13.13	7.39	8.90	11.10	17.82	13.93	9.02
MnO	.18	.28	.17	.27	.31	.32	.32	.25	.34	.26	.34
CaO	10.94	11.21	10.97	10.68	10.94	10.70	10.35	11.44	12.70	10.94	11.02
Na_2O	.91	1.85	2.21	2.59	1.46	2.42	2.43	1.51	.13	1.58	2.13
K_2O	2.32	.84	.06	.25	.33	.53	.62	1.85	.06	.26	.70
TiO_2	.14	.95	.83	.36	.54	1.09	1.06	1.78	.00	.21	.24
Cr_2O_3	.00	.03	.23	.00	.01	1.05	.00	.00	.00	.00	.00
ZnO	.00	.00	.00	.00	.00	.00	.00	.00	.00	.00	.03
TOTAL	98.12	95.24	96.03	96.85	97.91	97.19	96.32	96.64	96.35	97.02	96.08
FeO*	21.08	14.00	16.92	16.63	12.10	16.22	18.33	14.61	8.31	12.81	15.66
Fe_2O_3*	0.01	1.20	1.03	0.01	.90	3.33	0.01	.95	2.27	0.01	0.01

° ° Two amphiboles rocks.
†, ″ Inner/outer zones of zoned crystals.
* Recalculated after Papike *et al.* (1974).

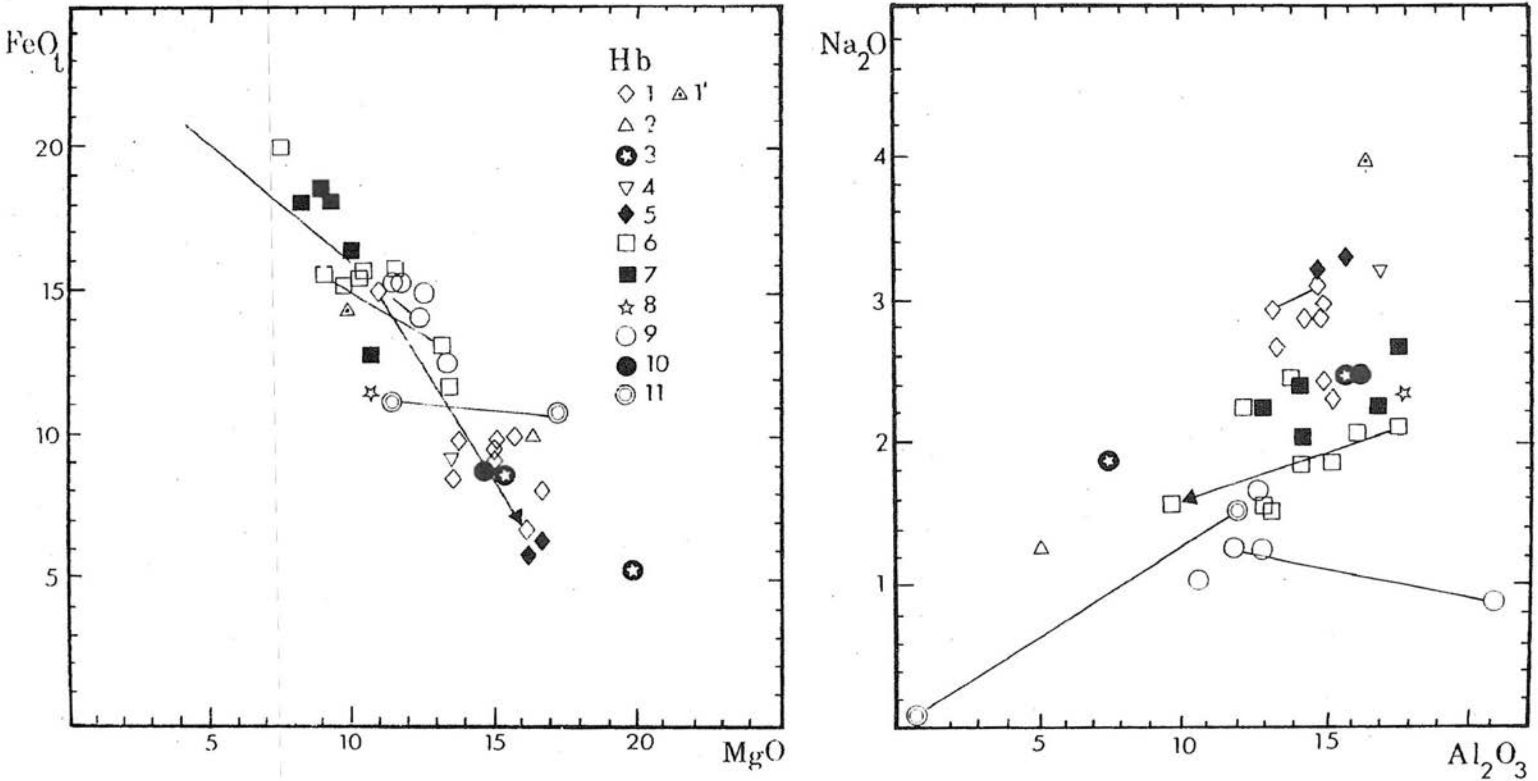

Fig. 17. Plots of FeO^T *vs.* MgO and Na_2O *vs.* Al_2O_3 contents (weight %) of Kohistan amphiboles (same symbols as Fig. 16)

Despite this correlation is far simple, the Kohistan zone C*b* and the lowermost part zone B*b* hornblendes show $0.7 < Al\,[vi] < 0.9$ while those from zone B*b* have $0.5 < Al\,[vi] < 0.7$. As discussed previously a load pressure (P_L) at the apparent base of the Kohistan arc of around 13–14Kb suggests that zone B*b* hornblendes would have been subjected to 8–11Kb during the D_1 metamorphic stage. With respect to chemical characteristics of the high grade amphiboles within the zone C*b* amphibolites, the granulitic belt and the Jijal-Patan complex, it seems no clear prograde chemical trends have survived D_2.

As shown by Fig. 16 and 17, the major chemical variations such as the correlations FeO^T versus MgO and Na_2O versus Al_2O_3 are more host-rock than P,T dependent. In Fig. 17 a good negative correlation is apparent between the Mg and Fe^T of the hornblendes. The latter are Mg-rich in the Jijal-Patan websterites, pyrigarnites, amphigarnites, garnetites, plagiopyrigarnites, plagioamphigarnites, and also in the olivine-bearing (troctolitic to dunitic) layered cumulates of the granulitic (metanoritic) belt. Opposite is the tone when considering the two (one)-pyroxene pyriclasites and the garnet-free or garnet bearing amphibolites i.e. a group of rocks whose hornblendes are Fe^T-rich or as rich in Fe^T as Mg. In Fig. 17 a crude positive correlation between the Na and Al content of the hornblendes plots suggests a "plagioclase buffering" so that the feldspar (mainly An40 ± 10) – bearing rocks (± garnet amphibolites, pyriclasites, troctolites and plagiopyrigarnites) are poorer in Na_2O ($1.0 < Na_2O < 2.5$) than the plagioclase-free rocks (garnetites, pyrigarnites, amphigarnites, dunites and websterites). Four probably late retrogressive amphiboles apart, the Al_2O_3 contents tend to be slightly higher in the Jijal-Patan ultramafites and the websteritic, dunitic, troctolitic cumulates of the granulitic belt than within the pyriclasites. In this respect the hornblendes from the garnet-free or garnet-bearing amphibolites are more scattered with intermediate position for Na_2O ($1.8 < Na_2O < 2.5$) but with $13 < Al_2O_3 < 18$.

Such features suggest the Fe^T, Mg, Na and Al contents of the studied amphiboles are host-rock dependent and the earlier conclusions about the prograde significance of the absolute values of Al [iv], Al [vi] and $(Na + K)^A$ in hornblende (Bard, 1970) have to be used carefully (see also Jan and Howie, 1982). As shown by Fig. 18 and 19 the partition of such major elements as Fe^T, Mg and Ca between coexisting high grade hornblendes, garnets, cpx and opx indicates bulk-composition controls and possible second-order overprints and/or changes in response to P,T progressive or retrogressive metamorphism. The Ca- distribution in cpx-hornblende pairs shows (Fig. 18, 19) that increasing Mg and Ca contents in both phases are probably controlled by the host-rock Mg and Ca contents. Fan-like aspects of the hb-cpx tie-lines from the Jijal-Patan mafic-ultramafic complex and from the granulitic belt suggest the hb-cpx have respectively reached near chemical equilibrium. Cross-cutting tie-lines of the Jijal-Patan pairs over those from the pyriclasites and associated rocks (see Fig. 19) would reflect higher P,T metamorphic conditions in the Jijal-Patan complex than within the granulitic belt. This is marked by a strong Mg-enrichment (and possibly a slight Ca-enrichment) of the

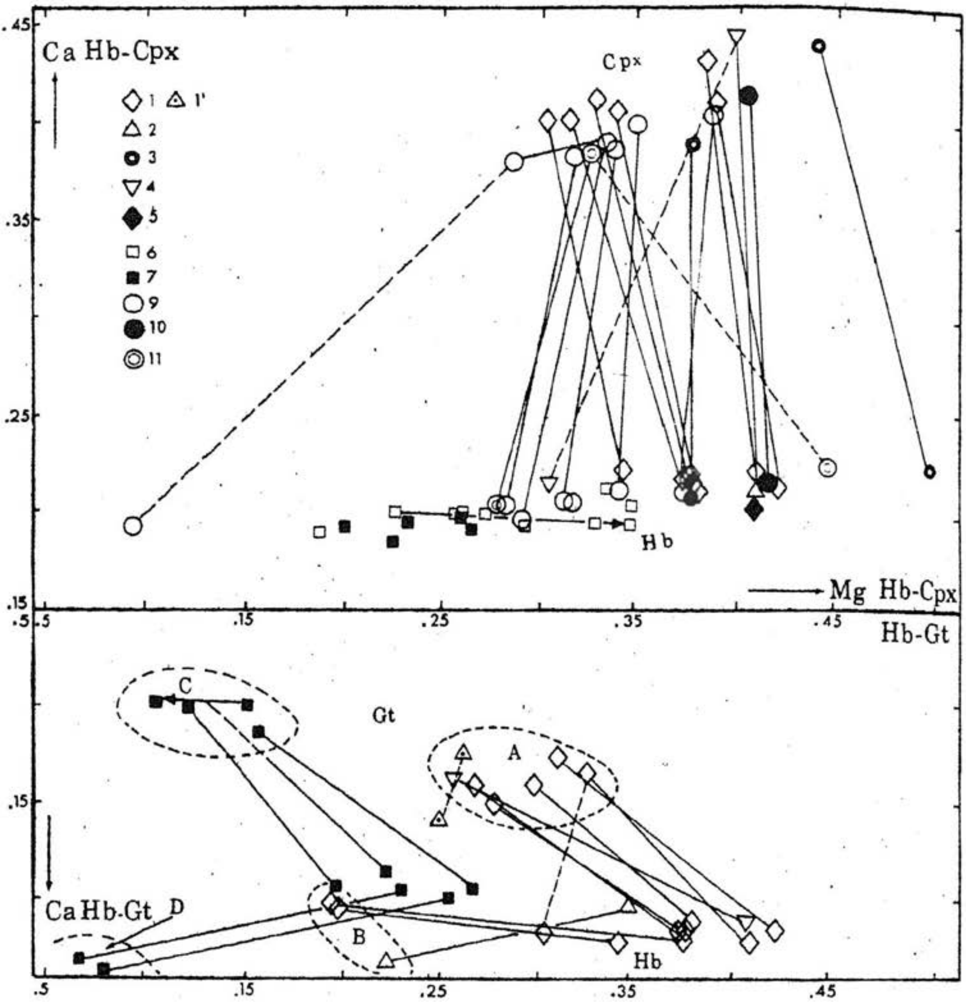

Fig. 18. Ca *vs.* Mg (mol. %) in amphiboles and coexisting amphibole-clinopyroxene and amphibole-garnet pairs. 1 : pyrigarnites; 1′ : garnetites; 2 : plagiopyrigarnites; 3 : metawebsterites; 4 : plagioamphigarnites; 5 : metadunites; 6 : garnet free amphibolites; 7 : garnet-amphibolites; 8 : ky-st-clinozoisite rocks near Jalkot (Indus Valley); 9 : pyriclasites; 10 : metatroctolites; 11 : retropyroclasites (arrow for zoned amphibole; full tie-lines for coexisting pairs; dotted tie-lines for cpx coexisting with a second amphibole in two amphiboles rocks; field A, B, C and D in lower diagram are discussed in the text).

Jijal-Patan hornblendes together with a slight Ca and Mg diminution in their associated cpx. The Mg-Ca partitioning between hornblende and garnet in cpx-free or cpx-bearing rocks (Fig. 18) seems more complicated and the following features may be pointed out :

i) clearly (one out of equilibrium hornblende apart) the hornblendes with Mg $\simeq 0.35$ are approximately in equilibrium with Ca-poor ($0.10 < Ca < 0.15$) pyrigarnites garnets (field A, Fig. 18). Significant cross cutting hb-gt tie-lines for a two-

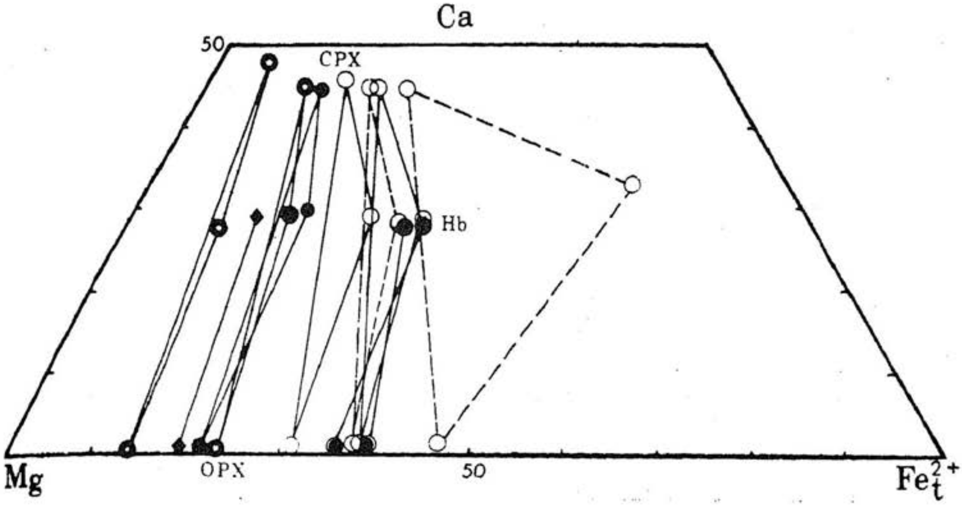

Fig. 19. Plots of coexisting hb-opx and hb-opx-cpx in the Ca-Mg-Fe_T'' triangle (mol. %). (Same symbols as Fig. 18; dotted circles for opx-hb pyriclasites; dotted tie-triangles for hb-opx-cpx associations from a thin layered pyriclasite containing two different cumulative layers in microprobe section).

amphibole pyrigarnite and one (plagio)amphigarnite suggest either a lower temperature of (re-)crystallization for the amphigarnite or the late-D_1 chemical changes of the high-grade (pargasitic) hornblende + (?) cpx rather than their coexisting garnet, in response to the retrogressive growth of a second (amphibolite facies) amphibole within this rock.

ii) hornblendes with $0.35 < Mg < 0.38$ may also coexist with Ca-rich ($0.20 < Ca < 0.25$) garnets in some pyrigarnites and plagio-pyrigarnites (field B, Fig. 18). These garnets are poorer in Mg than those previously mentioned, a feature which may be related to the bulk composition rather than to the lower P (and/or T conditions) of crystallization of the pyrigarnites they come from. Cross-cutting tie-line of the hb-gt from one plagiopyrigarnite indicates [together with the fact that this tie-line is subparallel to some hb-gt pairs from (lower T,P) garnet-bearing amphibolites (field D, Fig. 18)] that the plagiopyrigarnite was near equilibrium at lower T,P than the underlying pyrigarnites in Jijal-Patan complex.

iii) hornblendes with $Ca \simeq 0.20$ are Mg-poor ($0.14 < Mg < 0.27$) and apparently stable with Ca-rich and Ca-poor garnets in the cpx-free garnet amphibolites (respectively fields D and C in Fig. 18). Because the garnet compositions seem much more sensitive to host-rock chemistry than hornblendes, the two families of hb-gt tie-lines would reflect, as previously discussed, the possible occurrence of two different parental rocks for the amphibolites i.e. (?) Ca-poor and Ca-rich rocks. More chemical data are needed to test this hypothesis. Pargasitic hornblende coexisting with opx and opx-cpx again strongly suggest these amphiboles are near equilibrium with the granulitic pyroxenes. The partitioning of Ca, Mg and Fe^T (Fig. 19) shows clearly the Mg/Fe^T ratio in the coexisting three-phase assemblages increases progressively from the pyriclasites (metaleuconoritic to noritic rocks) to the plagioclase-free websterites via the troctolitic and the (cpx-free) dunitic cumulates, i.e. this is the proof that the Fe/Mg ratio is mainly host-rock dependent in the granulite unit and at least in one Jijal-Patan two-pyroxene + spinel ultramafite. Detailed study of the pyriclasites shows that cpx-hb-opx tie-triangles are crosscutting in such a way that it is not evident that the pyriclasites have crystallized under very different T conditions throughout the 10km thick granulitic belt or they have differently re-equilibriated with falling T (after D_1 metamorphism).

No compositional trends similar to those described by Rollinson (1981) for the Scourie hb-opx-cpx granulites in Scotland can be erected from Fig. 19, i.e. the latter conclusions seem acceptable. Dotted tie-triangles for a thin layered pyriclasite show this sample has two different hb-cpx-opx associations with one at least similar to the other pyriclasites and one containing a Mg-poor (Fe-rich) pargasitic hornblende. Textural evidence do not indicate the latter amphibole is a late (post-D_1) phase so it is suggested its composition is probably host-rock dependent (from an iron-rich metagabbroic cumulate).

Garnets

Eighteen garnets (Table 4) have been analysed (with one significantly zoned mineral) from the striped-amphibolites, the Jijal-Patan garnetites, pyrigarnites, amphigarnites, plagiopyrigarnites and one unique case of apparently equilibriated opx-gt association from the top (possibly neighbouring rocks) of the granulitic belt (Fig. 20). Two different groups of garnets occur in Kohistan rocks, i.e.

i) Garnets from the amphibolitic series with $20 < FeO^T < 30$, $2.0 < MgO < 6.0$ and $1.5 < MnO < 3.5$.

ii) Garnets from the Jijal-Patan rocks with $15 < FeO^T < 21.7$, $7.71 < MgO < 13$ and $0.5 < MnO < 0.8$.

Regarding these two groups, the garnets from the opx-gt gneisses are rich in Mg and Fe ($MgO \simeq FeO^T$) and low in Mn contents ($MnO \simeq 1$).

For quite uniform Al_2O_3 concentrations ($Al_2O_3 = 22.5 \pm 1$), the grossularite component is very variable but would discriminate Ca-rich from Ca-poor pyrope garnets in the Jijal-Patan complex. Here again the garnet from the opx-gt gneiss appears as a notably Ca-poor mineral ($CaO \simeq 2$). It is suggested that the different grossular contents of the almandine garnets from the striped-amphibolites would reflect different host-rock composition prior or during the D_1-metamorphism. Field data upon the grossular-rich garnets refer either to homogeneous fine-grained amphibolitic layers spotted by sub-automorphic garnet porphyroblasts or to thin felsitic intrafoliated injections (?) containing garnet up to 5cm. Grossular-poor garnet are found in different types of amphibolites which are at places similar to the latter types, the problem of this Ca-variations is still unsolved and needs more data to be discussed. For the pyrope-rich garnets, the apparent subdivision into Ca-rich and Ca-poor garnets is artificial when taking Jan and Howie's (1981) data on some Jijal-Patan pyrigarnites (plagioclase-free garnet granulites),

TABLE 4. MICROPROBE ANALYSES OF GARNETS

Analysis	1	2	3	4	5	6	7	8	9
Sample	P21	PK23A	PK22″	PK23B	PK23C	PK23E	P23C	GI12A	P23D
SiO_2	38.55	38.99	39.57	38.42	39.65	39.00	39.88	39.29	39.51
Al_2O_3	22.45	22.58	22.65	22.14	23.45	23.13	23.14	22.91	22.71
FeO^T	19.98	18.24	20.69	20.97	18.48	17.95	17.25	16.55	18.36
MgO	7.71	8.13	10.45	10.23	10.21	11.91	12.11	8.2	11.06
MnO	.73	.81	.54	.51	.67	.69	.67	.35	.41
CaO	11.27	11.3	6.89	7.62	7.93	7.82	7.31	13.38	8.58
Na_2O	.04	.05	.07	.04	.02	.00	.00	.01	.07
K_2O	.00	.03	.00	.05	.00	.00	.02	.00	.00
TiO_2	.07	.02	.00	.02	.10	.03	.06	.12	.05
Cr_2O_3	.00	.003	.00	0.03	.00	.00	.002	.00	.00
ZnO	.00	.00	.00	.00	.00	.00	.00	.00	.00
TOTAL	100.87	100.16	100.86	100.01	100.56	100.53	100.44	100.80	100.55

Table 4 continued (microprobe analyses of garnets).

Analysis	10	11	12	13	14	15	16	17	18
Sample	P24	P24′	GI16	GI18	P140	P142	P292†	P292°	P155
SiO_2	39.76	39.81	37.32	37.59	36.98	37.48	36.76	37.05	37.95
Al_2O_3	23.02	23.46	21.71	22.24	21.40	22.35	21.79	21.82	23.04
FeO^T	14.86	16.35	23.54	28.13	21.86	26.05	26.68	27.74	28.41
MgO	8.71	12.47	2.74	4.38	2.31	6.21	6.00	4.58	8.10
MnO	.42	.74	1.87	1.77	2.89	2.05	2.52	3.38	1.01
CaO	13.24	7.49	13.26	6.40	12.87	6.30	5.71	5.48	2.58
Na_2O	.01	.00	.00	.01	.05	.03	.02	.02	.01
K_2O	.00	.06	.00	.00	.00	.00	.03	.00	.02
TiO_2	.08	.06	.02	.11	.04	.01	.07	.00	.08
Cr_2O_3	.00	.006	.00	.00	.00	.00	.003	.00	.002
ZnO	.09	.00	.00	.02	.00	.00	.00	.09	.00
TOTAL	100.19	100.49	100.46	100.65	100.57	100.48	99.58	100.16	101.29

†, ° Inner/outer zones of zoned crystals.

TABLE 5. MICROPROBE ANALYSES OF EPIDOTES

Analysis	1	2	3°	4°	5°	6°	7	8	9°
Sample	PK22″	PK23B	GI12A	GI12A	P24	P24	GI20A	GI21A	GI16
SiO_2	38.11	37.61	38.58	38.12	38.75	38.02	37.02	36.86	38.42
Al_2O_3	27.90	28.94	32.43	29.06	31.56	29.39	25.76	27.77	33.70
FeO	8.04	6.55	2.19	6.23	2.72	5.67	9.91	7.05	.86
MgO	.14	.23	.05	.20	.10	.26	.07	.11	.00
MnO	.33	.06	.07	.00	.16	.40	.66	.21	.01
CaO	23.28	23.33	24.84	23.88	24.08	23.06	22.75	23.41	24.04
Na_2O	.03	.00	.00	.02	.02	.00	.14	.06	.01
K_2O	.21	.00	.00	.00	.05	.04	.05	.00	.03
TiO_2	.14	.05	.07	.00	.16	.40	.07	.13	.00
Cr_2O_3	.00	.00	.00	.00	.00	.00	.00	.15	.01
ZnO	.09	.00	.00	.00	.08	.14	.00	.55	.00
TOTAL	98.29	94.67	98.16	97.52	96.99	97.52	96.43	96.30	97.09

Table 5 continued (microprobe analyses of epidotes).

Analysis	10°	11°	12°	13	14	15	16	17	18
Sample	GI16	GI17B	GI17B	GI18	P136	P140	P142	P291	P292
SiO_2	36.98	37.79	36.81	37.05	36.24	36.72	37.26	36.26	36.19
Al_2O_3	25.93	33.55	27.05	26.77	25.78	26.54	26.97	26.21	23.52
FeO	9.81	.14	8.56	8.64	9.26	8.27	7.88	9.27	11.88
MgO	.06	.02	.11	.16	.00	.02	.22	.06	.00
MnO	.00	.00	.01	.23	.01	.06	.18	.23	.15
CaO	23.70	24.38	22.96	23.05	23.04	23.02	23.72	23.09	23.82
Na_2O	.00	.00	.13	.01	.00	.07	.02	.02	.05
K_2O	.00	.00	.01	.00	.01	.00	.01	.00	.00
TiO_2	.31	.00	.00	.19	.00	.11	.06	.16	.08
Cr_2O_3	.00	.00	.00	.00	.08	1.50	.00	.00	.00
ZnO	.00	.00	.29	.44	.06	.00	.00	.00	.00
TOTAL	96.81	95.89	97.09	96.54	94.48	96.63	96.33	95.29	95.70

° Two epidote-bearing rocks.
" Total iron determined as FeO although much of it is ferric in formula.

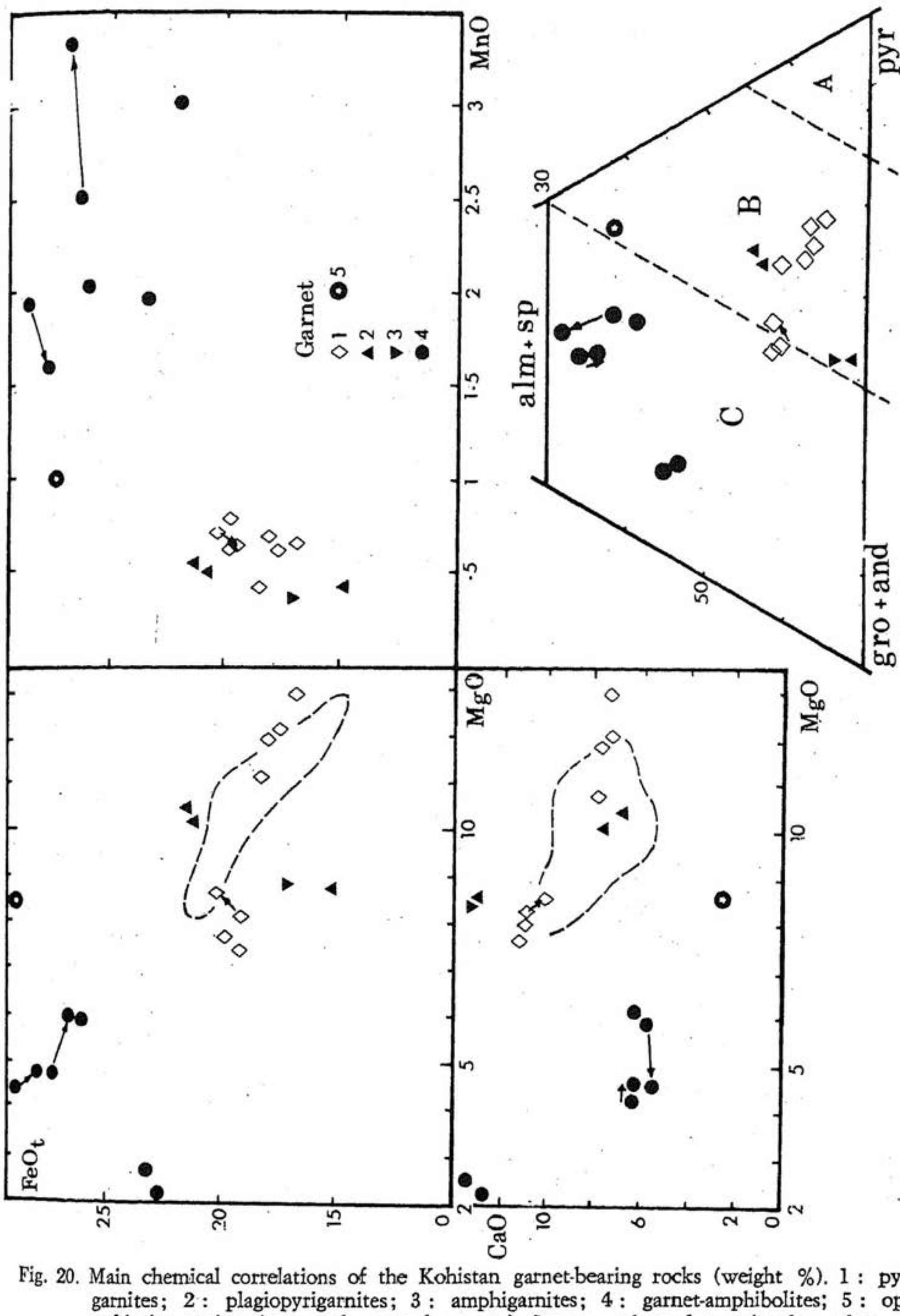

Fig. 20. Main chemical correlations of the Kohistan garnet-bearing rocks (weight %). 1 : pyrigarnites; 2 : plagiopyrigarnites; 3 : amphigarnites; 4 : garnet-amphibolites; 5 : opx-gt biotite gneiss; (arrows for zoned garnets). Lower end-members triangle : plots of the Kohistan garnets in Mysen and Heier's (1972) fields.

plagiopyrigarnites (garnet-anorthosites) and amphigarnites (garnet-hornblendites). In the Jijal-Patan complex, the garnets from the plagioclase-bearing rocks are richer in FeO^T than the mafic-ultramafic plagioclase-free rocks while their grossularite content seems more variable within a grossly negative correlation trend (Fig. 20) between CaO and MgO (or FeO^T). These features overprint a possible correlation (Coleman *et al.*, 1965; Green and Ringwood, 1972; Scharbert and Kuart, 1974; Smulikowski, 1972; Vrana *et al.*, 1975; Ellis and Green, 1979) between prograde P_L and grossular contents throughout the 6–8km thick Jijal-Patan complex. Comparisons with high-grade garnet from igneous mafic rocks (Fig. 20) show the Jijal-Patan garnets overlap on the eclogites-granulites field and plot mainly within the "B" (granulitic) garnet area. Almandine-rich garnets from the amphibolites plot in the "C" field and their low spessartine content ($\simeq 5 \pm 2\%$) indicate they have (Mysen and Heier, 1972) approached equilibrium under a relative high-P_L subfacies of the amphibolite facies. Absence of reactional textures so current in eclogitic rocks (i.e. keliphytic rims around corroded garnets, keliphytoid symplectites of (Na)–Cpx and Na-plagioclase, etc) as well as HP experiments on wet/dry tholeiitic to calc-alkaline systems (Green, 1967; Green and Ringwood, 1968), support the suggestion that the Jijal-Patan pyrigarnites have apparently not equilibriated during D_1 (or D_2) under the "eclogite facies" conditions. This is perhaps not the case for the deepseated amphibolites of the Kohistan sequence because some samples show retro-eclogite-like textures such as corroded garnets enfilled by numerous quartz and rutile inclusions and because some minerals show chemical zonations similar to those described (Vogel, 1967; Lasnier, 1977) in retroeclogitic rocks. In this respect the Kohistan garnets have either Fe-Mn (relatively)-rich cores grading progressively to a Mg-richest border in response to (?) syn-D_1 increasing P_L) or Fe-Ca (relatively) rich cores grading outwards to a Mn(+Mg)–richest rim probably in response to late D_1 – syn D_2 falling P_L and/or T.

Epidotes

Epidotes are common minerals in the amphibolites of Kohistan but also in the pyriclasites, the plagiopyrigarnites, pyrigarnites, garnetites and diopsidites. Within the two latter rock-types, textural evidence shows these minerals are either late D_2 or early (and at least) late D_1. Eighteen epidotes s.l. have been analysed from the amphibolites (15 an.), plagiopyrigarnites (4 an.) and one amphigarnite. The petrographical data suggesting the occurence in some samples of two epidotes also seem confirmed by microprobe and when two epidotes coexist they are classicaly a Fe-poor/Al-rich zoisite and a Fe-rich/Al-poor clinozoisite – pistacite. Zoisites are mainly retrogressive at the expense of the plagioclases but in the plagiopyrigarnites and amphigarnites these are radiating skeletal needles (associated with calcite) crosscutting An-rich (An70) plagioclase or building exsolution-like lamellae passing toward symplectitic tablets within (and towards the borders of) diopsidic-cpx. The latter habit strongly support the idea (Jan and Howie, 1981) that some epidotes may have crystallized during the late D_1 metamorphic stages. Clinozoisites and pistacites form large sub-automorphic crystals in pegmatoid post D_1-pre D_2 injections and within some scarce kyanite-staurolite-epidote felsitic rocks. The current habit of the clinozoisites is cauliflower-like symplectites enfilled by vermilar quartz in the pyrigarnites, plagiopyrigarnites and some garnet-free or garnet-bearing amphibolites. At some places these symplectites build up a coronitic rim around relict opx. In the two-epidotes samples, partitioning of Al and Fe''_T (Deer *et al.*, 1963; Holdaway, 1972) (in fact almost all iron as Fe_2O_3; see Table 5 structural formula on anhydrous basis of 25 oxygenes) between zoisite and clinozoisite-pistacite is not random (Fig. 21) despite it is obvious some parts are texturaly out of equilibrium. Zoisites from the amphibolites are richer in Al ($\simeq$ 0.38) than those from the Jijal-Patan plagiopyrigarnites and amphigarnites (Al $\simeq$ 0.32). The iron contents are also different, i.e. 0.2 in the amphibolites and 0.4 in the plagiopyrigarnites. Al-poor epidotes from the amphibolites and from the kyanite-staurolite felsites are poorer in Al (0.27 to 0.22) than those from Jijal-Patan epidotes (Al = 0.27 to 0.29) and respectively richer in iron (Fe''_T = 0.10 to 0.17; Fe''_T = 0.7 to 0.11). In contrast with the zoisites, CaO from the clinozoisites seems to be negatively correlated with FeO^T so possible Ca $\rightleftarrows$ Fe''_T (= Fe''') substitutions may have operated within these minerals. Plots of the Kohistan epidote pairs in Fig. 21 show a compositional miscibility gap between Al-poor and Al-rich epidotes (Deer *et al.*, 1963; Myer, 1966; Ackermand and Raase, 1973; Raith, 1973; Holdaway, 1972; Enami and Banno, 1980) and suggest this gap enlarges (for possible equilibriated pairs) from granulitic facies conditions towards lower T,P conditions. Taking into account the textural evidence, this conclusion seems errouneous because the zoisite-clinozoisite pairs from the Kohistan high-P amphibolite facies

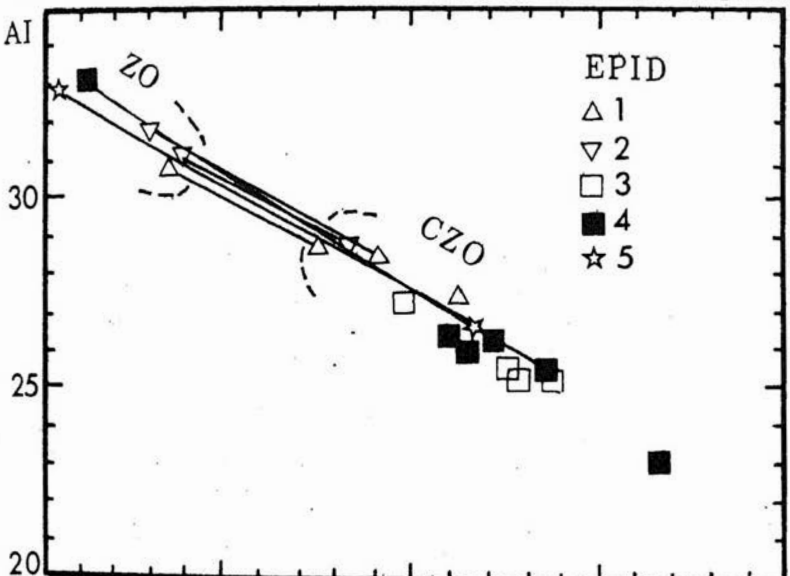

Fig. 21. Kohistan epidotes Al (total) *vs.* Fe''_T (in fact almost all the iron is present as Fe''' (mole %); 1 : plagiopyrigarnites; 2 : plagioamphigarnite; 3 : garnet-free amphibolites; 4 : garnet amphibolites; 5 : ky-st-clinozoisite rock near Jalkot (Indus Valley).

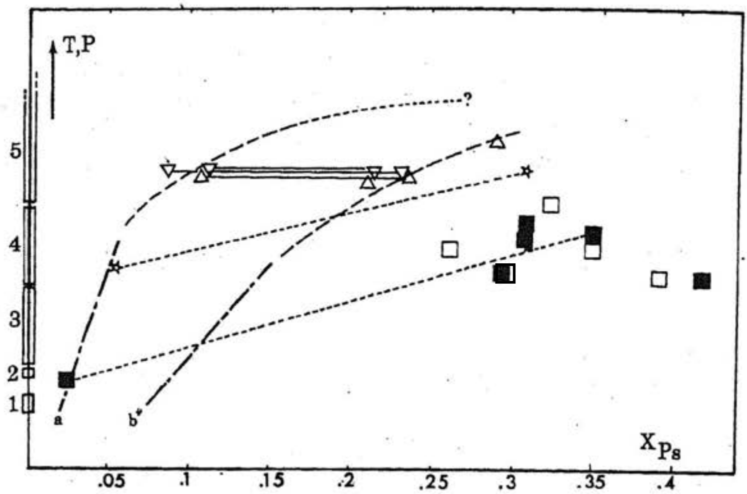

Fig. 22. Tentative empirical correlation between epidote X_{PS} contents ($= Fe^T/Fe_T + Al$; mol %) versus T,P conditions for greenschist (1), blueschist (2), epidote amphibolite (3), garnet-amphibolite (4) and granulite (5) facies after Enami and Banno (1981) (heavy dotted lines) and present approach (upper continuations); (same symbols as Fig. 21; full tie-lines for coexisting high-grade zoisite-clinozoisite pairs; dotted tie-lines for late zoisite growths in clinozoisite rocks; recalculations of total iron as Fe‴ do not change the present aspect of the miscibility gap between Fe-rich and Fe-poor epidotes).

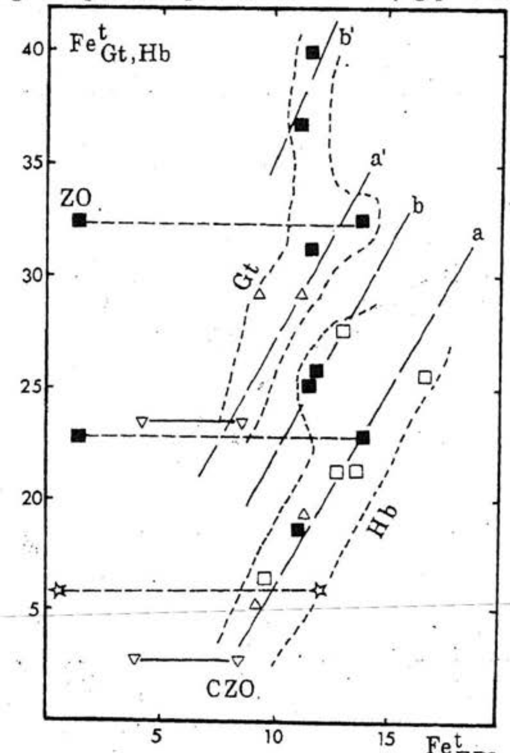

Fig. 23. Total iron (as Fe″ in mol. %) contents in coexisting epidote(s)-hornblende and epidote(s)-garnet rocks (same symbols as for Fig. 21-22; full tie lines for stable coexisting zoisite-clinozoisite pairs; dotted tie-lines for late zoisite-bearing rocks; lines a b, c, d, discussed in text).

are not synchronous and out of equilibrium. Tentative plotting of the Kohistan epidote pairs and single phases in Enami and Banno's (1970) empirical T/P versus $Fe'''/Fe''' + Al$ diagram (Fig. 21) would indicate the former miscibility gap tend to reduce at granulite facies conditions. If so, the zoisites would effectively be the common single high-T epidotes (Boettcher, 1970) stable above a compositional gap which have shifted towards the Fe''' -rich region in response to increasing temperature. As shown by Fig. 22, the partitioning of Fe''_T between coexisting hornblendes and Fe-epidotes and between garnets and Fe-epidotes have positive correlation suggesting near-equilibrium and host-rock control of the main chemical characters of these minerals. These correlations are shown as two possibly (?) different a, b and a', b' trends. It is possible these trends would reflect different Fe''/Fe''' ratios in the hb-ep or gt-ep pairs rather than to P_L, T controls of the iron partitioning in these complicated coexisting solid solutions during the synchronous growths being currently not surely established.

P,T ESTIMATIONS

Since the works from Bartholome (1962), Kretz (1961), Saxena (1968), Mueller (1960), etc., relative to the distribution of elements between coexisting Fe-Mg-Ca bearing-minerals, many workers have tried to construct geothermometers and/or geobarometers either on theoretical basis (requiring thermo-chemical data) or on experimental calibrations, in order to correlate distribution coefficients (K_D) of elements such as Fe'', Mg, Mn, Al, Ca, with T and/or P variables. For granulite and eclogite facies rocks, testing of most geothermometers commonly obtains results which seem consistent in absolute values with petrogenetic grids and facies series data. This is not always the situation; T (or P) estimates are sometimes not coherent. One of the numerous reasons for discrepancies is because most geothermometer equations imply to specify arbitrary P values so T estimates are more or less subjective with few exceptions when P_L is well approached by structural data and rock densities. It seems noteworthy this is the case in Kohistan where the actual 35–40km thick folded sequence (Fig. 5) lies under the S_1 – schistosity front i.e. it was probably at least around 45–50km thick during the D_1 – tectonometamorphic event. If correct, the distribution of rocks indicates an average density of 2.75 for the uppermost 15–20km thick units which overlie the granulitic belt i.e. the top of the latter was subjected to a P_L around 5–6kb during D_1. Assuming a thickness of 10km for the granulite unit in Indus Valley (average density 3.1), P_L would be close to 8–9 kb towards its base. With a density 3.3 for the 6–8km thick Jijal-Patan mafic-ultramafic complex, a $P_L \simeq 11$kb was operating at the top of the latter and 12–13kb towards the lowermost part of the (obducted) arc sequence during D_1. Using these P estimates, various geothermometers have been tested for reasonable P_L values between 6–8kb for the granulitic belt and 11–13kb for the Jijal-Patan complex. Identical pressure values have been estimated for these rocks by Jan and Howie (1980, 1981).

T estimates using two-pyroxenes geothermometers.

As shown by Fig. 24 we have plotted estimated T using the equations from Wood and Banno (1973) (revised by Wood, 1975 with T lowered $\simeq$ 60°C), Lindsley and Dixon (1976) (in Stormer and Whitney 1977), and Wells (1977) for six pyriclasites plus one troctolitic gneiss from the granulitic belt and for two websterites plus one opx + Al-spinel diopsidite from Jijal-Patan complex. From these methods the following remarks may be made :

i) the pyriclasites (with $K_D \simeq 0.59 \pm 0.2$) plot in narrow fields with T_1 (Wells) $\simeq 820 \pm 10$°C, T_2 (Lindsley-Dixon) $= 700 \pm 20$°C and T_3 (Wood-Banno) $\simeq 870 \pm 20$°C.

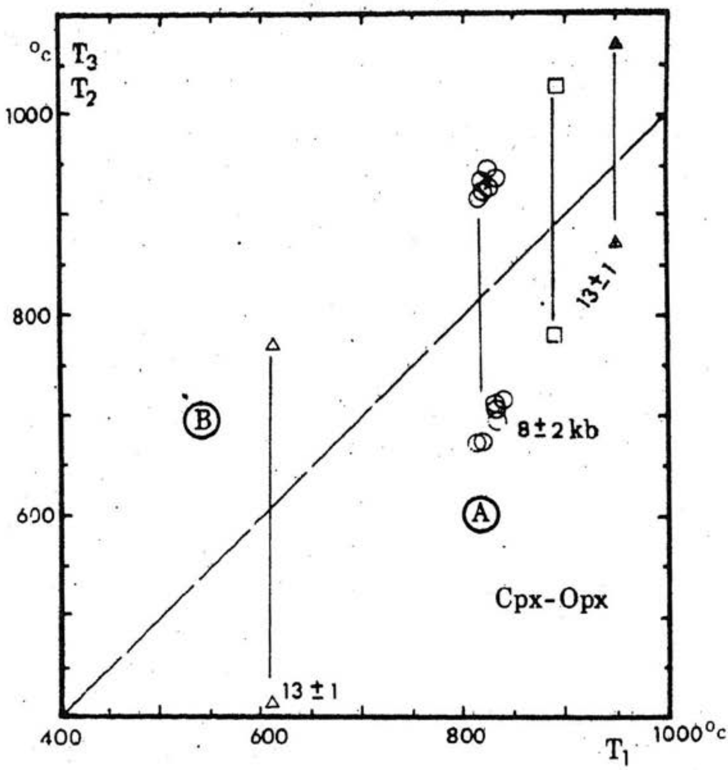

Fig. 24. Comparing temperature estimates using Wells (1977) (= T1), Lindsley and Dixon (1976) (= T2) and Wood and Banno (1973) (= T3) geothermometers for opx-cpx pairs in Kohistan high-grade rocks (circles : pyriclasites; square : metatroctolite; triangle : metawebsterite; dot in triangle : two-pyroxene spinel pyroxenite); (pressure estimates from field considerations).

ii) the troctolitic opx-cpx pair is 60 to 90°C higher than the pyriclasites.

iii) the websterites show low T (610–440, 390–450, 790–600°C) values while the opx + Al-spinel diopsidite temperature is 940, 870, 1070°C. Surprisingly and perhaps because our calculations use estimated Fe‴ and Fe″, the commonly observed discrepancy between Wells and Wood-Banno methods is not apparent. The low values of Lindsley and Dixon's method possibly reflect non-appropriate parameters in Henry *et al.*'s equation (see Stormer and Whitney (1977), p. 126, Tab. 2). For $P \simeq 8$kb, average temperature ($Tm = T1 + T2 + T3/3$) in pyri-

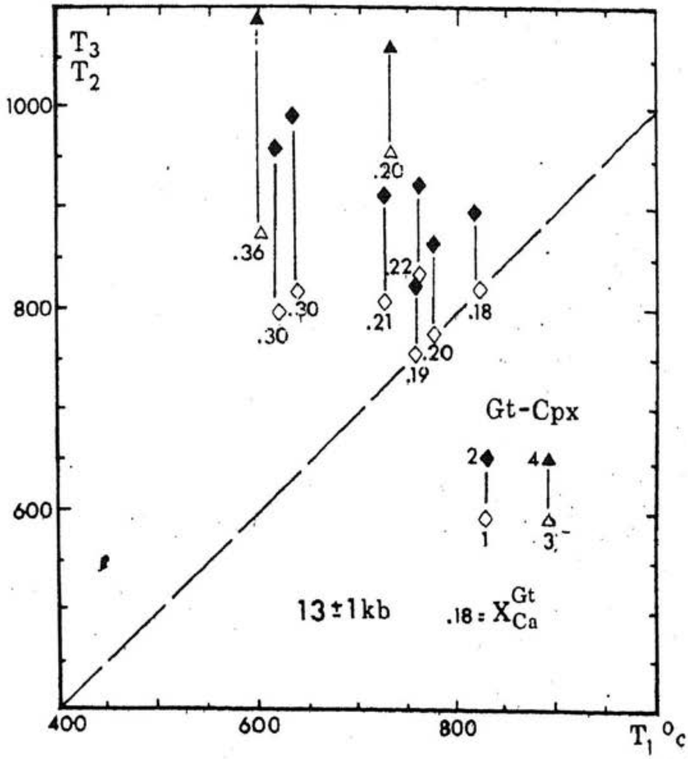

Fig. 25. Comparing temperature estimates using Saxena (1979) (= T1), Raheim and Green (1974) (= T2) and Ellis and Green (1979) (= T3) geothermometers for cpx gt pairs in Jijal-Patan complex (full symbols for T3 vs. T1; losangics : pyrigarnites; triangles : plagiopyrigarnites (pressure estimates from field considerations); X-Ca $_{GT}$ pointed for each studied garnet in gt-cpx pairs.

clasites, if significant, would give Tm 830°C ± 20°C. This is the same estimate as that of Jan and Howie (1980) for an heterogeneous sampling of two-pyroxenes rocks in Swat Kohistan. The troctolitic higher temperature (Tm ≃ 870°C) is problematical. The studied rock is from an interlayered cumulative bed associated with metanoritic rocks showing at least 60–80°C lower T. Among the possible explanations for such temperature difference in alternating beds is the fact that the troctolitic metacumulates show reactional coronitic (hb + spinel)-cpx-opx rims around relict olivine (now Fo_{80-81}) so reequilibration under the granulite facies conditions has not been achieved. Scattered T estimates for one Jijal-Patan websterite and one diopsidite with Tm = 610°C and 930°C strongly suggest : a) some Jijal-Patan rocks have undergone heterogeneous diffusive retrogression under the D_2 (?) – amphibolite facies conditions; b) on the contrary those ultramafites with Tm ≃ 930°C–950°C probably show inherited syn- to late D_1 temperatures. Such high T are quite similar to Jan and Howie's (1981) estimates for some Jijal-

Patan harzburgites, olivine-bearing and olivine-free websterites when using Wood-Banno (1973), Lindsley-Dixon (1976) and Wells (1977) methods.

T estimates using cpx-gt geothermometers.

Despite the fact that FeMg exchange reactions seem to be more T sensitive (Mori and Green, 1978) between cpx and garnet than cpx and opx, theoretical cpx-gt geothermometers of Ganguly (1979), Saxena (1979)* as well as experimental calibrations from Raheim and Green (1974), Ellis and Green (1979), Perkins and Newton (1980) show noticeable differences of 50–150°C in $K_{D\ Fe\text{-}Mg}$ versus T(P) thermometric estimates (Fig. 25). These discrepancies would reflect combined effects of parameters such as the non-ideal Ca ⇄ Mg substitutions (Ganguly, 1979; Ellis and Green, 1979) and the Mn, Al (and Na) contents of both the cpx and coexisting garnet in the K_D equations. Discussion of the different T estimates after Rollinson (1981) suggests that Ganguly's thermometer gives values 50°C higher than Ellis and Green at 800–1000°C, while in the same T-range Raheim and Green model gives up to 100 ± 80°C lower temperatures for pressures less than 20kb. For 12–15kb, Ellis-Green and Saxena's (Fig. 25) methods give respectively scattered 810–980° temperatures for the Jijal-Patan pyrigarnites and 1100–1200°C for the plagiopyrigarnites while Raheim-Green method shows narrow estimates 780° ± 50° and 900 ± 30°C for the same rocks. For the low $X\,Ca_{GT}$ (= .18) pairs, Ellis-Green's equation gives lower (≃ 50°C) temperatures than Raheim-Green's whereas this situation is reversed for $X\,Ca_{GT} \gg .18$, i.e. the former is higher by more than 70° with respect to the latter method. This suggests that the T-estimates are dependent on $X\,Ca_{GT}$. In agreement with Ellis-Green (1979), the remarks strongly indicate at least Ca ⇄ Mg substitutions in coexisting cpx-gt are non-ideal and K_D values are compositional dependent with more pronounced (not sole ?) $X\,Ca_{GT}$ effects at lower (larger non-ideal substitutions) than higher T. Taking in account these T discrepancies between Raheim-Green and Ellis-Green methods, it is questionable which equation is more appropriate for temperature estimates in the Kohistan cpx-bearing rocks. Assuming the ± 5% T-estimates for Ellis-Green, the Jijal-Patan pyrigarnites with $X\,Ca_{GT} \simeq .20 \pm 0.2$ would have equilibriated at temperatures quite similar to those predicted by Raheim-Green, i.e. 750–850°C with an average around 830°C. For the pyrigarnites cpx-gt pairs with $X\,Ca_{GT} = 0.33 \pm 0.03$, Ellis-Green's estimates minus 5% let the latter have equilibriated around 920 ± 20°C (810 ± 10°C after Raheim-Green's method). It is suggested these relatively higher temperatures for some pyrigarnites may represent the peak of D_1 – metamorphic stage throughout the Jijal-Patan complex. If not, cumulative effects of non-ideal substitution other than Ca ⇄ Mg in cpx and garnet on K_D values should be advocated; in this respect what would be the significance of the very hgih T – estimates for the two plagiopyrigarnites cpx-gt pairs i.e. 1143°C ± 60° ($X\,Ca_{GT}$ = .36) and 1050 ± 50°C ($X\,Ca_{GT}$ = .20) ? As discussed previously, it seems obvious at least one of this pair (the one which has a crosscutting tie-line in Fig. 15 and B) is possibly out of equilibrium. For the 1143°C ± 60°C cpx-gt pair,

* (Not revised calculation for error in published equation which lowers T-estimates 30 50°C).

the high $X\,Ca_{GT}$ is not correlated to lower P (Mori and Green, 1978) in the plagiopyrigarnites because the coexisting cpx is the Na, Al [iv] richest phase among the studied samples. The plagiopyrigarnite-cpx being always richer in Na and Al (see also Jan and Howie, 1981) than the underlying pyrigarnite-cpx, we had suggested these higher concentrations in the cpx have to be correlated to the host-rock Na/Al ratios in the plagioclase-bearing rocks. This would mean the "acmitic", "jadeitic" and Ca-Ts substitutions in the non-equivalent M_1 and M_2 cpx-sites are partly host-rock dependent and would reduce the K_D values in simulating high-T of equilibration. Accordingly, the same K_D differences are exposed between the plagioclase-free and the plagioclase-bearing "garnet-granulites" pairs from the Jijal-Patan rocks studied by Jan and Howie (1981). Recalculations (Ellis-Green equation at 12Kb) of the latter author's data show their two plagiopyrigarnites (S1 290 – S1 338) give also apparent high-T estimates (respec. 1130°C and 1150°C) while their pyrigarnites cpx-gt pairs show 150–200°C lower temperatures. Because the plagiopyrigarnites overlie the pyrigarnites in the Jijal-Patan complex, it seems reasonable to assert that they would have equilibriated (during D_1) in the same temperature range at around 12 and 13Kb respectively. The cpx-gt and cpx-opx estimates in the plagioclase-free ultramafic rocks have 880±50°C so the cpx-gt estimates in the plagiopyrigarnites are 150–200°C too high; various possibilities may explain this apparent difference :

i) theoretical approaches for correlating the K_D values in the cpx-gt pairs are correct; in such a case the high T estimates for the plagiopyrigarnites are significant and must receive an explanation in the thermal history of the Kohistan metamorphism during D_1.

ii) the cpx-gt K_D in the plagiopyrigarnites are derived from on-ideal solid solutions which are chemically different from those which allowed the actual temperature calibrations and empirical equations.

iii) the cpx-gt pairs from the Kohistan plagiopyrigarnites are out of equilibrium so their K_D values cannot be used for T estimates.

Points i and point iii in particular may be appropriate. Despite apparent textural equilibrium between gt and cpx in some plagiopyrigarnites, the fact that the garnet shows a very unusual mode of occurrence in other neighbouring plagiopyrigarnite suggests that the coexisting clinopyroxene and garnet have not equilibriated in the Kohistan granulitic rocks transitional area between the zones A and B granulites (Fig. 5).

P,T estimates using ol + an $\rightleftarrows$ cpx + opx + spinel.

As previously mentioned, the northern troctolitic metacumulates in the Indus Valley show coronitic textures quite similar to those described in metamorphic, sometimes layered, complexes containing plagioclase-gabbros, plagioclase-dunites and anorthositic rocks (De Waard, 1965; Saxena, 1969; Griffin, 1971; Murthy, 1958; Windley *et al.*, 1973; Lasnier, 1979; McLelland and Whitney, 1980); or mafic-ultramafic layered-bodies (Mason, 1967; Hamlyn, 1980). These textures present relict olivine rimmed by opx + green spinel symplectites in turn rimmed by cpx + green spinel symplectites with frequently an outer corona of Mg-pargasitic hornblende + vermicular green spinel symplectites. These reactional products are enclosed within an annealed plagioclase An 40 ± quartz matrix where they form more or less elongated patches or nodules oriented within the S_1 – foliation of the troctolitic layered gneisses. These "stretched" textural aspects strongly suggest the present coronitic assemblages are not late-magmatic but metamorphic with relict magmatic olivine having reacted, during D_1 to late-D_1, with surrounding (probably An-richer) plagioclase to give the end-products of the reaction :

(1) Olivine + An (in plagoiclase) ± H_2O ⇄ cpx + opx + Al (Fe, Mg) – spinel ± Mg-pargasite ± quartz.

Reaction (1) is a classical one in the zone between low-P and intermediate -P granulites (Ringwood, 1975). It has been calibrated by Kushiro and Yoder (1966), Green and Ringwood, (1967), Ito and Kennedy (1971) and Irving (1974) for the forsterite-anorthite system as well as for varoius basaltic (mainly tholeiitic) compositions. Uncertainties involved in determining the slopes of the reaction curves in plagioclase-olivine system have been discussed by Green *et al.* (1969), so the latter calibrations are not accurate (see Fig. 24) and may proceed wtihin a gently positive dipping "reaction zone" with approximate coordinates 1200°C/7.5–6.5kb. Introduction or transfer of water during the late stages of the reaction (1) is probably related to late-D_1 falling T and (?) P. Assuming (as previously discussed) that the granulitic belt in the area from which the metatroctolite comes suffered a P_L = 7kb., the temperature estimates using the latter calibrated curves were between 700°C and 880°C during the peak of D_1. Geothermometers (above discussion) gave Tm ≃ 870°C i.e. a temperature which fits with Well's equation and Irving *et al.*'s curve (Fig. 24). For the present study, it is noteworthy that the reaction (1) provides an explanation for a plagioclase + olivine "out" isograd in the Kohistan metamorphic pile during D_1 and that T in the granulitic belt was ≃ 879°C during D_1 and around 820°C during the late-D_1 tectono-metamorphic event at depths of 18–22km.

P,T estimates using clinozoisite + kyanite + staurolite + plagioclase + quartz.

Late-D_1 and D_2 – foliated coarse-grained (pegmatitic to aplitic) felsitic injections as well as some mafic coarse-grained amphibolitized rocks in the Southern amphibolites and north Mingora complex are clinozoisite + garnet bearing rocks containing at some (scarce) places kyanite ± staurolite ± corundum. Such rare assemblages have been described by Banno (1964) in the Sanbagawa belt (in association with eclogitic-like rocks), Mottana *et al.,* (1968) in eclogitic rocks from the type-locality in Austrian Alps, Vogel (1963) in eclogite-pyrigarnites at Cabo Ortegal (Spain) and recently by Nicollet *et al.* (1979) in high-pressure trondhjemitic metatects associated with retroeclogitic rocks in the French Massif Central. There are no doubts that these kyanite-clinozoisite assemblages represent high P associations and as experimentally studied by Boettcher (1970), the ky + zoi + q is the high pressure chemical equivalent of the associatoin anorthite + quartz (+ H_2O) and might represent solidus for the reaction :

(2) Liquid $\rightleftharpoons$ zoisite + kyanite + quartz + H_2O.

Calibrations of this reaction (Fig. 26) shows the right members may represent crystallization products of a trondhjemitic liquid which are stable at $T \simeq 750°C/P = 12kb$ and $T \simeq 820°C/P = 28kb$. Possible sub-solidus reactions (2') and (2") at lower P,T would allow the disappearance of at least one of these solid phases, i.e. :

(2') Zoisite + kyanite + quartz $\rightleftharpoons$ anorthite + H_2O.

(2") Anorthite $\rightleftharpoons$ garnet + kyanite + quartz.

This, with the fact the latter trondhjemitic liquid may precipitate An + zo + q (between 12–8kb and 750–770°C (negative slope)) or An + gt + q (between 8–6.5kb and 770° – 790°C) would explain most of mineralogical assemblages which occur in the late-to post D_1-syn-D_2 leucocratic (trondhjemitic) injections in the mid to the lowermost parts of the Kohistan metamorphic pile. The problem of the origin of these injections is unsolved and it is suggested on the basis of field observations that they may represent sub-autochthonous metatects from partial melting of the amphibolitic series. The kyanite-clinozoisite associations are thought to have equilibriated during late D_1 annealing process at $10 \pm 1kb$ and 720–740°C. This is in agreement with the pargasitic character of the amphibole from the neighbouring clinozoisite ± garnet amphibolites and with the high P stability field experiments for the Fe-Mg staurolites (Schreyer and Seifert, 1969; Ganguly, 1972; Richardson, 1968). EMA data (Table 6) show this is rather a Fe-staurolite ($X_{FeO} = .08$) acting as the main Fe – buffer in this assemblage. It is questionable whether this mineral is a melting product but one would note the hypothetical palingenetic origin or the kyanite-(clino)zoisite pegmatitic rocks may be advocated by the relative high-Cr contents of the kyanite ($\simeq .30$), staurolite ($\simeq .10$), clinozoisite ($\simeq 0.2$) and the Zn contents of the staurolite ($\simeq 0.5$). Whatever the solution of this problem, one will put the temperature estimates between the granulitic belt and the Jijal-Patan complex as notably $\simeq 100°C$ lower (during D_1 or late-D_1 stages) within the amphibolites which separate the latter mafic-ultramafic granulitized rocks in the Indus Valley.

In the north Mingora ultramafic-retrogranulitic complex (and probably south Timurgara (Jan and Kempe, 1973)), the growth of clinozoisite + kyanite, clinozoisite + garnet + kyanite, clinozoisite + kyanite + staurolite or clinozoisite + corundum together with Mg-chlorite + paragonitic mica ± rutile occur within amoeboid veinlets or within elongated centimetric patches in coarse-grained "amphibolitized" opx + cpx + green spinel mafic rocks. The textural evidence and the occurrence of two-pyroxene retropyriclasites nearby these rocks respectively suggest the former kyanite-bearing assemblages are late-D_1 and perhaps syn-D_2 retrogressive products formed at the expense of earlier plagioclase from troctolitic to websteritic metacumulates. With reference to Boettcher (1970), these kyanite-bearing associations would suggest T,P conditions similar if not identical to those previously discussed in the pegmatic veins south of Jalkot (Indus Valley) i.e. 750–790°C/8–12kb. Accordingly, the corundum under such conditons may occur as a stable (?) end-product of a plagioclase destruction process.

TABLE 6. MICROPROBE ANALYSES OF THE KY-ST-CLINOZ ROCK PHASES.

Mineral	Pl†	Pl°	Parag	Kyan	St
SiO_2	54.67	57.13	47.06	36.13	27.21
Al_2O_3	27.94	25.58	42.13	62.13	53.63
FeO^T	.03	.00	.44	.87	12.18
MgO	.01	.00	.00	.04	2.46
MnO	.02	.00	.00	.00	.00
CaO	9.47	7.26	1.28	.00	.00
Na_2O	6.15	7.32	6.10	01	.00
K_2O	.04	.04	.53	.00	.00
TiO_2	.00	.00	.00	00	.49
Cr_2O_3	.00	.00	.00	.29	.07
ZnO	.00	.00	.00	.00	.62
TOTAL	98.33	97.38	97.54	99.48	96.65
	An^{46}	An^{35}			

†, ° Inner/outer zones of zoned crystals.
For hornblende see table 3.
For Zoisite-clinozoisite see table 5.

TABLE 7. MICROPROBE ANALYSES OF OLIVINES AND SPINELS

Analysis	1	2	3	4	5	6	7	8	9
Sample	PK22	GI25B	GI56	GI58	PK22	GI9A	GI25b	GI56	GI58
SiO_2	39.22	39.07	42.61	38.67	8.87	0.00	0.00	0.00	.13
Al_2O_3	.00	.00	.02	.00	24.36	61.75	65.65	65.63	64.83
FeO^T	17.04	17.04	18.67	19.15	34.45	24.26	18.03	17.79	19.05
MgO	44.06	44.23	42.61	42.50	7.05	13.43	17.75	16.71	16.10
MnO	.38	.19	.31	.24	.40	.24	.19	.15	.29
CaO	.00	.00	.32	.00	4.00	.04	.16	.07	.27
Na_2O	.00	.04	.00	.00	.01	.00	.00	.00	.00
K_2O	.00	.00	.00	.00	.00	.00	.00	.00	.00
TiO_2	.00	.00	.00	.00	.32	.02	.00	.07	.00
Cr_2O_3	.00	.01	.00	.03	20.80	1.32	.57	.00	.02
ZnO	.17	.00	.04	.00	.23	.11	.00	.23	.03
TOTAL	100.88	100.58	100.42	100.60	100.48	101.17	101.80	100.58	100.71
	Fo^{81}	Fo^{81}	Fo^{81}	Fo^{80}					

P,T estimates using opx + an ⇄ cpx + gt + quartz.

Since De Waard (1965), it is now commonly recognised (Den Tex, 1972; Green, 1975) that the metamorphic quartz-saturated mafic rocks show stable opx + plagioclase at low P (granulitic "orthopyroxene-plagioclase subfacies") whereas the same rocks show coexisting garnet and cpx at higher P "cpx-almandine subfacies", so the schematic reaction :

(3) Opx + Ca-rich plagioclase (± pargasitic hb) ⇄ garnet + cpx + quartz + Na-rich plagioclase (± H_2O)

was occurring in rocks with various Fe/Mg and Na/Ca submitted to high grade metamorphism. Textural evidence supports this hypothesis (Griffin, 1971; Hansen, 1981; McLelland and Whitney, 1980; Savage and Sills, 1980; Vogel, 1967; Krogh, 1980; Jan and Howie, 1981) and experimental studies have been performed (Green and Ringwood. 1967; Green, 1970; Kushiro and Yoder, 1966; Hansen, 1981) on the garnet granulite transition so an equilibrium boundary has been grossly established with a positive slope around 100°C/kb in the field 600–1200°C/5–15kb (Fig. 26). Petrographic data show clearly the Kohistan plagiopyrigarnites have cpx–gt + quartz mainly at the expense of plagioclase + pargasitic hornblende and relict opx in coronitic assemblages and near a previously described network of joints and fractures. Under the 12kb P_L estimates, extrapolation at lower T and P of Hansen's curve (1981) would result in 700°C. This is lower than the high T estimates for the gt + cpx pairs in the plagiopyrigarnites which have been estimated around 850°C (with possible higher T_M values (?)) and fit rather well with Green and Ringwood (1967), Ringwood (1975) and Hansen (1976) extrapolated curves for quartz tholeiite compositions (Fig. 24) at 12kb. It is noteworthy that the first appearance of garnet by a reaction similar to (3) in the Kohistan granulitic rocks corresponds to a major second "isograd" (the "opx + plagioclase out") situated in the deep-seated part of the metamorphic pile, at the expense of hot (but water-poor) leuconoritic to noritic (layered) metagabros. Late leucocratic garnet-bearing patches and veinlets which cutacross the lowermost part of the granulitic belt are not related to this process but either to late-D_1 to syn-D_2 injections of garnet ± clinozoisite + plagioclase + quartz pegmatites or to late metasomatic transfers along cracks under high-pressure garnet-amphibolite facies conditions.

The solution for the problem of the petrological origin of the pyrigarnites may be approached by comparing the field relationships with the other rocks in the Jijal-Patan pile. It appears that the uppermost part of the pyrigarnites has either progressive (but rapid) feldspar-enrichments which grade to plagiopyrigarnites or the enclosure by pyrigarnites of alternating plagiopyrigarnitic bands and layers. Both structural patterns suggest the pyrigarnites are metacumulates that may have contained low modal fldspar proportions prior to their transformation (for some types) into plagioclase-free (plagioclase all consumed (?)) pyrigarnites. Actual mineralogical compositions as well as some textural evidences strongly suggest the pyrigarnitic rocks may have also contained opx, olivine and perhaps some cpx I, spinel and oxides prior to D_1 metamorphism. The chemographic approach would indicate that various (cumulative) parental rocks have reacte during D_1 to give the different pyrigarnites and associated rocks (O'Hara, 1968 Green and Ringwood, 1967; Griffin, 1971; Irving, 1974; Rollinson, 1981 McLelland and Whitney, 1980b; Jan and Howie, 1981), i.e. :

i) Garnetites from basic plagioclase orthopyroxenites (and/or clinopyroxenites ? by the metamorphic reactions :

(4) An + opx ⇄ garnet + quartz.

(4') An + Al-Sp ⇄ opx + garnet.

(4") An + cpx I ⇄ garnet + cpx II ± quartz (cpx-garnetite).

ii) Garnet diopsidites (pyrigarnites), diopsidites, Al-spinel diopsidites from basic plagioclase + olixine orthopyroxenites :

(5) An + forst + opx ⇄ garnet + cpx ± Al-sp.

(5') An + opx + Fe-oxide ⇄ garnet + cpx.

iii) Diopsidites from olivine orthopyroxenites :

(6) Forst + opx ⇄ cpx (Ca in opx).

iv) Garnet-diopsidites from spinel clinopyroxenites :

(7) Al-sp + cpx I ⇄ garnet + cpx II.

v) Spinel-diopsidites from basic plagioclase ± olivine orthopyroxenites :

(8) An + forst + opx ⇄ cpx + Al-sp ± quartz.

(8') An + opx ⇄ cpx + Al-sp + quartz.

vi) Meta-websteritic rocks from opx – clinopyroxenites and opx – cpx websterites .

(9) Opx I + cpx I ⇄ cpx II + opx II.

(10) Opx I + cpx I ⇄ cpx II ± opx II (± zoisite ± quartz).

vii) Metandunitic rocks from dunitic cumulates :

(11) Ol (± opx) ⇄ ol (± cpx).

Other P,T estimates.

Because of the relict character of most opx in the plagiopyrigarnites, the K_D for the opx-cpx pairs as well as the Al-contents of the opx in presence of garnet (Green and Ringwood, 1970; Wood, 1974; Newton, 1978; Perkins and Newton, 1980) have not been a priori calculated and related to T and/or P. Two-pyroxenes + garnet associations in the plagiopyrigarnites are however possible divariant assemblage that may be stable within a "divariant or multivarient bond" in the P,T diagrams for various host-rocks FeO/MgO ratios (Ringwood, 1975; Mysen and Boettcher, 1976; Hansen, 1981). Assuming a temperature of 750°C (which seems 100°C too low), Jan and Howie (1980) opx-gt pairs yield P estimates 10kb using $X\,Ca_{opx}$ (Mysen and Boettcher, 1976) and 17 ± 5kb using Al_2O_3 in opx coexisting with garnet and cpx (Akella, 1976). These P estimates give dubious average which is not far from the 13 ± 1kb proposed here for the Jijal-Patan plagiopyrigarnites which contain opx.

Garnet-opx associations in the cpx-free rocks seem scarce in Kohistan and one outcrop has been found near the apparent roof of the granulitic (metanoritic) belt. The rock is possibly a high-grade metatuffite (?) wtih alternating millimetric/centimetric plagioclase (An40) + quartz + opx "beds" interlayered with garnet biotite "layers". Chemical data on both opx and (not in contact) garnet have previously shown these minerals have quite distinguishing characteristics in the studied minerals series (Fig. 12), two of them being : i) – the high Al contents ($\simeq$ .20) of the opx; ii) – the high almandinous pattern of the garnet. Gt-biotite thermometer (Ferry and Spear, 1978) gives $T = 720 \pm 20°C$ and P_L (estimated) 6kb for these granulite (low P) facies rock in Kohistan.

DISCUSSION

The Metamorphic Evolution of Kohistan

Metamorphic zonation and structures.

From the textural and structural evidence two main sets of minerals and mineralogical assemblages may distinguish the D_1 and the D_2 tectono-metamorphic events. The D_1 metamorphic zonation (Fig. 27) is based on the early minerals and their distribution in the field. The following features may be pointed out :

a) The syn-to late D_1 metamorphic stages led to the development of six main prograde metamorphic zones in response to increasing T and depth (P_L) in "wet" ($P_L \simeq P_F \simeq P_{H_2O}$) and "dry" ($P_L > P_F \simeq P_{H_2O}$) rocks i.e. in the metasedimentary – metavolcanic sequences and in the metamafic-ultramafic complexes respectively. These six main progressive metamorphic zones are (Fig. 27) :

i) A "chlorite + epidote" low-grade zone which outcrops in the northernmost parts of Kohistan, within the Utror metavolcanic synform and, possibly, south of Chilas in Thak Valley,

ii) An "actinolite/blue green hornblende + epidote" zone with biotite + muscovite + andalusite associations in silico-aluminous layers,

iii) A "garnet + hornblende + epidote" zone with kyanite + clinozoisite + staurolite ± plagioclase associations in late D_1 – retrogranulitic rocks,

iv) A "basic migmatitic" zone with *in situ* syn- to late D_1 garnet-bearing leucosomes and hypersthene + garnet + biotite associations in some metagreywackes,

v) A "two pyroxene" zone covering rocks of magmatic origin among them metatroctolites which show a "plagioclase + olivine out" isograd with late D_1 amphibolitization, and

vi) A "garnet + cpx ± clinozoisite" zone corresponding to the late-D_1 destablisation of early opx + cpx ± Mg pargasite associations from relict two-pyroxene noritic or leuconoritic gneisses (pyriclasites) and associated rocks in the Jijal-Patan complex.

b) The granulitic assemblages develop mainly from H_2O-poor mafic ultramafic magmatic (layered) complexe(s) emplaced before the D_1 tectono-metamorphic event. It was suggested (Bard *et al.*, 1980) the Kohistan granulites formed at the expense of one or two (?) lopoliths built up by gabbro-noritic rocks and associated differentiated products. In this respect, this interpretation gives a possible explanation for the "sandwiched" occurrence of these granulites within the metamorphic pile. Recently, Coward *et al.* (1982) have claimed that the granulitic unit and the Jijal-Patan complex represent a single but very enormous magmatic complex affected by a large D_1 – recumbent fold. If so, the sandwiched occurrence of the granulite unit would be related to the fact that the granulites have a stratigraphic significance and would outcrop in the hinge of a mesozonal pennic-like fold. It seems that this interpretation is not supported by sufficient structural data (only some possible overturned cumulative layers locally situated towards the top of granulite unit near Chilas) and must be looked upon as a working hypothesis. If correct, it would mean that the Kohistan granulites represent the uppermost part of a roofless, at least 300km wide, calc-alkaline differented body underlying or intruding a volcanic arc.

c) The late-D_1 to syn-D_2 dioritic s.l. intrusions in Kohistan tend to emplace towards the northern edge of the granulite unit. Evidence for partial melting of the (wet) neighbouring amphibolites and/or retrogranulites during D_1 or late D_1 suggests that some of these dioritic injections may have originated by the partial anatexis of hot ($\simeq$ 850°C) and "wet" mafic rocks (Wyllie, 1977). Different devices may be advocated for the late-kinematic dioritic-tonalitic intrusions which outcrop around Utror and Gilgit.

P,T paths and metamorphic gradients.

The P,T paths during the metamorphic stages of the Kohistan sequence are tentatively drawn on Fig. 26. Taking in account P.H. Thompson's (1977) remarks for the "geotherm" aspects deduced from the isograd pattern across erosion surfaces, the estimated T-depth curves during D_1 (curves A, A′, A″ in Fig. 26) and D_2 (curve B) suggest the following :

a) The presence of andalusite in rare silico-aluminous beds indicates that D_1- late D_1 average "geotherms" (A, A′ and A″ were probably near 30°C ± 5°C/km in the upper part of the sequence which suffered the amphibolite facies conditions. Geothermometry estimates as well as the sharp transition zone of pegmatoid metatects and the destruction of olivine Fo_{80} in the presence of plagioclase strongly suggest the geotherms were $\simeq$ 80–100°C/km close to and inside the borders of the granulite unit, i.e. in the range 750–850°C. Within the latter, the T estimates would indicate no significant temperature elevation with depth and it is suggested

Tab. 8. Main mineralogical occurrences *versus* D_1 and D_2 deformations in Kohistan (medium and high grades) (1 : blue-green amphiboles; 2 : green; 3: brownish to greenish brown).

Table 8

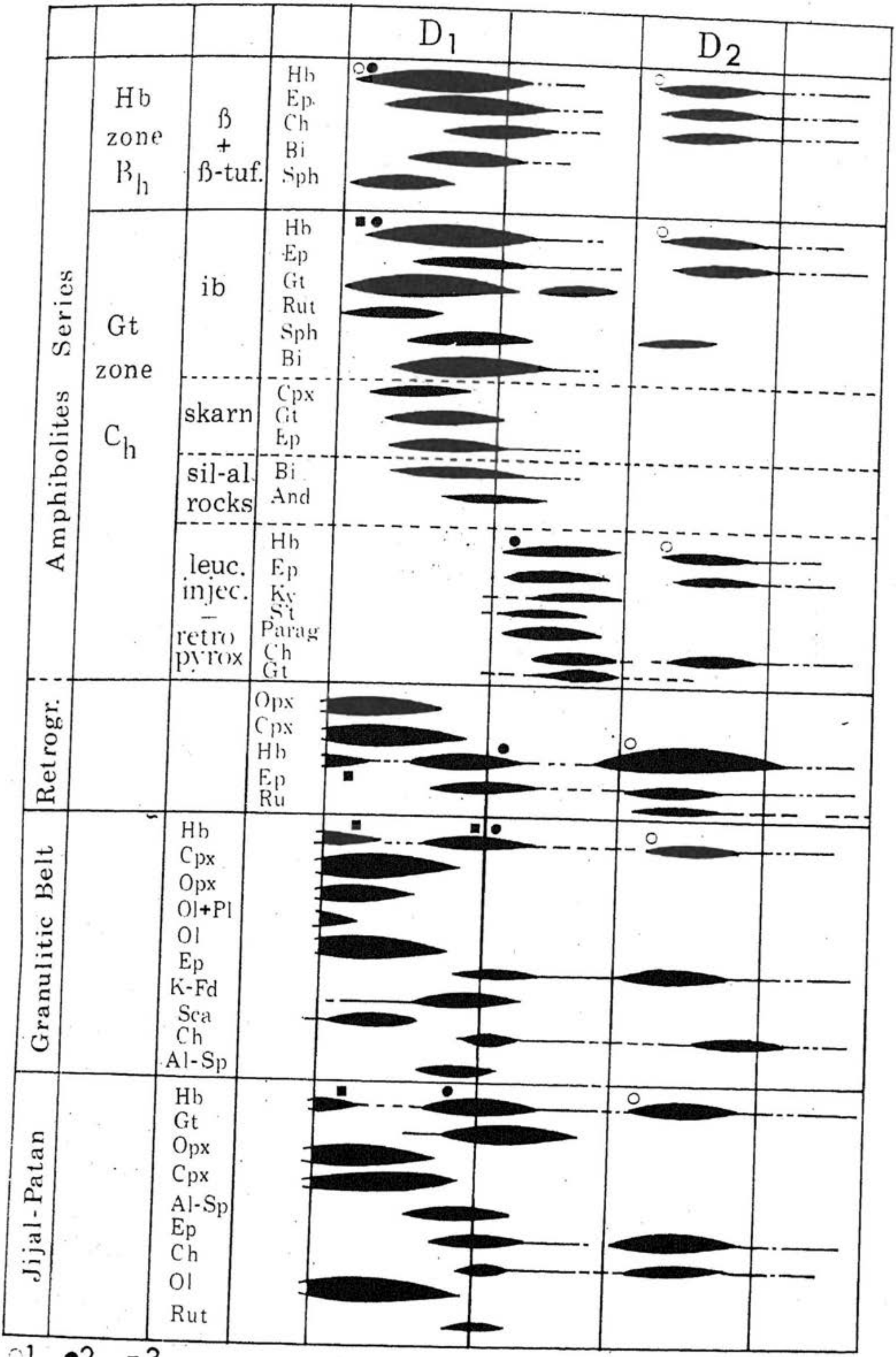
D1
D2
Amphibolites Series
Hb zone B_h
ß + ß-tuf.
Hb
Ep
Ch
Bi
Sph
Gt zone C_h
ib
Hb
Ep
Gt
Rut
Sph
Bi
skarn
Cpx
Gt
Ep
sil-al. rocks
Bi
And
leuc. injec. — retro pyrox
Hb
Ep
Ky
St
Parag
Ch
Gt
Retrogr.
Opx
Cpx
Hb
Ep
Ru
Granulitic Belt
Hb
Cpx
Opx
Ol+Pl
Ol
Ep
K-Fd
Sca
Ch
Al-Sp
Jijal-Patan
Hb
Gt
Opx
Cpx
Al-Sp
Ep
Ch
Ol
Rut

○1 ●2 ■3

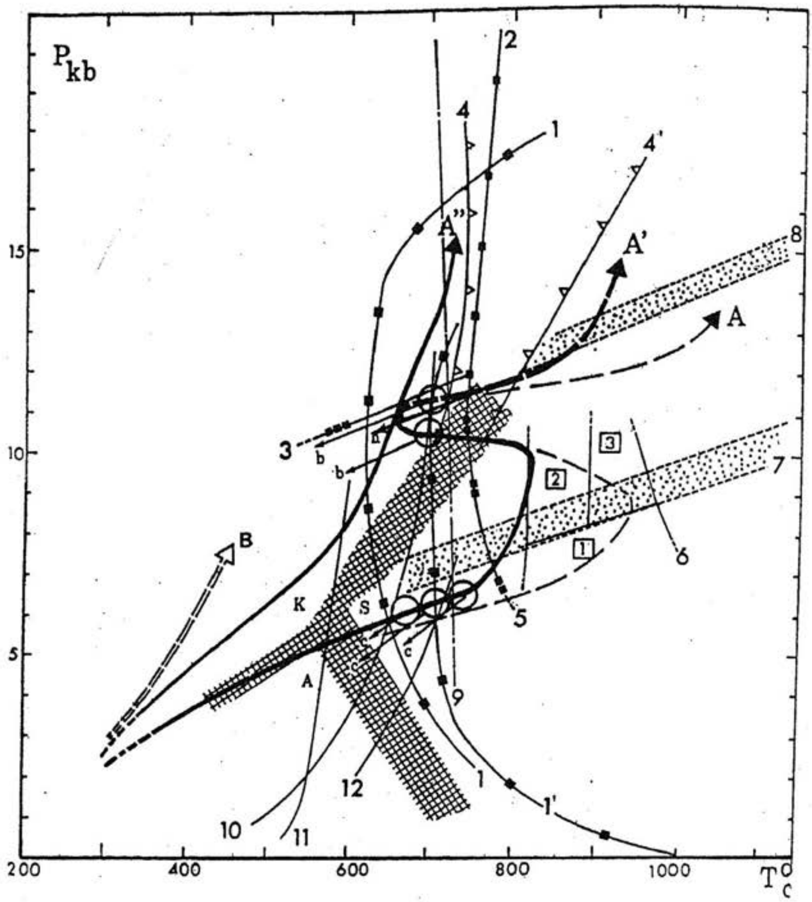

Fig. 26. Tentative $P(P_L)$,T paths during the metamorphic evolution of the Kohistan island arc; geotherms A, A′ respectively for earlier and late-D_1 event when crosscutting the granulitic belt (metanoritic layered intrusive) and the Jijal Patan complex (for A′ see also Fig. 28); geotherm A″ for syn- to late-D_1 event for the latter complexes (see also Fig. 28); geotherm B for syn- to late-D_2 event (K-S-A : average stability fields of the Al_2SiO_5 polymorphs); 1 : beginning of partial melting of water saturated gabbros (Wyllie, 1977); 1′ : approximate melting curve of amphibolitic rocks (Binns. 1969); 2 : zo + ky + quartz ⇄ H_2O + L (Boettcher, 1970); 3 : an + H_2O (low P ass.) ⇄ zo + ky + quartz (high P ass.) (Boettcher, 1970); 4 and 4′ : pure Mg-staurolite high-P stability fie'd (Schreyer and Seifert, 1969); 5 : an + zo + quartz ± gt + H_2O ⇄ L (Boettcher, 1970); 6 : various stability fields in the system CaO-MgO-Al_2O_3- SiO_2-H_2O : [1]: an + forst + H_2O, [2]: an + hb + cpx + sp H_2O, [3]: an + cpx + opx + H_2O; 7 : approximative reaction field of ol + an ⇄ opx + cpx + sp in tholeiitic basalts (see literature in Ringwood, 1975; and Griffin, 1971); 8 : approximative reaction field of opx + an ⇄ cpx + gt in tholeitic basalts (Ringwood, 1975; Griffin, 1971); 9 : Al-ep⇄zoisite (Holdaway, 1972); 10): epidote + q⇄gt + an + mgte + H_2O (Liou, 1973; NNO buffer); 11 : chlorite "out" in metabasites (Liou *et al.*, 1974) as isograd separating the greenschist facies from the so-called epidote-amphibolite facies; 12 : epidote "out" from reaction ep + An0-20⇄An30-40 + q + H_2O under HM buffer conditions (high fO_2 conditions) Liou et al., 1974. Circles with arrows : possible sub-*in situ* melting of amphibolitic rocks giving late D_1 uprising ky +zo + st (a) and/or + zo trondhjemitic melts (b) and dioritic subautochthonous intrusives (c).

that the dT/dP decreased towards the apparent bottom of the granulite unit to become negatively 80 ± 5°C/km and progressively return to a positive slope 25 ± 5°C/km in the southern amphibolitic unit. Occurrence of andalusite and kyanite respectively upon and under the granulite unit as well as the P,T estimates on the gabbro + H_2O partial melting conditions (Wyllie, opt cit.) are in agreement with the drawn aspects of possible early (A) and late (A′) geotherms during D_1. Because of the need to take into account the T estimates in the granulite unit, the conclusion is that the D_1-geotherms are affected by a loop turned toward the T axis in the range 6–10kb. Such a feature is not evident for the geotherm in the western area (Tal) of Kohistan where no granulites occur. Here, the T,P curve shows a classical morphology (curve A″) i.e. it is mainly similar to the geotherms in conductive models of heat transfers from depth.

The aspects of the P,T curves A and A′ towards the deepest parts of the metamorphic pile are not well established. Here, the P–T estimates and textural evidence in the Jijal-Patan complex would indicate a second drop of the temperature and a shifting of the P–T curve towards the T axis. This drop might have been more pronounced during the earlier D_1 – stage (curve A), a feature which may explain : i) – the relict two-pyroxene ± pargasite associations in the Jijal-Patan plagiopyrigarnites, ii) – the late-D_1 opx + plagioclase "out" reaction in these rocks, iii) – some relict (?) and problematical high temperatures (≥ 900°C) in some websterites and two pyroxene-spinel pyroxenites from the mid and upper part of the Jijal-Patan complex.

The reality of a second high-grade loop affecting the D_1 – geotherms may be disputed if the Jijal-Patan complex is supposed to be either the top of an ascending mantle derivated diapir or the remnant of the lowermost part (the level 3 plus the underlying upper mantle) of the oceanic crust as logical basement of the intra-oceanic island arc the Kohistan would represent. The second origin has been claimed by Tahirkheli *et al.* (1979). More recently, Jan and Howie (1981) have also interpreted the pyroxenites and peridotites of Jijal as alpine, i.e. an ophiolite with but an uncommon thickness of clinopyroxenites and dunites. These interpretations are apparently supported by the fact the Jijal-Patan complex seems roughly similar to the classical models (Cann, 1974; Moores and Vine, 1974; Dewey and Kidd, 1977; Juteau *et al.,* 1978) for the transitional zone between the upper mantle under the oceanic crust (harzburgitic tectonites, dunites, pyroxenites) and the layered (cumulative) gabbros and associated rocks of the lowermost parts of the oceanic crust. If so and if no major fault at the top of the Jijal-Patan complex, this would suggest the overlying mafic rocks would present classical features from oceanic crust sections and ophiolitic bodies. This is not clearly the situation (see Fig. 7) because if the overlying material are tholeiitic (Jan, 1977) coarse-grained Flaser-gabbros, blastomylonites and striped amphibolites, they also contain numerous lenses of mafic-ultramafic retrogranulites which are quite identical to the metamorphosed layered calc-alkaline intrusives which built up the Kohistan main "granulite unit". The hypothesis that the Jijal-Patan complex represents in fact an intrusion emplaced throughout the deepest parts of the Kohistan sequence during

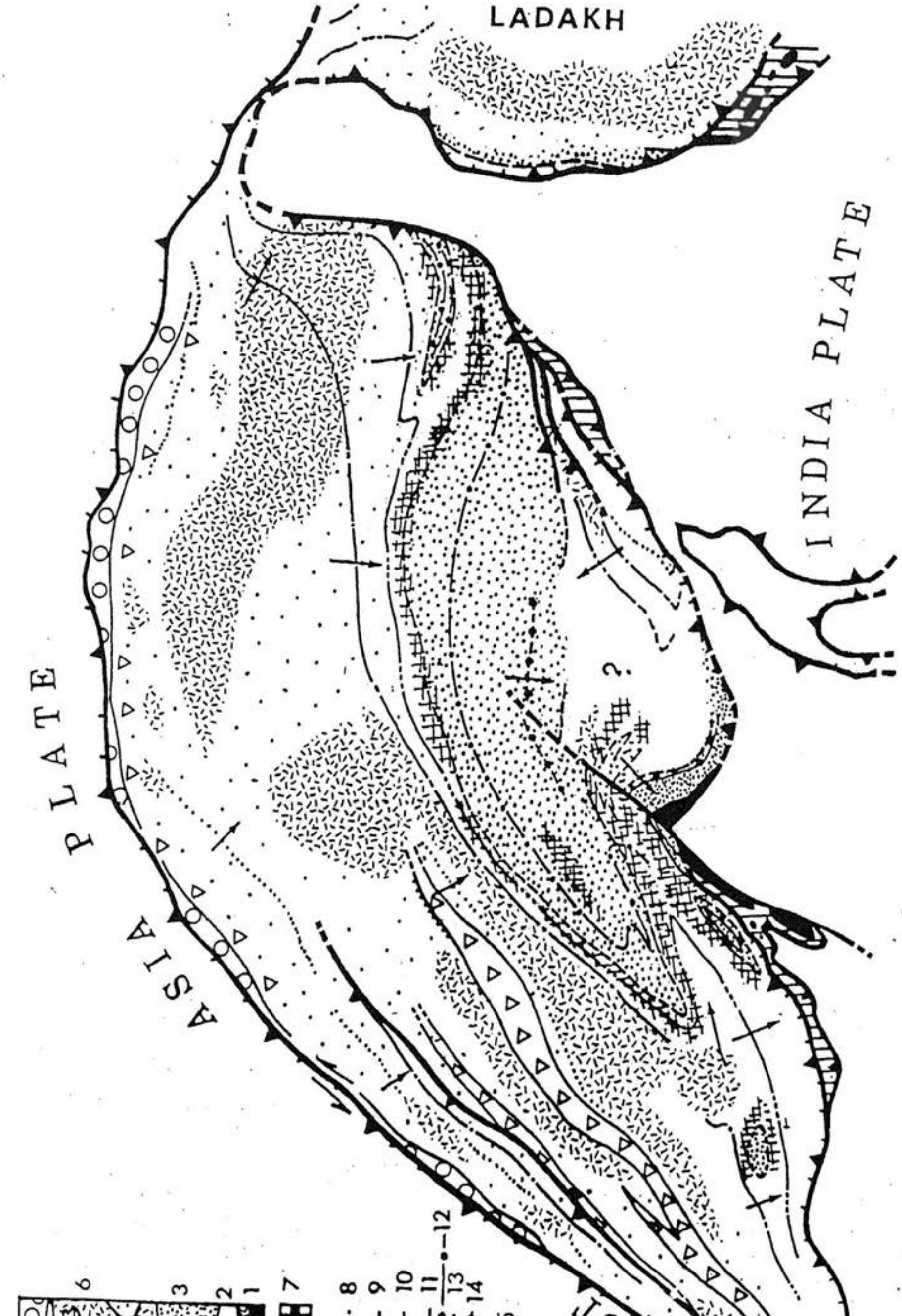
LADAKH
ASIA PLATE
INDIA PLATE
N. SUT
MMT
?
km
0
50
100
5
4'
4
6
3
2
1
7
8
9
10
11
12
13
14
15

the arc building stages is favoured by the following points : i) – the transition between the plagiopyrigarnites of Jijal-Patan and the neighbouring amphibolites – layered retrogranulites is progressive, ii) – the plagiopyrigarnites show inherited websteritic, troctolitic, noritic, and leuconoritic associations with structural and cumulative patterns quite similar to those presented by the granulite unit (i.e. a layered intrusion). In other words, because the Jijal-Patan complex would be a still hot magmatic formation during D_1 (and not a necessary "cold" remnant of the oceanic crust under the arc) its presence in the metmorphic pile would have the same thermal disturbance on the P,T curve aspect as the thermal loop the former intrusion introduces in the mid portion of the Kohistan sequence. This interpretation may explain why the dT/dP (Fig. 26) during D_1 in the lowermost area of the metamorphic pile becomes again strong so it tends to be suparallel to the transition zone where two-pyroxene granulites transform into garnet-cpx granulites (and no true eclogitic rocks with Na-rich cpx) with temperatures estimates accordingly around 850°C at ≃ 40km. Such a feature gives also a convincing explanation for the occurrences of a swarm of late-D_1 pegmatoid injections containing clinozoisite + garnet or clinozoisite + kyanite + staurolite. The latter have parageneses which are in agreement with the experimental data from Boettcher (1970) and Wyllie (1977) on the melting products from H_2O – gabbros systems. For the present purpose, it is again suggested these injections with trondhjemitic to quartz-dioritic compositions are sub-in situ metatects from the high pressure partial melting of amphibolitic rocks.

Mineralogical data on the syn- to late D_2 metamorphic event (Table 8) allow the drawing of the geotherm aspect during D_2. No significant disturbances correlated with the granulite or the Jijal-Patan complexes seem to occur at this time and it is suggested the geotherm has a slope ≃ 25–20°C/km in the mid and lower part of the Kohistan sequence.

Significance of the amphibolitic rocks between the granulite unit and the Jijal-Patan complex.

South of the granulite unit both in Swat Valley and between Jalkot and Patan (Indus Valley), the amphibolitic rocks in contact with the two-pyroxene or garnet-bearing granulites are coarse-grained Flaser-gabbros, opx-bearing retrogranulites and various metawebsteritic metadiopsiditic and metadunitic rocks. The occurrence of the latter rocks suggests parts of the amphibolitic rocks situated between the Jijal-Patan complex and the granulite unit (as well as those which outcrop in the north Mingora U.M. complex) were parts of pre-D_1 calc-alkaline intrusions. Taking in account the field and textural data, an attempt to approach the

Fig. 27. Schematic metamorphic zonation related to D_1-late D_1 metamorphic stage in Kohistan; 1 : Jijal-Patan complex; 2 : amphibolitic series; 3 : granulitic belt; 4 : Utror volcanics; 4' : metasediments; 5 : Yasin group; 6 : dioritic-granulitic late intrusives; 7 : Blueschist-belt and associated "tectonic melange"; 8 : biotite "in" in silico-aluminous rocks; 9 : hornblende "in" in metabasic rocks; 10 : garnet "in" in amphibolitic rocks; 11 : olivine + plagioclase "out" in granulitic rocks; 12 : garnet "in" and opx + plagioclase "out" in granulitic rocks; 13 : garnet in late D_1 leucocratic veinlets crosscutting the granulitic belt (arrows for increasing metamorphic grades during D_1).

geometry of these pre-D_1 magmatic rocks suggests the granulite unit and the Jijal-Patan complex could be remnants of a single magmatic body (Fig. 5). If so, it is suggested synkinematic water transfers along S_1 and along late-D_1 / syn-D_2 shear zones may have occurred throughout the lowermost parts of this magmatic body so the previously (early-D_1) granulitic assemblages transformed into at least late-D_2 high-P amphibole (+ clinozoisite)-rich associations. As shown by Fig. 28 A, we put the hypothesis that the granulite unit and the Jijal-Patan complex (+ the north Mingora rocks) are from a single calc-alkaline pluton possibly cut by a ductile maga-shear zone (DMZ) along which hydratation processes occurred. Late-D_1 water transfer on the margins of this pluton as well as late-D_1 "degranulitization" along the latter shear zone would explain the actual occurrences of the Kohistan retro-granulites and the textural, structural patterns exposed by some striped – amphibolites and Flaser-gabbros.

Geochronological data on D_1 and D_2 events.

As discussed by Bard *et al.* (1980), the great part of the Kohistan sequence was built before the Albian times ($\simeq$ 100 MY) i.e. before the deposition of the unconformable fossiliferous Yasin detrital series. Because of possible Eocene microfossils around Dir and Late Cretaceous limestones in the Deosai plateau east of Kohistan, it is suggested the Kohistan arc was covered by clastic deposits of these ages before or during the first D_1 tectonometamorphic event. This latter develops clearly around 85 MY (i.e. Upper Cretaceous) with the following data :

i) 80 MY on zircons of the Swat pyroxene granulites (U/Pb method, Neisser, pers. comm. (metamorphic event (?))).

ii) 80 MY on phengite from the blueschist belt near Shang La Pass (Maluski, in preparation, $^{39}Ar/^{40}Ar$ method).

iii) 67 MY on a hornblende from a pegmatite cutting the foliation of the granulitic belt around Bahrein (Swat Valley K/Ar method; Jan and Kempe, 1973).

iv) 82 ± 6 MY on a hornblende from a syenitic rock intruding the metamorphosed Dras volcanics (= Utror volcanics) at Kargil in Ladakh-Deosai east of the Kohistan ($^{39}Ar/^{40}Ar$ method; Brookfield and Reynolds, 1981).

These data point to a major Upper Cretaceous event (D_1) in Kohistan that is synchronous with the blueschist metamorphism in the MMT suture. It is suggested on the other hand that the calc-alkaline volcanism and plutonism in Kohistan is probably Lower-Mid Cretaceous (110 ± 10 MY) and some late intrusions are perhaps Late Cretaceous (90 ± 10 MY).

In Yasin area, measurements of syn-to late D_2 diorites have ages ranging betwen 37 and 56 MY (lit. in Bard et al., 1980). $^{39}Ar/^{40}Ar$ method has recently given 50 ± 5 MY ages on biotite from late kinematic diorite east of Deosai and on biotite from metamorphic orthogneisses (Bunner orthogneisses) and surrounding metasediments within the Indian plate series south of Kohistan (Maluski, in preparation). Similar method used by Brookfield and Reynolds yields about 42 MY from micas in a deformed (D_2) granodiorite north of MMT suture near Skardu

(Deosai-Ladakh area). All these measurements indicate D_2 is probably Upper Eocene/Lower Oligocene in the Kohistan-Ladakh and this tectono-metamorphic event is probably approximately synchronous with the first alpine phase within the Indian plate south of MMT suture.

CONCLUSIONS

Thermal models during D_1 and D_2.

The zonographic patterns related to the D_1 tectono-metamorphic phase in Kohistan (Fig. 27) as well as the aspects of the geotherms (Fig. 26) during this event suggest the D_1 – isotherms are centered on the orthoderivated granulites of the Kohistan sequence. The magmatic origin of the granulites has been discussed above so the question arises whether theoretical and/or experimental data are compatible with the conclusion that the thermal structure during D_1 was mainly controlled by still very hot pluton(s) in the Kohistan arc. For this purpose the work of Wells (1980) is of a particular interest because this author has predicted that the "distorted" aspect of the geotherms in a crustal segment may persist 20 MY after the emplacement of large magmatic intrusion(s). Injection of enormous 1000–1100°C calc-alkaline plutons in a volcanic arc must introduce heat sources that may slowly cool so 20 ± 5 MY after their emplacement, the local "normal" geotherms may be modified by the plutons. Because the Kohistan "granulitic belt" (i.e. a layered noritic pluton) and the Jijal-Patan complex formed at least a 30000 km³ body probably 15–25 MY before the D_1 event, it seems the D_1 thermal features of the Kohistan sequence could be related to a large calc-alkaline pluton(s) which intruded the arc during the Mid Cretaceous. As discussed by A.B. Thompson (1981), Wells's (1980) magmatic accretionary models are accordingly such processes which provide the most efficient means of simultaneous heating and evolving tectonically thickened crust so as to expose low-to intermediate pressure facies series at the surface. The Kohistan situation fits nicely with these models and as shown by the Fig. 28A, it is suggested the thermal structure during D_1 was closed to the drawn aspects of the isotherms in the D_1 – deformed Kohistan sequence. The fact D_1 seems synchronous with the blueschist metamorphism in the MMT "tectonic melange" together with petrological and mineralogical studies by Guiraud *et al.* (in preparation), the isotherms (Fig. 28A) throughout the MMT suture are thought to have had the aspects predicted by the models of Oxburgh and Turcotte (1974), Graham and England (1976), England and Richardson, (1977) or Bird (1978) for various situations of overthrusting slabs i.e. a strong narrow downbowing structure of the isotherms between the obducting Kohistan arc (Tahirkheli *et al.,* 1979; Bard *et al.,* 1980; Coward *et al.,* 1982) and the downgoing Indian plate. From a general viewpoint, it is noteworthy that the blueschist facies conditions cannot be again convincingly related to early subduction stages (Miyashiro, 1972; Ernst, 1973) but rather during (Mattauer *et al.,* 1977) and perhaps after (Thompson *et al.,* 1981; Caron *et al.,* 1981) obduction processes in colliding orogens.

Apart from the northern areas invaded by syn- to late D_2 dioritic-granodioritic intrusions, it seems the isotherm distribution during D_2 would be a relatively simple one (Fig. 28B). In response to a slow thermal re-equilibration, these isotherms have become flat so they crosscut the earlier metamorphosed calc-alkaline pluton(s). Assuming the D_2 tectonometamorphic event is Oligocene and synchronous with the first alpine tectonometamorphic phase in the Indian plate south of the MMT suture, the thermal structure of northern Pakistan 40–50 MY ago was probably in agreement with possible (?) "folded" isotherms and inverse metamorphism (Le Fort, 1975) in those parts affected by synmetamorphic magashears similar to the polyphase MCT shear zone (Gansser, 1964; Brunel and Andrieux, 1980). The downward-bowed aspect of the isotherms in the reactivated MMT suture is probably notably less pronounced (Guiraud *et al.*, opt. cit.) than during D_1 so D_2 – mesozonal Barrovian-type recrystallisations may have overprinted the earlier blueschist paragenesis.

The D_1 and D_2 thermal stuctures and the plate-scale models for the Kohistan and neighbouring areas.

Recently proposed plate-scale models for the Kohistan (Tahirkheli *et al.*, 1979; Bard *et al.*, 1980), the Afghanistan (Tapponnier *et al.*, 1981) and the Deosai-Ladakh areas (Brookfield and Reynolds, 1981) raise questions as to how the D_1 and D_2 tectono-metamorphic phases would fit into the proposed models. The D_1 thermal structure is compatible with the suggestion that the Kohistan is a Lower-Mid Cretaceous intraoceanic island arc obducted onto the Indian continental margin during the Upper Cretaceous. The absence of sialic material within the arc implies that the suggestion that the Kohistan sequence formed on a continental margin during the

---

Fig. 28. Possible aspects of the thermal structures in the Kohistan obducted island arc during its tectonometamorphic evolution. A : *Intraoceanic subduction stage with arc building* $\simeq$ 100*MY ago* i.e. just after the last emplacement of calc alkaline plutonic and volcanic rocks [1 : hypothetic ascending upper mantle diapir (4) under the arc; 2 : partial melting of the diapir giving rise to the Jijal-Patan type cumulative (1, 4, 21) mafic-ultramafic rocks and to the layered lopolithic intrusion (which will be the future granulite belt of Kohistan); 3 : basaltic tuffs and lavas (tholeiitic, with abyssal and/or arc affinities, up to calc-alkaline (1, 51): 4 : Utror andesites, dacites and rhyodacites (calc-alkaline series) (7); the ocean relict between the Kohistan arc and India was probably 800km wide (15) (?) 100MY ago; Asia was at 6500-6000km from the arc]. B : *Obduction stage* $\simeq$ 85*MY ago and* D_1 *event* (A′ and A″ = vertical profiles for "geotherms" A′ and A″ in Fig. 3; 1 : granulite unit from a metamorphic calc-alkaline layered pluton; 2 : Jijal-Patan complex as remnant of an ascending mantle diapir which suffered partial melting; 3 : basic anatexis around the granulite and amphibolitization of the latter in response to H_2O transfers from the neighbouring amphibolite units and associated metasediments; o.c. : oceanic crust as the basement of the Kohistan arc sequence (note that the HP metamorphism in the blueschist belt under MMT is related to D_1); MMT : Main Mantle Thrust; DMZ : ductile northwards main zone (approximative attitude). C : *Oligocene collision of India (north-western edge) against Asia during the* D_2 *tectonometamorphic event* (note here that the 50 40MY syn- to late-D_2 intrusives are not related to a Late Eocene-Oligocene southwards subduction on Andean type margin (10, 18) but rather correlated (not proved) to partial anatectic process (with possible hybridization with products from melting of the arc crust + underlying mantle) of the Indian plate under the obducted Kohistan arc).

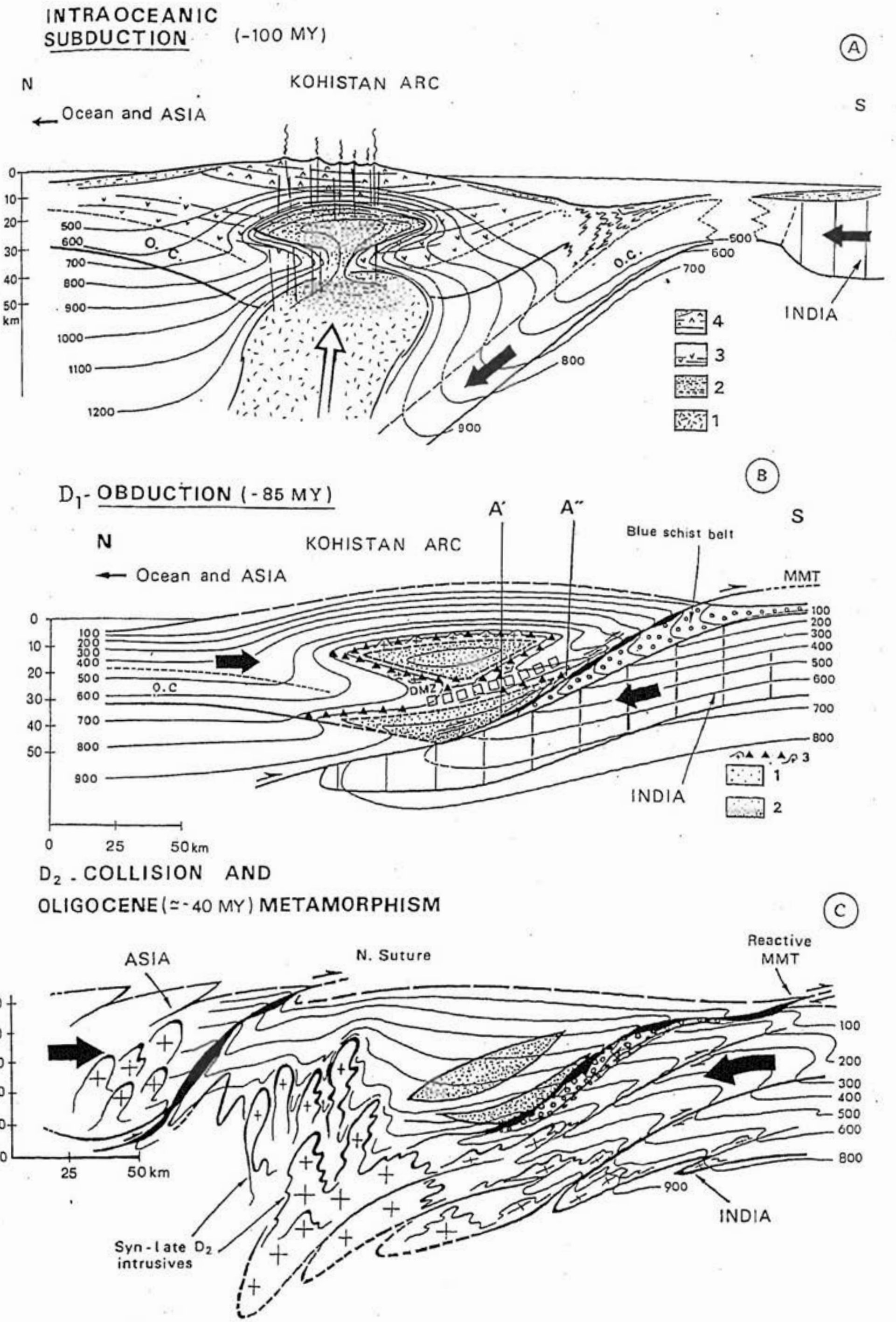
INTRAOCEANIC SUBDUCTION (-100 MY)
A
N
KOHISTAN ARC
S
← Ocean and ASIA
O. C.
O.C.
INDIA
0
10
20
30
40
50
km
500
600
700
800
900
1000
1100
1200
500
600
700
800
900
4
3
2
1
B
D1- OBDUCTION (-85 MY)
A′
A″
S
N
KOHISTAN ARC
Blue schist belt
← Ocean and ASIA
MMT
O.C
DMZ
100
200
300
400
500
600
700
800
900
3
1
2
INDIA
0
25
50 km
D2 . COLLISION AND
OLIGOCENE (≃-40 MY) METAMORPHISM
C
ASIA
N. Suture
Reactive
MMT
0
10
20
30
40
50
25
50 km
100
200
300
400
500
600
800
900
INDIA
Syn-late D2
intrusives

Mid Cretaceous (Andrews-Speed and Brookfield, 1982) is incorrect. The results of the present work are in agreement with Tapponnier *et al.* (1981) in that they do not support the idea D_1 is synchronous with a Late Cretaceous-Early Eocene collision (Andrews-Speed and Brookfield, opt. cit.) between India and Asia. The opening rates (Molnar and Tapponier, 1975) of the Indian Ocean introduce constraints for the Tethys closure that require the beginning of collision and welding of Asia and India during the Late Eocene-Lower Oligocene i.e. $\simeq$ 40MY ago. This time corresponds to the D_2 tectono-metamorphic event in Kohistan, Ladakh and south of MMT in northern Pakistan and Kashmir. The emplacement of the syn- to late D_2 heterogeneous gabbro-dioritic-granodioritic intrusions in northern Kohistan and Ladakh would correspond in such a collision proces to the early and late ascent of anatectic products from the melting of the Indian plate and uper mantle 50--80km beneath the obducted island arc (Fig. 28B). An alternative possibility (Brookfield and Reynolds, 1981) is that the 40–50MY intrusions are the products of a second calc-alkaline series corresponding to an Andean type magmatism in response to a southwards subduction (Fig. 28B') during the Late Eocene-Oligocene. No structural and geochemical data support this hypothesis.

Origin of the rocks of the granulite unit and the Jijal-Patan complex.

Among the numerous problems in Kohistan is the primary source of the rocks of the granulite unit and the Jijal-Patan complex. The pioneer work of Jan (1977) considered that the two associations were not petrogenically linked and the Jijal-Patan complex was interpreted as a possible alpine-ultramafic complex, i.e. an ophiolite. More recently Bard *et al.* (1980), Jan (1980), and Coward *et al.* (1982) suggested that the Jijal-Patan complex is a layered calc-alkaline pluton with the same origin as the rocks of the layered "granulitic belt" i.e. a large differenciated gabbro-noritic intrusion. [It may be noted that Jan and Howie (1981) considered the pyrigarnites and plagiopyrigarnites of the Jijal-Patan complex to be comagmatic with the pyriclasites (noritic granulites) but the diopsidites-peridotites forming the lower unit of the Jijal-Patan complex were considered to be a mantle diapir]. These suggestions thus imply that the parental rocks of the granulite unit and the Jijal-Patan complex are comagmatic. As previously discussed they would represent the remnants of either a simple large plutonic complex or two layered lopoliths possibly emplaced during a Cretaceous arc building stage in the Paleotethys. If correct, this would be a major contribution to the knowledge of the internal structure and petrographical pattern of an intra-oceanic island arc. In this respect it is noteworthy to quote there are strong similarities between the former calc-alkaline layered pluton(s) of Kohistan and, for example, the nature of the blocks and inclusions (cumulative and layered troctolites, norites, leuconorites, etc.) found within the volcanoes of the Lesser Antilles island arc (Arculus and Wills, 1980). Taking in account the geological setting of the Kohistan calc-alkaline pluton(s), it is suggested the source of the latter may be a mantle derived diapir which had suffered partial melting at depths near 50km. Such a process would have left Fo_{90} – harzburgitic restites and would have generated olivine-tholeiitic melts (Green and Ringwood, 1968; Ringwood, 1975; Jaques and Green, 1980) that may have precipitated near in-situ (Jijal-Patan) or escaped to crystallize and "accumulate" dunites, orthopyroxenites and cpx ± opx ± olivine (Fo_{90}) ± plagioclase bearing rocks (i.e. the Jijal-Patan and the granulite unit rock -types). With respect to the disputed origin of calc-alkaline sequences in active orogenic belts associated with consuming plate margins, the Kohistan plutonic rocks could provide valuable informations even though they have suffered metamorphic overprints and ductile deformation.

Acknowledgements. The present study was possible after field studies in 1978, 1979 and 1981 with the financial support of the Centre National de la Recherche Scientifique (A.T.P. INAG "Geodynamique II"). EMA were performed with the aid of the latter organisation, the L.A. 266 and the Laboratoire de Petrologie des Zones Profondes (University of Montpellier II).

I gratefully acknowledge Prof. Dr. Tahirkheli and Prof. Dr. Jan from the Center of Geology of the University of Peshawar for all the facilities they offered to visit the splendid Kohistan geology. I am grateful for valuable and enthusiastic discussion with these colleagues and with members of the Himalayan team of Montpellier (Dr. Proust, Maluski, Matte and Burg). I also thank Dr. Dupuy for pertinent criticism of the petro-chemical discussion of this study. The paper also benefited from perceptive comments by Dr. P.H. Thompson who also aided to correct the English translation. Mrs. Lanco typed the paper, Mr. Boeuf drew some figures and Mr. Tejedo made the thin sections, with their usual skill, good nature and efficiency.

APPENDIX

The present microprobe analyses were performed by the author with a three spectrometers automatised CAMEBAX MPA at the University of Sciences and Techniques of Languedoc (Montpellier) : operating conditions ordinarily were 15KV, sample current near 10nA and beam diameter around 5-1 μ : present data are average from three to six analyses on each mineral.

Sample locations and petrography :

P21 : 4km north of Jijal (Indus Valley), Pyrigarnite : cpx + gt (+ greenish hb).

P23c : 4.5km north of Jijal, Pyrigarnite : gt + cpx (+ green hb + clinoz + ores + rutile).

P23d : 4.6km north of Jijal, Hb-pyrigarnite : gt + greenish brown Hb + cpx (+ ores)

P24 : 4.6km north of Jijal, Plagiopyrigarnite : cloudy pl + cpx + zoi (symplect) + gt + clinoz (+ calcite + albite + chlorite).

P24' : 4.7km north of Jijal, Hb-pyrigarnite : gt + cpx + zoned green (II) hb (+ clinoz + ore + sphene + chlorite + blue-green actinolite around gt).

P127 : Bahrein village (Swat Valley), Sheared amphibolite : An50 + greenish brown hb + q (+ clinoz).

P130 : Bahrein village, Pyriclasite : An50 + cpx + opx (+ brownish green hb + ilmenite).

P135 : 1km south of Fathepur, Hb-pyriclasite : An45 + opx + light green hb (+ biotite + ores + rutile).

P136 : 5km north of Bahrein, Striped opx-gt gneiss : An35 + opx + q + An30 + gt + bi (+ ores + clinoz + chlorite).

P140 : 7km south west of Fathepur, Striped garnet amphibolite : An30→25 + green hb + garnet (+clinoz + q + sphene).

P142 : 10km west of Khwazakhela, Garnet-amphibolite : An27→5 + green hb + gt + clinoz + q (+ chlorite + pistacite + rutile).

P155 : 7km north of Bahrein, Opx - gt gneiss : An35 + opx + q and q + An30 + gt + bi (+ ores + clinoz + chlorite).

P291 : 11km south of Timurgara (Panjhkora Valley), Striped-amphibolite : An27→18 + green hb + pistacite / clinoz + q (+ rutile + ilmenite).

P292 : 10.5km south of Timurgara, Garnet-amphibolite : Cloudy plag + green hb + gt + pistacite + q (+ leucoxene + ores + sec. chlorite + apatite).

P293 : 4km south of Timurgara, Retrogranulite : cloudy plag → An02 rim + brown-green hb + relic. cpx + actinolite (+ chlorite + pistacite).

P297 : 4km south of Timurgara, Flaser-gabbro : An45→35 + green hb + q (+ ilmenite + rutile + apatite + clinoz).

PK22 : 4km north of Jijal (Indus Valley), Olivine-clinopyroxenite : Cr-cpx + Fo_{90} + chromite.

PK22" : 4km north of Jijal, Garnetite : gt (+ white mica + blue green hb + clinoz + cloudy plag).

PK23a : 4.5km north of Jijal, Pyrigarnite : cpx + gt + pale-green hb (+ sphene + rutile + chlorite + ilmenite + clinoz).

PK23b : 4.5km north of Jijal, Plagiopyrigarnite (cataclastic) : cpx + gt + cloudy plag + clinoz + q (+ rutile + blue-green hb + pistacite).

PK23c : 4.8km north of Jijal, Hb-pyrigarnite : cpx + gt + green hb (+ ilmenite/Ti-mgt + white mica).

PK23e : 4.8km north of Jijal, Hb-pyrigarnite : cpx + gt + green hb (+ clinoz + q + ores).

GI5a : 3.5km north of Jijal, Diopsidite : cpx (+ ores + chlorite).

GI7 : 3.8km north of Jijal, Hb-websterite : cpx + opx + pale green-brown hb.

GI9a : 4km north of Jijal, Spinel-diopsidite : cpx + opx + green spin (+ pale green hb + ores + apatite).

GI9b : 4km north of Jijal, Websterite : cpx + opx (+ ores + chlorite).

GI12a : 5km north of Jijal, Amphigarnite : An70 + gt + pale green hb + clinoz + zo (+ calcite + q).

GI16 : 3km north of Patan (Indus Valley), Garnet amphibolite : cloudy plag→An02 + green hb + gt + clinoz + zo + q (+ rutile + sphene + apatite + ores + chlorite).

GI17b : 5km north of Patan, Ky-clinoz felsite : q + An46→35 + clinoz + kyanite + staurolite (+ paragonitic mica + chlorite + calcite + rutile + green hb).

GI18 : 5.2km north of Patan, Garnet amphibolite : An40→30 + green hb + gt + q + clinoz (+ biotite + chlorite + ores).

GI19 : 6km north of Patan, Coarse-grained amphibolite : An48→37 + green hb + q (+ sphene + apatite + ores).

GI20a : 6.5km north of Patan, Leucoamphibolite : An37 + q + green/blue green hb + clinoz (+ biotite + sphene + rutile + apatite + ores).

GI21a : 6.6km north of Patan, Flaser-gabbro : cloudy plag + green hb + clinoz (+ rutile + sphene + apatite).

GI25b : 10km north of Jalkot (Indus Valley), Contact dunite/troctolite (cumulates) : Fo_{82} + cpx + pale green hb / An45 + cpx + green spinel verm. + (relict olivine + q).

GI41 : 12km west of Chilas (Indus Valley), Pyriclasite : An70 + cpx + opx + green hb (+ q + clinoz + biotite + ores).

GI42 : 11km west of Chilas, Layered pyriclasite : opx + cpx + pale green-brown hb + An50/opx + cpx + green hb + An48 (+ ilmenite).

GI45 : 10.5km west of Chilas, Pyriclasite : cpx + opx (+ An50).

GI53 : 10km west of Chilas, Pyriclasite : An47 + cpx + opx + green hb (+ q + biotite + chlorite + white mica + calcite + apatite + ores).

GI56 : 9km west of Chilas, Dunite : Fo_{81} + opx + pale green hb (+ green spinel + plag).

GI58 : 9km west of Chilas, Troctolite : An95 + opx + cpx + pale brown-green hb + green spinel + relictual olivine Fo_{80} (+ q + magnetite + biotite).

REFERENCES

Ahmed, Z., 1977. Electron probe composition of the spinel phases from a lherzolite near Bar-Bandai, Swat District, Pakistan. Geol. Bull. Punjab Univ. 14, 45—50.

Ackermand, D., & Raase, P., 1973. Coexisting zoisite and clinozoisite in biotite schist from the Hohe Tauern, Austria. Contrib. Miner. Petr. 42, 333—341.

Akella, J., 1976. Garnet pyroxene equilibria in the system $CaSiO_3 — MgSiO_3 — Al_2O_3$, and in a natural mineral onexture. Amer. Miner. 61, 589—598.

Anastasiou, P., & Seifert, F., 1972. Solid solubility of Al_2O_3 in enstatite at high temperatures and 1-5kb water pressure. Ibid. 34, 272—287.

Andrews-Speed, C.D., & Brookfield, M.E., 1982. Middle Paleozoic to Cenozoic geology and tectonic evolution of the northern Himalaya. Tectonophysics 82, 253—275.

Atkins, F.B., 1969. Pyroxenes of Bushweld intrusion, South Africa. J. Petr. 10, 222—249.

Banno, S., 1964. Alumina content of orthopyroxene as geologic barometer. Japan. J. Geol. Geogr. 35, 115—121.

Bard, J.P., 1970. Hornblendes formed during the Hercynian progressive metamorphism of the Aracena metamorphic belt (SW Spain). Contrib. Miner. Petr. 28, 117—134.

——, Maluski, H., Matte, P., & Proust, F., 1980. The Kohistan sequence : crust and mantle of an obducted island arc. In : Proc. Int. Com. Geodyn., Gr. 6, Mtgs. Peshawar; Spec. Iss. Geol. Bull. Univ. Peshawar 13, 87--93.

Bartholome, P., 1962.Iron-magnesium ratio in associated pyroxenes and olivines. Bull. Geol. Soc. Amer. Buddington Vol., 1—20.

Binns, R.A., 1969. Experimental studies of metamorphism at Broken Hill. In "Broken Hill Mines". Aust. Inst. Min. Metall., 199—205.

Bird, P., 1978. Stress and temperature in subduction shear zones : Tonga and Mariana. Geophys, J.R. Astr. Soc. 55, 411—434.

Blattner, P., 1976. Replacement of hornblende by garnet in granulite facies assemblages near Milford Sound, New Zealand. Contrib. Miner. Petr. 55, 181—190.

Boettcher, A.L., 1970. The system $CaO\text{-}Al_2O_3\text{-}SiO_2\text{-}H_2O$ at high pressures and temperatures. J. Petr. 11, 337—379.

Boyd, F.R., 1970. Garnet peridotites and the system $CaSiO_3\text{-}MgSiO_3\text{-}Al_2O_3$. Miner. Soc. Amer., Spec. Paper 3, 63—75.

—— & England, J.L., 1964. The system enstatite-pyrope. Carn. Inst. Washington Ann. Rep., 157—161.

Brookfield, M.E. & Reynolds, P.H., 1981. Late Cretaceous emplacement of the Indus suture zone ophiolitic melanges and an Eocene-Oligocene magmatic arc on the northern edge of the Indian plate. Earth. Plan. Sci. Letters 55, 157—162.

Brunel, M. & Andrieux, J., 1980. Sur un modele tectonique explicatif du metamorphisme "inverse" Himalayen. C.R. Acad. Sci. 291, 609—612.

Cann, J.R., 1974. A model for oceanic crustal structure developed. Royal. Astro. Soc. Geophys. J. 39, 169—187.

Caron, J.M., Parrot, J.F. & Whitechurch, H., 1981. Blueschist metamorphism and collision. Terra cognita., Sp. issue, 66 (Abstract).

Coleman, R.G., Lee, D.E., Beatty, L.B. & Brannock, W.W., 1965. Eclogites and eclogites : their differences and similarities. Geol. Soc. Amer. Bull. 76, 483—508.

Coward, M.P., Jan, M.Q., Rex. D., Tarney, J., Thirlwall, M. & Windley, B.F., 1982. Structural evolution of a crustal section in the western Himalaya. Nature 295, No. 5844, 22—24.

Deer, W.A., Howie, R.A. & Zussman, J., 1963. Rock forming minerals, Vol. 2. Longmans, London.

Den Tex, E., 1972. The facies groups and facies series of metamorphism and their relation to physical conditions in the earth's crust. Lithos 4, 23—41.

De Waard, D., 1965. A proposed subdivision of the granulite facies. Am. J. Sci. 263, 455—461.

Dewey, J.F. & Kidd, W.S.F., 1977. Geometry of plate accretion. Geol. Soc. Amer. Bull. 88, 960—968.

Edgar, A., Mottana, A. & Macrae, N.D., 1968. The chemistry and cell parameters of omphacite and related pyroxenes. Miner. Mag. 37, 61—74.

Eichelberger, J.C., 1978. Andesitic volcanism and crustal evolution. Nature 275, 21—27.

Ellis, D.J. & Green, D.H., 1979. An experimental study of the effect of Ca upon garnet-clinopyroxene Fe-Mg exange equilibria. Contrib. Miner. Petr. 71, 13—22.

Enami, M. & Banno, S., 1980. Zoisite clinozoisite relations in low- to medium-grade high-pressure metamorphic rocks and their implications. Min. Mag. 43, 1005—1013.

Engels, J.P., 1972. The catazonal poly-metamorphic rocks of Cabo Ortegal (NW Spain), a structural and petrographic study. Leid. Geol. Meded. 48, 83—133.

England, P.C. & Richardson, S.W., 1977. The influence of erosion upon the mineral facies of rocks from different metamorphic environments. J. Geol. Soc. London 134, 201—213.

Ernst, W.G., 1973. Blueschist metamorphism and P,T regimes in active subduction zones. Tectonophysics 17, 255—272.

Ferry, J. & Spear, F.S., 1978. Experimental calibration of the partitioning of Fe and Mg between biotite and garnet. Contrib. Min. Pet. 44, 250—274.

Fleet, M.E., 1974. Partition of major and minor elements and equilibrium in coexisting pyroxenes. Contrib. Min. Pet. 44, 259—274.

Ganguly, J., 1972. Staurolite stability and related parageneses : theory, experiments and applications. J. Pet. 13, 335—365.

——— 1979. Garnet and pyroxene solid solutions and geothermometry based on Fe Mg distribution coefficients. Geochim. Cosmochim. Acta 43, 1021—1029.

Gansser, A., 1964. Geology of the Himalayas. Interscience, J. Wiley and Sons, London.

——— 1980. The division between Himalaya and Karakorum. Proc. Int. Com. Geodyn., Gr. 6, Mtgs. Peshawar; Spec. Issue Geol. Bull. Univ. Peshawar 13, 9—22.

Gorshkov, G.S., 1969. Intraoceanic islands, east-Pacific ridge, island arcs : volcanism and upper mantle. Tectonophysics 8, 213—221.

Graham, C.M. & England, P.C., 1976. Thermal regimes and regional metamorphism in the vicinity of overthrust faults : an example of shear heating and inverted metamorphic zonation from southern California. Earth Planet. Sci. Letters 31, 142—152.

Green, D.H., 1964. The petrogenesis of the high-temperature peridotite intrusion in the Lizard area, Cornwall. J. Pet. 5, 134—188.

——— & Ringwood, A.E., 1967. An experimental investigation of the gabbro to eclogite transformation and its petrological applications. Geochim. Cosmochim. Acta 31, 767—833.

——— & ——— 1970. Mineralogy of peridotitic compositions under upper mantle conditions Phys. Earth Planet. Interiors 3, 359—371.

——— & ——— 1972. A comparison of recent experimental data on the gabbro-garnet granulite-eclogite transition. J. Geol. 80, 277—288.

Green, T.H., 1967. An experimental investigation of sub-solidus assemblages formed at high pressure in high alumina basalt, kyanite eclogite and grosspydite compositions. Contrib. Min. Pet. 16, 84—114.

——— & Ringwood, A.E., 1968. Genesis of the calc-alkaline igneous rock suite. Contrib. Min. Pet. 18, 105—162.

——— 1970. High pressure experimental studies on the mineralogical constitution of the lower crust. Phys. Earth Planet. Interiors 3, 441—450.

Griffin, W.L.. 1971. Genesis of coronas in anorthosites of the upper Jotun nappe, Indre Sogn, Norway. J. Pet. 12, 219—243.

Hamlyn, P.R., 1980. Equilibration history and phase chemistry of the Panton sill, western Australia. Amer. J. Sci. 280, 631—668.

Hansen. B.F., 1981. The transition from pyroxene granulite facies to garnet-clinopyroxene granulite facies. Experiments in the system CaO-MgO-Al_2O_3-SiO_2. Contrib. Min. Pet. 76, 234—242.

Hensen, B.H.. 1976. The stability of pyrope-grossular garnet with exces silica. Contrib. Min. Pet. 55, 279—292.

Hess, J.J., 1960. Stillwater igneous complex, Montana. Geol. Soc. Amer., Mem. 80.

Holdaway, M.J.. 1972. Thermal stability of Al-Fe epidotes as function of F_{co_2} and Fe content. Contrib. Min. Pet. 37, 307—340.

Howie, R.A., 1965. The pyroxenes of metamorphic rocks.. In : Controls of metamorphism (Oliver & Boyd Ed.), London, 319—326.

Irving, O.J., 1974. Geochemical and high pressure experimental studies of garnet pyroxenite and pyroxene granulite xenoliths from the Delegate basaltic pipes, Australia. J. Pet. 15, 1—40.

Ito,K. & Kennedy, G.C., 1971. An experimental study of the basalt-garnet granulite-eclogite transition. In : The structure and physical properties of the earth's crust. Amer. Geophys. Union, Monograph 14, 303—314.

Jan, M.Q., 1977. The mineralogy, geochemistry and petrology of Swat Kohistan, NW Pakistan. Unpubl. Ph.D. Thesis, Univ. London.

——— 1980. Petrology of the obducted mafic and ultramafic metamorphites from the southern part of the Kohistan island arc sequence. Geol. Bull. Univ. Peshawar 13, 95—107.

——— 1982. Chemical changes accompanying the granulite to amphibolite transition in Swat, NW Pakistan. In 'Contemporary Geoscientific Researches in Himalaya, 2', (A.K. Sinha ed.), 49—52.

——— & Howie, R.A., 1980. Ortho- and clinopyroxenes from the pyroxene granulites of Swat Kohistan, northern Pakistan. Min. Mag. 43, 715—726.

——— & ——— 1981. The mineralogy and geochemistry of the metamorphosed basic and ultrabasic rocks of the Jijal complex, Kohistan, NW Pakistan. J. Pet. 22, 85—126.

——— & ——— 1982. Hornblendic amphiboles from basic and intermediate rocks of Swat-Kohistan, northwest Pakistan. Am. Mineral. 67, 1155—1178.

——— & Kempe, D.R.C., 1973. The petrology of the basic and intermediate rocks of Upper Swat, Pakistan. Geol. Mag. 110, No. 3, 285—300.

Jaques A.L. & Green. D.H., 1980. Anhydrous melting of peridotites at 0-15Kb pressure and the genesis of tholeitic basalts. Contrib. Min. Pet. 73, 287—310.

Juteau, T., Nicolas, A., Dubessy, J., Fruchard, J.C. & Bouchez. J.L., 1978. Structural relationships in the Antalya ophiolite complex, Turkey : possible model for an oceanic ridge. Geol. Soc. Amer. Bull. 88, 1740—1748.

Kostyuk, E.A. & Sobolev, V.S., 1969. Paragenetic types of calciferous amphiboles of metamorphic rocks. Lithos 2, 67—81.

Kretz, R., 1961. Some applications of thermodynamics to coexisting minerals of variable composition. Examples : orthopyroxene-clinopyroxene and orthopyroxene-garnet. J. Geol. 69, 361—387.

Krogh, E.J., 1980. Compatible P-T conditions for eclogites and surrounding gneiss in the Kristiansund area, western Norway. Contrib. Min. Pet. 75, 387—393.

Kuno, H., 1968. Differenciation of basaltic magmas. In : Basalts (Hess, H.H. & Poldervaart, A. Ed.), Willey, New York, 623—688.

Kushiro, I. & Yodger, H.S., 1966. Anorthite-forsterite and anorthite-enstatite reactions and their bearing on the basalt-eclogite transformation. J. Pet. 7, 337—362.

Lasnier, B., 1977. Persistance d'une serie granulitique au coeur du Massif Central francais (Haut-Allier); les termes basiques, ultrabasiques et carbonates. Unpubl. Thesis, Un. Nantes, France.

Leake, B.E., 1978. Nomenclature of amphiboles. Min. Mag. 42, 533—563.

Le Fort, P., 1975. Himalayas : the collided range; present knowledge of the continental arc. Am. J. Sci. 275 A, 1—44.

Lindsley D.K.H. & Dixon. S.A., 1976. Diopside-enstatite equilibria at 850° to 1400°C, 5 to 35Kb. Am. J. Sci. 276, 1285—1301.

Liou, J., 1973. Synthesis and stability relations of epidote, $Ca_2Al_2FeSi_3O_{12}$. J. Pet. 14, 381—413.

———, Kuniyoshi, S. & Ito. K., 1974. Experimental studies of the phase relations between greenschist and amphibolite in a basaltic system. Am. J. Sci. 274, 613—632.

Majid, M. & Paracha, F.A., 1980. Calc-alkaline magmatism at destructive plate margin in Kohistan, Northern Pakistan. Proc. Int. Com. Geodyn., Grp. 6, Mtgs. Peshawar, Spec. Iss. Geol. Bull. Univ. Peshawar 13, 109—120.

McLelland, J.M. & Whitney. P.R., 1980a. Compositional controls on spinel clouding and garnet formation in plagioclase of olivine metagabbros, Adirondack Mountains, New York. Contrib. Min. Pet. 73, 243—251.

——— & ———, 1980b. A generalized garnet-forming reaction for metaigneous rocks in the Adirondacks. Contrib. Min. Pet. 72, 111—122.

Mason, R., 1967. Electron-probe microanalysis of coronas in a troctolite from Sulitjelma, Norway. Min. Mag. 36, No. 280, 504—514.

Mattauer, M.. Proust, F. & Tapponnier, P., 1977. Tectonic mechanism of obduction in relation with high pressure metamorphism. Orogenic mafic and ultramafic associations. Coll. Int. CNRS. 272, Grenoble, 197—201.

Medaris. L.R., 1972. High-pressure peridotites in southwestern Oregon. Bull. Geol. Soc. Amer. 83, 41—58.

Mercier, J.C., 1980. Single-pyroxene thermometry. Tectonophysics 70. 1—38.

Miyashiro, A., 1972. Metamorphism and metamorphic belts. G. Allen and Unwin Ltd.. London.

Molnar, P. & Tapponnier. P., 1975. Cenozoic tectonics of Asia : effects of a continental collision. Science 189, 419—426.

Moores, E.M. & Vine, J.F., 1974. Ophiolites and oceanic crust. Nature 250, 136—138.

Mori, T. & Green, T.H., 1978. Laboratory duplication of phase equilibria observed in natural garnet lherzolites. J. Geol. 86, 83—97.

Mottana. A.A., Church, W.R. & Edgar, A.D., 1968. Chemistry, mineralogy and petrology of an eclogite from the type locality (Saualpe, Austria). Contrib. Min. Pet. 18, 338—346.

Mueller, R.F., 1960. Compositional characteristics and equilibrium relations in mineral assemblages of a metamorphosed iron formation. Am. J. Sci. 258, 449—493.

Murthy, M.V.N., 1958. Coronites from India and their bearing on the origin of corona. Bull Geol. Soc. Amer. 69, 23—38.

Myer, G.H., 1966. New data on zoisite and epidote. Bull. Geol. Soc. Amer. 64, 364—385.

Mysen, B.O. & Boettcher, A.L., 1976. Melting of a hydrous mantle : III, Phase relations of garnet-websterite + H_2O at high pressures and temperatures. J. Pet. 17, 1—14.

——— & Heier, K.S., 1972. Petrogenesis of ecologites in high-grade metamorphic gneisses exemplified by the Hareidland eclogite, western Norway. Contrib. Min. Pet. 36, 73—94.

Newton, A.E., 1975. Composition and petrology of the earth's mantle. McGraw Hill, New York.

Nicollet, C., Levrelou. A. & Dupuy, C., 1979. Petrogenesis of high pressure trondhjemitic lavers in eclogites and amphibolites from southern Massif Central. France. In : Trondhjemites, dacites, and related rocks (Barker, F. Ed.), Amsterdam, 435—463.

O'Hara. M.J., 1968. The bearing of phase equilibria on synthetic and natural svstems on the origin and evolution of basic and ultrabasic rocks. Earth. Sci. Rev. 4, 69—113.

Oxburgh, E.R. & Turcotte, D.L., 1970. Thermal structure of island arcs. Bull. Geol. Soc. Amer 81, 1665—1688.

——— & ———, 1974. Thermal gradients and regional metamorphism in overthrust terrains with special reference to the Eastern Alps. Schweiz. Min. Pet. Mitt. 54. 641—662.

Papike, J.J.. Cameron, K.L. & Baldwin, K., 1974. Amphiboles and pyroxenes : characterisation of other than quadrilateral components and estimation of ferric iron from microprobe data. Geol. Surv. Amer., Poster Sess, Miami. 22 p.

Perkins III, D. & Newton. R.G.. 1980. The composition of coexisting pyroxenes and garnet in the system CaO-MgO-Al_2O_3-SiO_2 at 900°-1100°C and high pressures. Contrib. Min. Pet. 75, 291—300.

Powel. R . 1978 The thermodynamics of pyroxene geotherms. Phil. Trans. Royal Soc. London 288, 457—469.

Raheim, A. & Green. D.H.. 1974. Experimental determination of the temperature and pressure dependence of the Fe-Mg partition coefficient for co-existing garnet and clinopyroxenes. Contrib. Min. Pet. 48, 179—203.

Raith M.. 1976 The Al-Fe(III) epidote miscibility gap in a metamorphic profile through the Pennic series of the Tauern window, Austria. Contrib. Min. Pet. 57, 99—117.

Richardson S.W., 1968. Staurolite stability in a part of the system Fe-Al-Si-O-H. J. Petrol. 9, 467—488.

Ringwood, A.E., 1975. Composition and petrology of the earth's mantle. McGraw Hill, New York.

Rollinson. H R.. 1981. Garnet-pyroxene thermometry and barometry in the Scourie granulites, NW Scotland. Lithos 14, 225—238.

Rossi-Ronchetti, C.. 1975. Rudiste e Narinae del Cretaceo di Yasin (Pakistan nord-occidentale). In : Desio's Ital. Exped. Karakorum-Hindu Kush, Scientific Rep. IV, No. 1, 229—272.

Savage, D. & Sills, J.D.. 1980. High-pressure metamorphism in the Scourian of NW Scotland : evidence from garnet-granulites. Contrib. Min. Pet. 74, 153—163.

Saxena S.K., 1968. Crystal-chemistry aspects of distribution of elements among certain co-existing rock-forming minerals. N.Jb. Min. Abh. 108, No. 3, 292—323.

——— 1969. Distribution of elements in coexisting minerals and the problem of chemical des-equilibrium in metamorphosed basic rocks. Contrib. Min. Pet. 20, 177—197.

——— 1979. Garnet-clinopyroxene geothermometer. Contrib. Min. Pet. 70, 229—235.

Sharbert, H.G. & Kuart, G., 1974. Distribution of some elements between coexisting ferro-magnesian minerals in Moldanubian granulite facies rocks, Lower Austria. Tschermaks Min. Pet. Mitt. 21, 110—134.

Shreyer, W. & Seifert. F., 1969. High-pressure phases in the system MgO-Al_2O_3-SiO_2·$\mathbf{H_2O}$. Am. J. Sci. 267-A, 407—443.

Smulikowski, K., 1972. Classification of eclogites and allied rocks. Krystalinikum 9, 107—230.

Steinberg, M., Desprairies. J.F., Fogelsang, A., Martin, D., Caron, D., & Blanchet, R., 1977. Radiolarites et sediments hypersiliceux oceaniques : une comparison. Sedim. 24, 547—563.

Stormer, J.C. Jr. & Whitney, J.A., 1977. Two feldspar geothermometry in granulite facies metamorphic rocks : sapphirine granulites from Brazil. Contrib. Min. Pet. 65, 123—133.

Tahirkheli, R.A.K., Mattauer, M., Proust, F. & Tapponnier, P., 1979. The India-Eurasia suture zone in northern Pakistan : some new data for an interpretation at plate scale. In : Geodynamics of Pakistan. Geol. Surv. Pakistan, 125—130.

Tapponnier, P., Mattauer, M., Proust, F. & Cassaigneau, C., 1981. Mesozoic ophiolites, sutures and large-scale tectonic movements in Afghanistan. Earth Planet. Sci. Letters 52, 355—371.

Thompson, A.B., 1981. The pressure-temperature (P,T) plane viewed by geophysicists and petrologists. Terra Cognita 1, No. 1, 11—20.

———, Beiss. W. & England, P.C., 1981. Pressure-temperature- time (P-T-t) paths of the Earth's crust during metamorphism and orogeny. Terra Cognita Spring Issue, 90 (Abstract L. 13).

Thompson, P.H., 1977. Metamorphic P-T distributions and the geothermal gradients calcuated from geophysical data. Geology 5, 520—522.

Vogel, D.E., 1967. Petrology of an eclogite and pyrigarnite polymetamorphic rock complex at Cabo Ortegal, Spain. Leidse Geol. Meded. 40, 121—213.

Vrana, S., Prasad, R. & Fedivkova, E., 1975. Metmorphic kyanite eclogites in the Lufilian arc of Zambia. Contrib. Min. Pet. 51, 139—160.

Wells, P.R.A., 1977. Pyroxene geothermometry in simple and complex systems. Contrib. Min. Pet. 62, 129—139.

——— 1980. Thermal models for the magmatic accretion and subsequent metamorphism of continental crust. Earth Planet. Sci. Letters 46, 253—265.

White, A.J.R., 1964. Clinopyroxenes from eclogites and basic granulites. Am. Miner. 49, 883—888.

Windley, B.F., Herd. R.K. & Bowden. A.A., 1973. The Fiskenaesset complex, western Greenland. I. Gronl. Geol. Unders. 106, 1—80.

Winkler, H.G.F., 1967. Petrogenesis of metamorphic rocks. 2nd Ed. Springer Verlag, Berlin.

Wood, B.J.. 1974. The solubility of alumina in orthopyroxene coexisting with garnet. Contrib. Min Pet. 46, 1—15.

——— 1975. The influence of pressure, temperature and bulk composition on the appearance of garnet in orthogneisses : an example from South Harris, Scotland. Earth Planet. Sci. Letters 26, 299—311.

——— & Banno, S., 1973. Garnet-orthopyroxene and orthopyroxene-clinopyroxene relationships in simple and complex systems. Contrib. Min. Pet. 42, 109—124.

Wyllie, P.J., 1977. Crustal anatexis : an experimental review. Tectonophysics 43, 41—71.